UNIVERSITY OF CALIFORNIA, SAN DIEGO

Investigation of the potential anticancer and antifungal active secondary metabolites from marine natural products

A dissertation submitted in partial satisfaction of the requirements for the degree

Doctor of Philosophy

in

Oceanography

by

Chollaratt Boonlarppradab

Committee in charge:

Professor William Fenical, Chair
Professor Lihini L. Aluwihare
Professor Katherine A. Barbeau
Professor Douglas H. Bartlett
Professor Theo N. Kirkland

2007

The dissertation of Chollaratt Boonlarppradab is approved, and is acceptable in quality and form for publication on microfilm:

_____

_____

_____

_____

_____

_____

Chair

University of California, San Diego

2007

TABLE OF CONTENTS

LIST OF FIGURES

Chapter III.1

Chapter III.2

Chapter III.3

Chapter III.4

Chapter III.5

LIST OF TABLES

Chapter III.5

LIST OF ABBREVIATIONS

AMBR	amphotericin B resistant
CD	circular dichroism
DNA	deoxyribonucleic acid
DEPT	distortionless enhancement by polarization transfer
EI	electron ionization
ESI	electrospray ionization
FAB	fast atom bombardment
FDA	food and drug administration
COSY	correlation spectroscopy
HCT-116	human colon adenocarcinoma tumor cell line 116
HMBC	heteronuclear multiple bond correlation
HMQC	heteronuclear multiple quantum coherence
HPLC	high performance liquid chromatography
HSQC	heteronuclear single quantum coherence
HR	high resolution
IC_{50}	concentration at which 50% survival is observed
IR	Infrared
J	NMR coupling constant
LC/MS	liquid chromatography / mass spectroscopy
LR	low resolution
MALDI	matrix-assisted laser desorption/ionization

MIC	minimum inhibitory concentration
MS	mass spectroscopy
NOESY	nuclear Overhauser effect spectroscopy
NMR	nuclear magnetic resonance
ROESY	rotating frame nuclear Overhauser effect spectroscopy
TOCSY	total correlation spcetroscopy
TOF	time of flight
UV	ultraviolet

ACKNOWLEDGEMENTS

There are many people who provided me with help and great support during the course of my Ph.D., that I couldn't express enough appreciation and gratitude toward. First of all, I would like to convey my sincere appreciation to my distinguished advisors, Professor William Fenical and Professor John Faulkner. John gave me a valuable opportunity to participate in this terrific Ph.D. program at Scripps and guided me through my earlier year here. Bill has been an exceptionally insightful and understanding advisor, who led me through the rest of my thesis study. I also thank Professors Douglas Bartlett, Theo Kirkland, Katherine Barbeau, and Lihini Aluwihare for their precious suggestion about my research and enthusiastic participation in my thesis committee.

My thesis research could not have been complete without Dr. Paul Jensen and Chris Kauffman. I appreciate Paul's significant efforts in collection and discovering phylogenetically novel marine microbial strains. I would like to thank Chris for his tremendous help in microbial fermentation, recovering of lost production and culture optimization. I also appreciate the support from Matt Woolery regarding the use and maintenance of LC/MS and other machines in the lab. I also thank Alejandra Prieto Davo, and Erin Gontang for their great efforts in collecting marine actinomycetes strains from various locations, and genetic identification of those strains.

I would like to thank Dr. Lyndon West, Hak Cheol Kwon, Chambers Hughes, Ratnakar Asolkar and Takashi Fukuda for their generous and valuable guidance in the isolation process, structure elucidation, and chemical reactions. I also thank

Catherine Sincich and Sara Kelly for performing the antimicrobial and HCT-116 assays. I greatly appreciate Sara's effort in the instruction of the preparation of antifungal bioassay.

I also thank my friends who came to the Faulkner and Fenical lab, and gave me confidence and constant support. I was able to carry out through the Ph.D. course together with Wendy Strangman by supporting each other. I would like to thank Dr. Grace Lim for her patience in sharing the lab and office with me during the time I was in Faulkner lab, as well as Dr. Joel Sandler, Melissa Lerch, Koty Sharp and Roman De Jesus who were the members of the Faulkner lab at that time. I also thank Dong-Chan Oh and Ana Paula Espindola for helping me with the problem regarding the NMR and also for being great friends in the Fenical lab.

To my family, I will not be able to thank my mother and father enough for their love and contribution during the difficult time in my Ph.D. study. I also thank my grandmother, aunt, uncle and brother for their care and endless support. Without their consideration, I could not have finished my study at Scripps.

The text of II.3, in full, is the manuscript to be submitted to an academic journal as it appears in Boonlarppradab, C.; Faulkner, D. J. Adociasulfate 13, an antifungal merotriterpenoid from the Red Sea sponge *Haliclona* (aka *Adocia*) sp. *Tetrahedron Lett.* The dissertation author was the primary author and directed and supervised the research, which forms the basis for this chapter.

The text of II.4, in full, is the manuscript submitted to an academic journal as it appears in Boonlarppradab, C.; Faulkner, D. J. Eurysterols A and B, Cytotoxic and Antifungal Steroidal Sulfates from a Marine Sponge of the Genus *Euryspongia*. *J. Nat.*

Prod. **2007**, *70*, 846-848. The dissertation author was the primary author and directed and supervised the research, which forms the basis for this chapter.

The text of III.4, in part, is the manuscript to be submitted to an academic journal as it appears in Boonlarppradab, C.; Kauffman, C. A.; Jensen, P. R.; Fenical, W. Marineosins A and B, A new class of macrocyclic pyrroles from the marine actinomycete "MAR3" clade. *Org. Lett*. The dissertation author was the primary author and directed and supervised the research, which forms the basis for this chapter.

VITA

2001 B.S. Biology (concentrated in chemistry), Haverford College.

2007 Ph.D. Oceanography (marine natural products chemistry), Scripps Institution of Oceanography, University of California, San Diego.

PUBLICATIONS

Boonlarppradab, C.; Faulkner, D. J. Eurysterols A and B, Cytotoxic and Antifungal Steroidal Sulfates from a Marine Sponge of the Genus *Euryspongia*. *J. Nat. Prod*. **2007**, *70*, 846-848.

Boonlarppradab, C.; Faulkner, D. J. Adociasulfate 13, an antifungal merotriterpenoid from the Red Sea sponge *Haliclona* (aka *Adocia*) sp. *Tetrahedron Lett.* submitted.

Boonlarppradab, C.; Kauffman, C. A.; Jensen, P. R.; Fenical, W. Marineosins A and B, A new class of macrocyclic pyrroles from the marine actinomycete "MAR3" clade. *Org. Lett.* submitted.

ABSTRACT OF THE DISSERTATION

Investigation of the potential anticancer and antifungal active secondary metabolites from marine natural products

by

Chollaratt Boonlarppradab

Doctor of Philosophy in Oceanography

University of California, San Diego, 2007

Professor William Fenical, Chair

The oceans are a unique resource that has contributed greatly to the field of natural products chemistry. Secondary metabolites from natural sources still play an important role in drug discovery and development by providing pharmaceutical candidates with novel structures that are valuable for synthetic modification. Of the marine organisms described to date, the vast majority of marine natural products derive from invertebrates such as sponges, ascidians, bryozoans, and tunicates. Recently, marine microbes have also come to the forefront of natural products research since they are now being recognized as a significant new source of diverse and unique chemical compounds. With the existence of various diseases which pose a dangerous threat to human health, many bioassays have been developed in an attempt to find suitable agents as cures to those symptoms. Among recognizable infectious diseases, fungal infection is one of the significant causes of mortality and morbidity. As there are only few numbers of antifungal drugs available for

therapeutic treatment, searching for new classes of active compounds proves to be crucial. This thesis discusses different methods for screening extracts of marine organisms in search of novel antifungal agents that possess relevant clinical value, with emphasis on the isolation and characterization of these compounds.

Chapter I introduces the concept of the main thesis research that is described in subsequent chapters. Chapter II provides details of the discovery of new secondary metabolites from marine invertebrates, including sponges and ascidians, through a bioassay-guided screening process. The new compounds that were isolated include the merotriterpenoid adociasulfate, steroidal sulfates, and a pyridoacridine alkaloid. This chapter also describes antifungal bioassays that were performed and the results of the screening. Chapter III describes the isolation of new secondary metabolites from marine actinomycete strains selected based upon the results of a liquid antifungal assay. In this latter chapter, the problem regarding the screening of marine microbes using the liquid antifungal assay, and the subsequent adjustment by assay modification are described. The isolation and identification of new quinoline alkaloids, a bacterial sesterterpenoid and a novel cytotoxic macrolide are also discussed in detail, with respect to structural elucidation and biological activity.

I

Introduction to the thesis research

General overview of marine natural products

The oceans are a unique resource that has contributed significantly to the field of natural products. The large area, over 70% of the earth's surface, is covered by the ocean. This incredible and potential resource comprises more than 300,000 described species of plants and animals, as well as countless numbers waiting to be discovered and explored.[1] Nevertheless, research institutions and the pharmaceutical industry started to become interest in the ocean only approximately 50 years ago with the discovery of antiviral nucleosides, spongothymidine and spongouridine, from the sponge *Cryptotethia crypta*.[2] Of the marine organisms described to date, the vast majority of marine natural products derive from invertebrates such as sponges, ascidians, bryozoans, mollusks, and tunicates. Recently, marine microbes have also emerged to the forefront of natural products research since they are now being recognized as an important new source of diverse and unique secondary metabolites. In total, over 14,000 novel compounds have been isolated from marine organisms with an increasing trend in numbers.[3] The process of natural selection and ecological pressures such as competition for space, predation, self-protection, or fouling, exert great influences on the development and evolution of unique secondary metabolites that possess distinct biological activities.[4]

In addition to novel chemical structures, marine natural products chemistry research has yielded significant numbers of important bioactive metabolites that are now being developed as drug candidates. Secondary metabolites from natural sources still play a crucial role in drug discovery and development by providing potential drug candidates with novel skeletons that are valuable for synthetic modification.[5] The importance of

natural products in this field has been demonstrated by the fact that 5 % and 23 % of drugs approved by the FDA over the last 25 years between 1981 and 2006 are natural products or natural product-derived molecules.[6] Additionally, at least 21 natural products or natural product derived drugs have been approved in the United States, Europe or Japan during the 6 years between 1998 and 2004.[7] Not surprisingly, quite a few clinically effective drugs have also been developed by the pharmaceutical industry through marine natural product drug-discovery programs. Approximately 15 promising marine derived compounds are scheduled to begin or are currently undergoing clinical evaluation, mostly in the area of anticancer chemotheraphy.[3] These include the potent marine alkaloid anticancer agent ecteinasidin-743, isolated from the tunicate *Ecteinascidia turbinata*, bryostatin-1, a macrolide with potent antitumor activity from the common bryozoan *Bugula neritina*, and halichondrin B, a potent anticancer agent derived from a New Zealand deep water sponge *Lissodendoryx* spp.[8]

Anitifungal drug discovery and development

Over past two decades, the incidence of fungal infection in humans has significantly increased. These rising trends have occurred not only in superficial infections of the skin, but also in more serious systemic infections of the internal organs, particularly in immunocompromised patients.[9] Invasive fungal infections are now considered to be a significant cause of mortality and morbidity. The frequency of systemic fungal infections has risen in conjunction with the increasing number of patients with immunodeficiency. For example, patients who receive cancer chemotherapy,

immunosuppressive therapy, and those infected with HIV are particularly susceptible. As a result, there is a critical need for the development of new antifungal drugs. This urgency stems from the therapeutic limitations of the present antifungal agents, the emerging development of widespread antifungal drug resistance, the toxicity of current drugs, and non-optimal pharmacokinetics and hazardous drug-drug interactions.

Despite the fact that invasive fungal diseases have become more frequent than in the last 50 years, there are still difficulties in clinical diagnosis. One of major problems in therapeutic treatment is limitation of antifungal agents for pharmaceutical use. Since the 1950s, only two classes of natural products (griseofulvin and polyenes), one class of semi-synthetically derived natural product (echinocandins), and four classes of synthetic chemicals (allylamines, azoles, flucytosine, and phenylmorpholines) have been identified as clinically viable drugs for medical treatment against fungal infections.[10] The difficulties in antifungal drug development also stem from the fact that pathogenic fungi are eukaryotic as are mammalian cells. Hence, searching for cellular targets upon which antifungal agents could act, without serious side-effects, proves to be very difficult to achieve. This could explain why only a few classes of chemical compounds represent the major portion of antifungal drugs.

As it was mentioned earlier, several therapeutic antifungal drugs in the market were derived from natural sources.[7] This evidence suggests that natural products are prominent candidates in the area of antifungal drug development. The field of antifungal drug discovery research is being directed toward the screening for lead compounds with defined mechanisms of action that can function as templates for

further development and modification as potent therapeutic agents. Researchers aim to discover compounds possessing a broad spectrum of antifungal activity against crucial pathogenic fungi, such as *Candida albicans,* non-albicans *Candida* (e.g. *C. krusei, C. glabrata,* and *C. parapsilosis*), *Aspergillus fumigatus* and *Cryptococcus neoformans*. Stemming from the fact that marine organisms possess novel secondary metabolites, which differ from those in terrestrial organisms in term of both structures and specific bioactivities, it is believed that marine organisms may be significant resources for providing antifungal agents with selective modes of action. The screening of marine organisms for antifungal metabolites has led to the discovery and characterization of a significant number of novel natural products with distinct chemical structures and clinically relevant antifungal activities.

As the main focus of my thesis research, I hypothesized that careful investigation of both marine invertebrates and marine microbes by wisely manipulating antifungal and cytotoxic bioassays as screening methods would be the effective approach to the discovery of novel secondary metabolites with potent and selective antifungal activity. Thus, the objective of this dissertation research was to examine novel natural products from marine organisms, and to isolate, purify, and elucidate the structures of the new chemical compounds potentially useful as effective antifungal therapeutic agents.

Chapter II discusses new bioactive secondary metabolites from marine invertebrates, such as sponges and ascidians. Two different types of antifungal bioassays that were conducted as screening tests and their results are discussed there in detail. Reported are merotriterpenoids of the adociasulfate class from a marine sponge of the genus *Haliclona*, steroidal sulfate metabolites from a marine sponge of the genus

Euryspongia, and cytotoxic pyridoacridine alkaloids from a marine ascidian of the genus *Eudistoma*.

Chapter III describes the discovery and structure determination of novel secondary metabolites from marine microorganism of the subclass actinomycetales. The bioassay-guided screening method was also applied to marine microbial sources for selection of the promising strains, although the approach that was taken is slightly different from that applied to the marine invertebrates. This chapter also discusses an unexpected pitfall regarding the use of liquid antifungal assay with microbial strains, and the method that was developed to resolve this problem. These studies include the isolation of quinoline alkaloids, a bacterial terpenoid, and a new class of cytotoxic macrolides with a novel skeleton from marine actinomycetes of the newly recognized MAR3 clade.[11]

References

(1) Donia, M.; Hamann, M. T. *Lancet Infect. Dis*. **2003**, *3*, 338-348.

(2) Bergmann, W.; Feeney, R. *J. Org. Chem.* **1951**, *16*, 981-987.

(3) Proksch, P.; Edrada-Ebel, R.; Ebel, R. *Mar. Drugs* **2003**, *1*, 5-17.

(4) Belarbi, E. H.; Gomez, A. C.; Chisti, Y.; Camacho, F. G.; Grima, E. M. *Biotechnol. Adv.* **2003**, *21*, 585-598.

(5) Clardy, J.; Walsh, C. *Nature* **2004**, *432*, 829-837.

(6) Newman, D. J.; Cragg, G. M. *J. Nat. Prod*. **2007**, *70*, 461-477.

(7) Butler, M. S. *Nat. Prod. Rep.* **2005**, *22*, 162-195.

(8) Munro, M. H. G.; Blunt, J. W.; Dumdei, E. J.; Hickford, S. J. H.; Lill, R. E.; Li, S.; Battershill, C. N.; Duckworth, A. R. *J. Biotechnol*. **1999**, *70*, 15-25.

(9) Andriole, V. T. *J. Antimicrob. Chemother*. **1999**, *44*, 151-162.

(10) Odds, F. C. *J. Mycologist* **2003**, *17*, 51-55.

(11) Fenical, W.; Jensen, P. R. *Nat. Chem. Biol.* **2006**, *2*, 666-673.

II

New secondary metabolites from marine invertebrates

Chapter II describes three different invertebrate projects providing different types of bioactive compounds, which were isolated by the bioassay-guided fractionation method. The major focus of this chapter is based on the investigation of marine invertebrates for potential antifungal candidates that may prove to be useful as therapeutic agents. Chapter II.1 provides an introduction and a few examples of potent antifungal metabolites from marine invertebrates. The following chapter II.2, discusses two standard antifungal susceptibility tests that were chosen for screening of marine invertebrates, as well as the obtained results.

Chapter II.3 details the most promising project, a sponge of the genus *Haliclona* that was chosen based upon the result of antifungal screening of over one hundred marine invertebrate samples. This chapter demonstrates a successful example of the isolation and characterization of the selective antifungal metabolite with potent antifungal activity with insignificant cytotoxicity.

In chapter II.4, two new cytotoxic and antifungal steroidal sulfates, isolated from an undescribed species of marine sponge *Euryspongia* sp., are discussed in detail. The slight differences in their structures proved to have a significant impact on their biological activity in both antifungal and HCT-116 assays.

Chapter II.5 describes the isolation of a cytotoxic pyridoacridine alkaloid from a purple ascidian of the genus *Eudistoma*. The new derivative isolated is a sagitol-type compound, which was isolated along with a few known metabolites through the process of bioassay-guided fractionation.

II.1

Antifungal metabolites from marine organisms

II. 1. Antifungal metabolites from marine organisms

The marine environment supports a great biodiversity with a correspondingly great potential for the discovery of unique and pharmaceutically active secondary metabolites. Various species of macroscopic plants and animals are known to adapt to different regions of the oceans , which include polar, temperate or tropical seas. In particular, the Indo-Pacific Ocean has been reconized to comprise the world's greatest tropical marine biodiversity.[1] The high diversity in species is particularly noticeable on coral reefs where up to 1000 species per m^2 occur in certain areas.[1] These highly competitive locations are founded on an intense ecological pressure which serves as a significant driving force that led to the evolution and development of biologically active marine natural products.

According to the literature up until the year 1998, the Porifera has been the most studied phylum, followed by the Cnidaria, Chromophycota, Rhodophycota, Mollusca, Chordata and the Echinodermata.[2] In comparison to terrestrial organisms such as plants and microorganisms, published screening data from the US National Cancer Institute (NCI) clearly indicated that marine invertebrates are a preferred pharmaceutical potential source as it shows much higher incidence of significant biological activity, particularly with regard to anticancer activity.[2] As can be expected, marine natural products contribute mostly in the area of anticancer chemotherapy. The list of compounds currently undergoing clinical investigation strongly supports this argument. Among marine invertebrates, the intensive investigation reveals that certain groups of organisms, including sponges, molluscs,

tunicates and bryozoans, have a higher incidence of biological or pharmacological activity from their secondary metabolites.[2]

As for the research in the field of antifungal active compounds, the investigation of marine invertebrates has led to the isolation and characterization of unique and unprecedented natural products with distinct bioactivity. Since many of the secondary metabolites from marine sources appear to be structually different from their terrestrial counterparts, it is hypothesized that effective antifungal compounds with selective modes of action could be obtained from marine organisms.

The first example of a marine-derived antifungal compound is jasplakinolide (**1**), a 19-member macrocyclic cyclodepsipeptide isolated from a marine sponge *Jaspis* sp. collect in Fiji.[3] Jasplakinolide, also known as jaspamide, exhibits selective *in vitro* antimicrobial activity with MIC value of 25 μg/mL against *Candida albicans*, while at the same time shows *in vivo* topical activity (2% solution) against *Candida* vaginal infection in mice.[3]

The extremely potent antifungal agents, gambieric acids, have been isolated from an epiphytic marine dinoflagellate *Gambierdiscus toxicus*. Gambieric acids are the first representative group of antifungal compounds that possess novel brevetoxin-type (fused polyether rings) structures, consisting of nine contiguous ether rings and one isolated tetrahydrofuran. Gambieric acids A (**2**) and B (**3**) inhibit the growth of *Aspergillus niger* at the concentration of 10 and 20 ng/disk, respectively, and the potency exceeds that of the clinically efficacious drug amphotericin B by 2000-fold.[4]

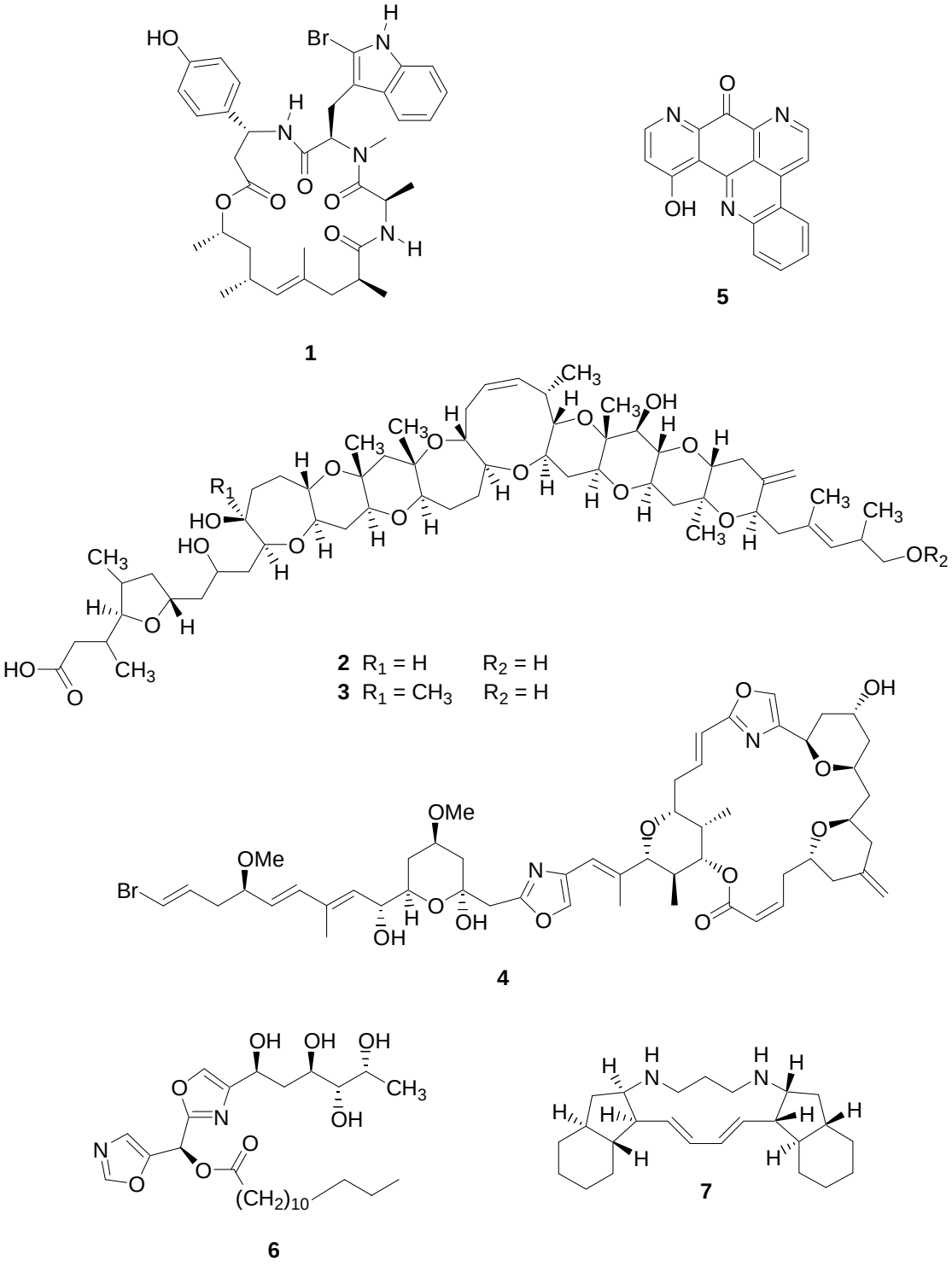

Figure II.1.1 Antifungal metabolites from marine natural products

The cytostatic and antifungal macrolides, phorboxazoles, were derived from a marine sponge of the genus *Phorbas* collected in Western Australia. The phorboxazoles represent a new class of macrolides which are composed of a unique oxazole-trisoxane fused ring system. Phorboxazole A (**4**) showed a 9 mm zone of inhibition in the agar disk diffusion assay against *C. albicans* at the concentration of 0.1 μg/disk.[5]

McCarthy *et al*. reported a polycyclic alkaloid, meridine (**5**), isolated from a deep water Bahamian marine sponge *Corticium* sp. The study showed that meridine was highly active against pathogenic fungi *C. albicans* and *Cryptococcus neoformans* at MIC values of 0.2 and 0.8 μg/mL respectively.[6] Meridine was also tested against various strains of filamentous fungi with significant activity being observed against *Trichophyton mentagrophytes* and *Epidetmophyton fIoccosum*.[6]

Bengazoles, unique bis(oxazoles) with a carbohydrate-like polyol side chain, which were characterized from a marine sponge of the genus *Jaspis,* were reported to have excellent antifungal activity.[7,8] Bengazole A (**6**) is very potent ergosterol-dependent agents whose activity against *C. albicans* and *Saccharomyces cerevisiae* is comparable to that of amphotericin B. In a simple agar disk diffustion assay, 9 to 10.5 mm zone of inhibition at 0.5 μg/disk were observed.[7]

Extraction of a bright red sponge *Haliclona* sp. from Palau, followed by purification, lead to the characterization of haliclonadiamine (**7**), an antifungal alkaloid which

showed growth inhibition against *C. albicans* at concentrations of 1.0 to 0.5 μg/disk in the standard disc assay.[9]

Despite the fact that marine invertebrates represent a great source for novel bioactive chemicals with potential as pharmaceuticals, molecular probes, cosmetics, or nutritional supplements, there is one major limiting factor that often prevents further development in these fields. As one can imagine, a serious problem with marine invertebrates is the limitation of supply of most marine-derived compounds.[10] More often, the active metabolites only occur in trace amounts in the organism, and the limited harvest that can be performed without disrupting the ecosystem or depleting the resource will not provide enough target compound for the development in each field. In particular, drug discovery and development program usually require large amounts, ca. 100 gm, of chemical compounds for preclinical studies.

Apart from the supply problem, most antifungal metabolites from marine organisms usually turn out to be very cytotoxic toward human cells. Consequently, these compounds are not considered to be suitable antifungal agents for pharmaceutical drug development. In most cases, it will be necessary to assess whether antifungal activity outweighs cytotoxic effects. Given the fact that most marine-derived antifungal compounds possess high cytotoxicity, the modification of the target molecule to improve therapeutic index will be extremely crucial.

References

(1) Donia, M.; Hamann, M. T. *Lancet Infect. Dis.* **2003**, *3*, 338-348.

(2) Munro, M. H. G.; Blunt, J. W.; Dumdei, E. J.; Hickford, S. J. H.; Lill, R. E.; Li, S.; Battershill, C. N.; Duckworth, A. R. *J. Biotechnol*. **1999**, *70*, 15-25.

(3) Crews, P.; Manes, L. V.; Boehler, M. *Tetrahedron Lett.* **1986**, *27*, 2797-2800.

(4) Nagai, H.; Murata, M.; Torigoe, K.; Satake, M.; Yasumoto, T. *J. Org. Chem*. **1992**, *57*, 5448-5453.

(5) Searle, P. A.; Molinski, T. F. *J. Am. Chem*. *Soc.* **1995**, *117*, 8126-8131.

(6) McCarthy, P. J.; Pitts, T. P.; Gunawardana, G. P.; Kelly-Borges, M.; Pomponi, S. A. *J. Nat. Prod*. **1992**, *55*, 1664-1668.

(7) Molinski, T. F. *J. Nat. Prod.* **1993**, *56*, 1-8.

(8) Searle, P. A.; Richter, R. K.; Molinski, T. F. *J. Org. Chem*. **1996**, *61*, 4073-4079.

(9) Fahy, E.; Molinski, T. F.; Harper, M. K.; Sullivan, B. W.; Faulkner, D. J. *Tetrahedron Lett.* **1988**, *29*, 3427-3428.

(10) Proksch, P.; Edrada-Ebel, R.; Ebel, R. *Mar*. *Drugs* **2003**, *1*, 5-17.

II.2

Antifungal bioassay-guided screening of marine invertebrates

II. 2. Antifungal bioassay-guided screening of marine invertebrates

Introduction

Pathogenic Fungal Infections

Of the numerous fungal genera known to date, most pathogenic fungal diseases in humans are caused by only 10 to 15 different species, even though these strains can be deadly if the patient has a weaken immune system. Since the 1980s, an increasing trend of fungal infections has been observed with the parallel emergence of new fungal pathogens and opportunistic fungi which can cause infection in the immunocompromised host.[1] The incidence and fatality rates of several specific mycoses were also examined with the result of *Candida* species being accounted for most infections.[2] During this past three decades, *Candida* has emerged worldwide as a significant cause of bloodstream infections.

Pathogens of the genus *Candida* are opportunistic fungi that infect primarily immunocompromised human hosts. They are the leading cause of invasive infections in hospitalized patients. These pathogens are the fourth most common cause of bloodstream infections in the United States with an attributable mortality rate of 19% up to 49%.[3,4] The increasing rate of invasive infections by *Candida* species is likely to result from an increased prevalence of susceptible hosts, who have received intensive care therapies or immunosuppressive therapies associated with organ transplantation, cancer chemotherapy or the use of broad-spectrum antibiotics. There is also an increased awareness of the high morbidity and mortality rate associated with fungal

infections caused by resistant fungi in various groups of patients. The clinical consequences of antifungal resistance can be seen from treatment failures in infected patients especially with *Candida* species. Despite the fact that there are over 100 species of *Candida* that have been described, only a few species have been associated with clinical infections.[4] Overall, most infections are caused by *C. albicans.* Within the group of patients infected by pathogenic fungi, from approximately 30% up to over 50% are caused by *C. albicans*[5-7] as shown in Figure II.2.1.[8]

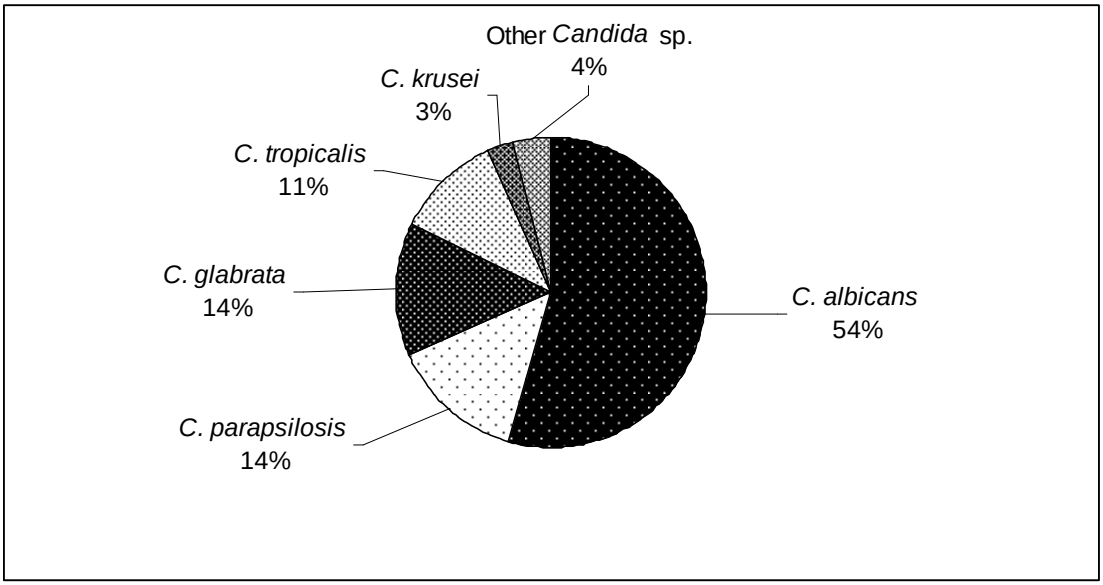

Figure II.2.1 Distribution of *Candida* species from 8,197 clinical isolates obtained internationally from 91 medical centers from 2001 through 2004.

Due to the high rate of infection by *C. albicans*, and its importance as a major human pathogenic fungus, the specific target for my discovery program was *C. albicans* wild type (ATCC32354) and the amphotericin B resistant strain available from the American Type Culture Collection (ATCC90873). The wild type *C. albicans* strain is used as the standard test organism for my screening of crude extracts in order to identify active projects.

Antifungal Susceptibility Tests

In the field of drug discovery and development from marine natural products, selection of the appropriate biological assay is one of the crucial factors that can lead to the discovery of novel target compounds with the desired bioactivity from the sources of interest. Generally, there are various types of methods that may be suitable for different type of samples, or serve the purpose of the screening better one way than the other. Typically, primary assays are designed for the initial screening of large numbers of crude extracts, with the purpose of identifying active extracts. Most primary assays do not usually give accurate quantitative results but are more qualitative and still provide sufficient data for the selection of interesting projects with appropriate levels of biological activity. On the other hand, secondary assays are usually designed for more specific purpose, such as the quantification of activity of the pure chemical compound or the activity observed in the primary assay (MIC values).

As there are various types of antifungal assays available to select from, it was important to search for the most appropriate screening method that could best provide the anticipated results. The criteria for choosing the proper antifungal assay for this

study was mainly based on the reliability, reproducibility, simplicity and the cost of the assay system. For marine invertebrate extracts as the main screening target, the antifungal susceptibility tests that were chosen for the screening step, consisted of two types of assays, the “Disc Diffusion Method” and a dilution “Liquid Assay” (Broth Dilution Antifungal Susceptibility Testing).

Disc Diffusion Method

The Disc diffusion assay is the simplest and most widely used approach for initial screening of crude extracts. This assay relies on the diffusivity of the active compound(s) into the agar matrix which has been surface inoculated with the test fungal strain. The metabolites that possess antifungal activity will generate zones of inhibition of fungal growth around the zone of application. This method utilizes the small filter-paper disc to which the potential active mixtures are applied, and allowed to diffuse from. A known concentration of liquid from the crude extract is applied to a circular paper disc with a diameter of 6.5 mm that is subsequently placed on the *C. albicans* innoculated petri dish. The fungal petri dishes are then incubated at 37º C for 24 hours and inhibition zones are determined. The diameter of the zone of inhibition extending outward from the paper disk is read as a zone of inhibition (in mms). This method does not yield a quantitative number, such as a minimal inhibitory concentration (MIC), but gives a rough estimation of activity in terms of the diameter of the zone of inhibition. Using this approach, the interpretation of the data is more qualitative than quantitative.

This method has one major limitation, which is that the activity is dependent upon the diffusivity of the test compound. Certain types of molecules, such as extremely non-polar compounds, do not diffuse well in the agar matrix and result in a small zone of inhibition, while molecules with higher polarity and diffusivity can create larger inhibiting zones, regardless of their antifungal activity. Hence, the ability of chemical metabolites to diffuse through agar matrix has a great effect on the size of zone of inhibition, and often leads to the misinterpretation of antifungal potency.

A Dilution Liquid Assay (Broth Dilution Antifungal Susceptibility Testing)

The liquid antifungal assay is the most widely used quantitative susceptibility measurement that defines the concentration of the test compounds. *C. albicans* cultures, containing serial dilutions of the test agents, are used to establish the lowest drug concentration that prevents detectable fungal growth. This method provides a more accurate measurement of antifungal activity by generating a specific Minimum Inhibitory Concentration (MIC value), which can be used to estimate therapeutic concentrations *in vivo*. The endpoint of a susceptibility measurement depends on the starting microbial cell concentration, conditions of temperature and pH, and how early or late in the growth cell cycle that results are obtained. AlamarBlue, which is an oxidation-reduction (REDOX) indicator, can be utilized as the growth indicator in this assay. During cell growth, metabolic activity maintains a reduced environment, while the inhibition of growth results in an oxidized environment. Therefore, continued growth of fungal cells will result in the chemical reduction of AlamarBlue that can be observed as the change in color from blue (oxidized form) to pink (reduced form).

During the inoculum preparation, *C. albicans* was cultivated in the RPMI 1640 medium (GIBCO) and shaken at 37 °C overnight. The density of cell suspensions was counted using a haemocytometer. These cell suspensions were eventually diluted to make the final concentration of 1 x 10^4 cells/mL. Subsequently, AlamarBlue (Trek Diagnostic System, Inc.) was added to the cultivation solution at 1% concentration.

For the purpose of my screening program, this liquid assay technique is divided into two different methods, the Single Concentration Method and the Serial Dilution Method.

1) Single Concentration Method

This method is designed to test the antifungal activity of the extract at a single concentration against *C. albicans*. This assay will not yield an exact MIC value, but rather indicates whether there is growth inhibition at a preselected concentration. Hence, it is a useful method for the primary screening of the large number of samples in a short period of time. The assay was set up using a 96-well plate format. The crude extracts (10 µl) were added into each well (column 1 to 10) and mixed with 100 µl of *C. albicans* inoculum solution. The standards, DMSO (10 µl) and amphotericin B (Sigma) solution (10 µl, 0.5 mg/mL) were added to 190 µl of *C. albicans* inoculum solution at the top row of column 11 and 12, respectively, as the negative and positive control. Subsequently, a half-fold serial dilution was performed in these two columns by mixing the top row and transferring 100 µl of mixtures down the plate. The dilution process was repeated down the plate (vertical wells) until the mixtures were

diluted 128 times in the last row and the final 100 µl of mixtures were discarded. After that, the plate was incubated at 37 ºC for 12-16 hours. The results of antifungal activity can simply be indicated by turbidimetric visualization.

2) Serial Dilution Method

The principal of this method is very similar to the first one, but instead of focusing at one single concentration, this assay employs a half-fold serial dilution method for all the tested samples. Hence, this method can be used to determine the exact MIC values of the antifungal metabolites. This assay is usually performed to test pure chemical compounds or antifungal-active extracts from the primary screening to derive specific MIC values.

For the basic procedure, each chemical extract (10 µl) was added to a 190 µl of *C. albicans* inoculum solution in the first row. Each vertical column (from 1 to 10) was designated for a single test sample, while DMSO and amphotericin B were added to columns 11 and 12 , as was done in the first method as the negative and positive controls. The half-fold serial dilution method was utilized entirely for both the tested compounds and the standards. The MIC value was determined from the concentration of the last well that retained blue color in each column. The range of concentration in each column from the first row to the last row depends on the initial concentration of the test compound as illustrated in Table II.2.1. The numbers in the first row represent concentrations of the test materials, while numbers in each column stand for MIC values expressed as µg/mL.

Table II.2.1 The range of MIC values for various starting concentrations of the tested compounds

Row	0.5 mg/mL	5 mg/mL	10 mg/mL	20 mg/mL	25 mg/mL
A	25	250	500	1000	1250
B	12.5	125	250	500	625
C	6.25	62.5	125	250	312.5
D	3.125	31.3	62.5	125	156.3
E	1.56	15.6	31.3	62.5	78.1
F	0.78	7.8	15.6	31.3	39.1
G	0.39	3.9	7.8	15.6	19.5
H	0.19	1.95	3.9	7.8	9.8

Marine Invertebrates Screening

In this chapter, the main sources of potential active leads were marine sponges and ascidians. The initial screening method for the crude extracts was performed by the disc diffusion method, and samples were obtained from different locations and collections, including Palau, South Africa and Red Sea. The average hit rate was 10% or less, and more importantly, those antifungal active extracts were also significantly cytotoxic.

What I discovered was that the more antifungal the samples were, the more cytotoxic they were likely to be in the HCT-116 colon carcinoma assay. These projects are, therefore, not suitable candidates for antifungal drug development, since the ideal project should be non-cytotoxic to human cells. From an available collection of marine invertebrates, it proved to be extremely difficult to find a project with selective antifungal activity. This is one of the major reasons that later on, the focus was shifted toward marine microbes.

Nonetheless, on the basis of primary screening by the disc diffusion method using the invertebrate collection, promising chemically-oriented projects were chosen and the crude extracts were fractionated using appropriate chromatographic methods. The resulting fractions were tested for antifungal activity in the dilution liquid assay, and it was found that more than half of them showed no activity at all. This outcome illustrates the uncertainty of data from the disc diffusion method. Most samples that showed activity from the disc diffusion method lacked comparable activity in the antifungal liquid assay. (Table II.2.2) The difference may stem from the compound

being degraded or the pharmacokinetic properties of the active molecules. For that reason, the disc diffusion method was eventually discarded in favor of the more reliable liquid antifungal assay in the initial process of screening crude extracts.

Table II.2.2 Antifungal screening results of marine invertebrates using disc diffusion and liquid broth dilution methods.

Collection	**Number of the Crude Extracts**	**Number of Antifungal Active Extracts**		**HCT-116 (IC_{50} >20 μg/mL)**
		Disc Diffusion Method	**Liquid Assay**	
South Africa (2003)	100	6	4	2
Palau (1999)	167	20	6	1
Red Sea (2000)	54	NA	6	2

According to the overall results of the antifungal screening for the marine invertebrate extract collection, approximately 5% of total extracts showed antifungal activity. Of all the test mixtures, only less than 1.5% possess selective antifungal activity with a low level of cytotoxicity. Even though, the screening process yields only few promising projects, chemical investigation for those extracts were conducted in order to isolate and identify those potent antifungal metabolites.

Dereplication of known chemical metabolites from active extracts

The crude methanol extracts of marine invertebrates that exhibited antifungal activity in the liquid antifungal assay, were fractionated first using HP20SS column chromatography. By utilizing the bioassay-guided fractionation method, the active fractions were further separated and purified by High Performance Liquid Chromatography (HPLC) to obtain pure chemical compounds. The structures of known compounds were identified by a dereplication procedure and confirmed as known by direct comparison of ESI-MS and NMR spectroscopic data to those in Marinlit^{TM}.

Isolation of Agelasine F (Ageline A) from marine sponge of the genus *Agelas* (Project 99-446)

The marine sponge *Agelas* sp., designated 99-446, was collected by members of the Faulkner research group in Palau in 1999 by scuba diving. The specimen (1 kg wet weight) was kept frozen immediately after collection until being processed. The sponge was exhaustively extracted with methanol and the extract was tested in the liquid antifungal assay. The crude extract exhibited antifungal activity at MIC values less than 156 μg/mL in the antifungal assay, while showing cytotoxicity with an IC_{50} value (HCT-116 assay) at 25.4 μg/mL. In addition, a zone of inhibition of 12 mm was also observed in the disc diffusion assay.

The crude methanol extract was separated by HP20SS column chromatography, using an acetone-water gradient from 10% to 100%, into approximately 50 fractions. Fraction 29 which was eluted with a 60% acetone/water mixture was found to deposit crystals after sitting on the lab bench for 3 to 4 days. The ^{1}H NMR spectrum indicated that the compound appeared to be very pure. The compound was recrystallized from the same solvent condition in order to obtain the highest quality crystals. Unfortunately, both ^{1}H NMR and MS spectral data pointed out that the compound was the previously reported, agelasine F (also known as ageline A), which is known to possess potent antimicrobial activity. Agelasine F, which belongs to a group of 7,9-dialkylpurinium salts, also exhibits strong activity against *Mycobacterium tuberculosis*.[9] The liquid antifungal assay showed this compound to possess very potent antifungal activity with MIC value less than 2.0 μg/mL, unfortunately with moderate cytotoxicity showing IC_{50} of 4.8 μg/mL in the HCT-116 assay.

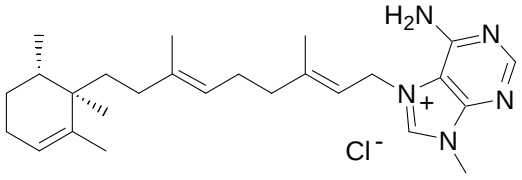

Agelasine F (Ageline A)

Isolation of psammaplysin A from marine sponge of the order *Verongida* (Project 99-371)

An unidentified marine sponge (600 g wet weight) of the order *Verongida*, designated 99-371, was collected from Palau in 1999. The crude methanol extract showed slight antifungal activity from disc diffusion method, but did not possess significant cytotoxic activity (IC_{50} over 40 μg/mL in the HCT-116 assay). The crude extract was fractionated by HP20SS column chromatoraphy eluting with acetone/water gradients from 10% to 100%. Fractions 21 to 23 (60% acetone/water fractions) were discovered to contain one major halogenated metabolite, which by mass spectrometry was found to contain four bromine atoms. This chemical compound, as directly derived from HP20SS chromatography was fairly pure and didn't require further purification by HPLC. However, the ^{1}H NMR and MS data from this compound indicated that it is a known antibiotic, psammaplysin A.[10] In pure compound testing, psammaplysin A was active in the HCT-116 assay with IC_{50} = 50 μg/mL, while the antifungal activity against *C. albicans* (MIC value of 250 μg/mL) showed the compound to have little pharmaceutical potential.

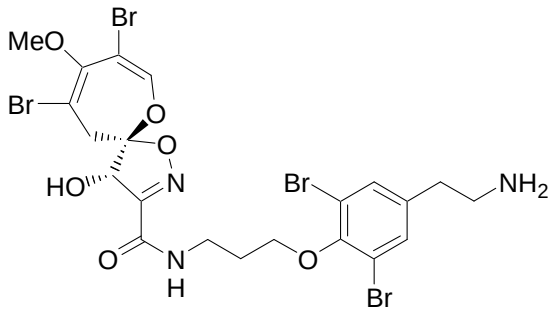

Psammaplysin A

References

(1) Kauffman, C. A. *Curr. Opin. Microbiol*. **2006**, *9*, 483-488.

(2) Lagrou, K.; Verhaegen, J.; Peetermans, W. E.; De Rijdt, T.; Maertens, J.; Van Wijngaerden, E. *Eur. J. Clin. Microbiol. Infect. Dis.* **2007**, *26*, 541-547.

(3) Zaoutis, T. E.; Argon, J.; Chu, J.; Berlin, J. A.; Walsh, T. J.; Feudtner, C. *Clin. Infect. Dis.* **2005**, *41*, 1232-1239.

(4) Pfaller, M. A.; Pappas, P. G.; Wingard, J. R. *Clin. Infect. Dis.* **2006**, *43*, S3-S14.

(5) Mokaddas, E. M.; Al-Sweih, N. A.; Khan, Z. U. *J. Med. Microbiol*. **2007**, *56*, 255-259.

(6) Morgan, J. *Curr. Infect. Dis. Rep.* **2005**, *7*, 429-439.

(7) Jarvis, W. R. *Clin. Infect. Dis.* **1995**, *20*, 1526-1530.

(8) Pfaller, M. A.; Boyken, L.; Hollis, R. J.; Messer, S. A.; Tendolkar, S.; Diekema, D. J. *J. Clin. Microbiol*. **2006**, *44*, 760-763.

(9) Capon, R. J.; Faulkner, D. J. *J. Am. Chem. Soc*. **1984**, *106*, 1819-1822.

(10) Rotem, M.; Carmely, S.; Kashman, Y.; Loya, Y. *Tetrahedron* **1983**, *39*, 667-76.

II.3

Adociasulfate 13, an antifungal merotriterpenoid from the Red Sea sponge *Haliclona* (aka *Adocia*) sp.

Abstract

A new hexaprenoid hydroquinone sulfate, adociasulfate 13, was isolated from the sponge *Haliclona* (aka *Adocia*) sp. collected in the Red Sea. This compound, together with the previously reported adociasulfates 2, 5, and 6, were isolated by tracing their antifungal activities using bioassay guided-fractionation. The structure of adociasulfate 13 was elucidated by interpretation of spectroscopic data. Adociasulfate 13 exhibited significant antifungal activity against amphotericin B-resistant and wild-type strains of *Candida albicans* with MIC values of 4.3 μM.

Keywords: adociasulfate; sponge; marine natural product; merotriterpenoid; antifungal, cancer cell cytotoxicity

Introduction

Merotriterpenoids belong to an uncommon class of metabolites produced by both terrestrial and marine organisms. A wide range of triterpenoid hydroquinone sulfates have been obtained from marine sources, and found to possess remarkable biological activities. Akaterpin, isolated from the marine sponge *Callyspongia* sp., was discovered to be a phosphatidylinositol-specific phospholipase C inhibitor.[1] The shaagrockols, toxicols, and toxiusol from the Red Sea sponge *Toxiclona toxius* were reported to show inhibition against HIV reverse transcriptase.[2-4] In particular, sponges of the genus *Adocia* (order Haplosclerida, family Chalinidae) have been shown to contain an interesting group of biologically active hexaprenoid hydroquinone sulfates, the adociasulfates.[5-10] So far, there were twelve adociasulfates that have been isolated. Adociasulfate 1-6 and 10, isolated from a Palaun sponge, were reported as kinesin motor protein inhibitors.[5,8] In addition, adociasulfates 1, 7 and 8, derived from marine sponge of the same species collected in Australia, were shown to act as inhibitors of the H^+-ATPase proton pump activity.[6]

As part of our program to investigate marine natural products that exhibit selective antifungal activity with no significant cytotoxicity, both the aqueous and organic extracts of 321 sponges and ascidians collected in Palau, the Red Sea, and South Africa were evaluated using both antifungal (*Candida albicans*) and HCT-116 colon carcinoma cytotoxicity assays. The extracts that were found to be effective in fungal inhibition with negligible cytotoxicity were chosen for further examination. Among the most promising candidates from the initial screening was the crude extract of the sponge *Haliclona* (aka *Adocia*) sp. collected in the Red Sea. The partially purified

material showed inhibition against *C. albicans* at a MIC value of 25 μg/mL, whereas no significant activity was observed in the cytotoxic assay (IC_{50} > 78 μg/mL). Using antifungal bioassay guided-fractionation, we isolated a new antifungal merotriterpenoid, adociasulfate 13 (**1**), along with the three known compounds, adociasulfates 2 (**2**), 5 (**3**) and 6 (**4**). This chapter describes the isolation and structural elucidation of **1**, and the biological activities of these four adociasulfates.

Results and Discussion

The sponge (Figure II.3.2), identified as a *Haliclona* sp., was collected by Faulkner group members using scuba in Egyptian waters in the Red Sea in 2000, and the specimen was kept frozen until being processed. The sample (213.1 g) was later defrosted, exhaustively extracted with excess MeOH, and then dried *in vacuo*. The yellow crude extract was first fractionated by partition on HP20SS resin, subsequently eluting with acetone/water mixtures to obtain 20%, 40%, 50%, 60%, 70%, 80% and 100% acetone fractions. The 80% acetone fraction (617 mg), which proved to exhibit the most potent antifungal activity, was further purified by reversed-phase C_{18} HPLC to yield adociasulfate 13 (**1**, 5.4 mg) along with the previously reported compounds, adociasulfates 2, 5, and 6 (1.5 mg, 21 mg, and 4.2 mg, respectively).

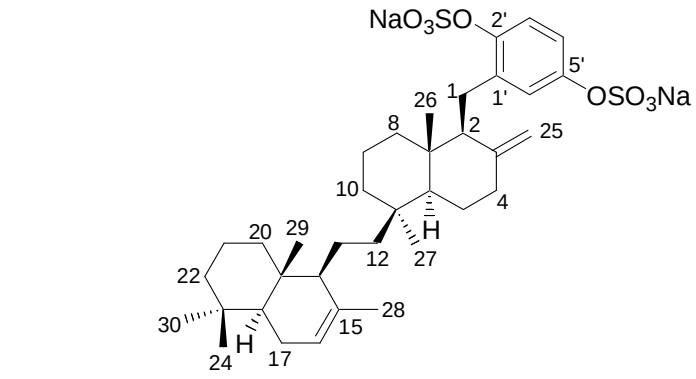

1

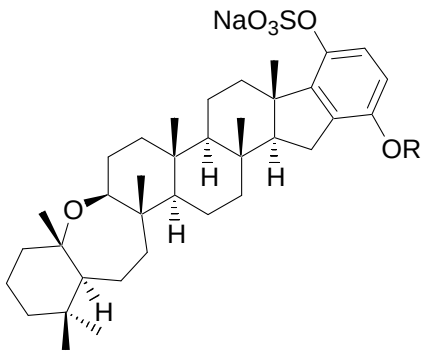

2 R = SO_3Na
4 R = H

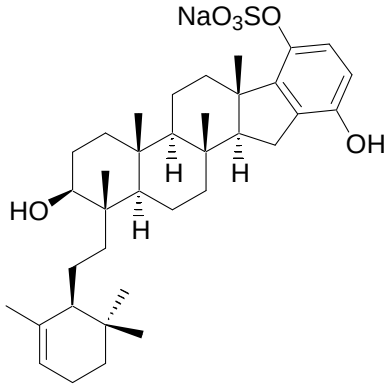

3

Figure II.3.1. The structures of adociasulfates 2 (**2**), 5 (**3**), 6 (**4**), and 13 (**1**)

Figure II.3.2. Photograph of the Red Sea sponge *Haliclona* (aka *Adocia*) sp.

Adociasulfate 13 (**1**) was isolated as an amorphous white solid, which analyzed for the molecular formula $C_{36}H_{52}O_8S_2Na_2$ by analysis of NMR data (Table II.3.1) and high-resolution ESITOFMS data ($[M+Na]^+$ = *m*/*z* 745.2794). The HRMS spectrum also showed ions that analyzed for $[M–Na]^–$ at *m*/*z* 699.2998 which suggested the presence of two sodium sulfate ester groups in this compound. Furthermore, analysis of the IR spectroscopic data showed strong broad absorption bands at 1269 cm^{-1} and 1042 cm^{-1}, both of which supported the presence of sulfate groups. The molecular formula of **1**, which required ten degrees of unsaturation, were assigned to an aromatic ring and two olefinic bonds by interpretation of ^{13}C NMR data, which revealed 26 aliphatic and 10 aromatic/olefinic carbons. Based upon this initial analysis of ^{13}C NMR data, the additional four degrees of unsaturation suggested the presence of a tetracyclic ring system connected to an aromatic ring. The overall data, and considering the source, suggested the tetracyclic ring system was of a terpenoid origin.

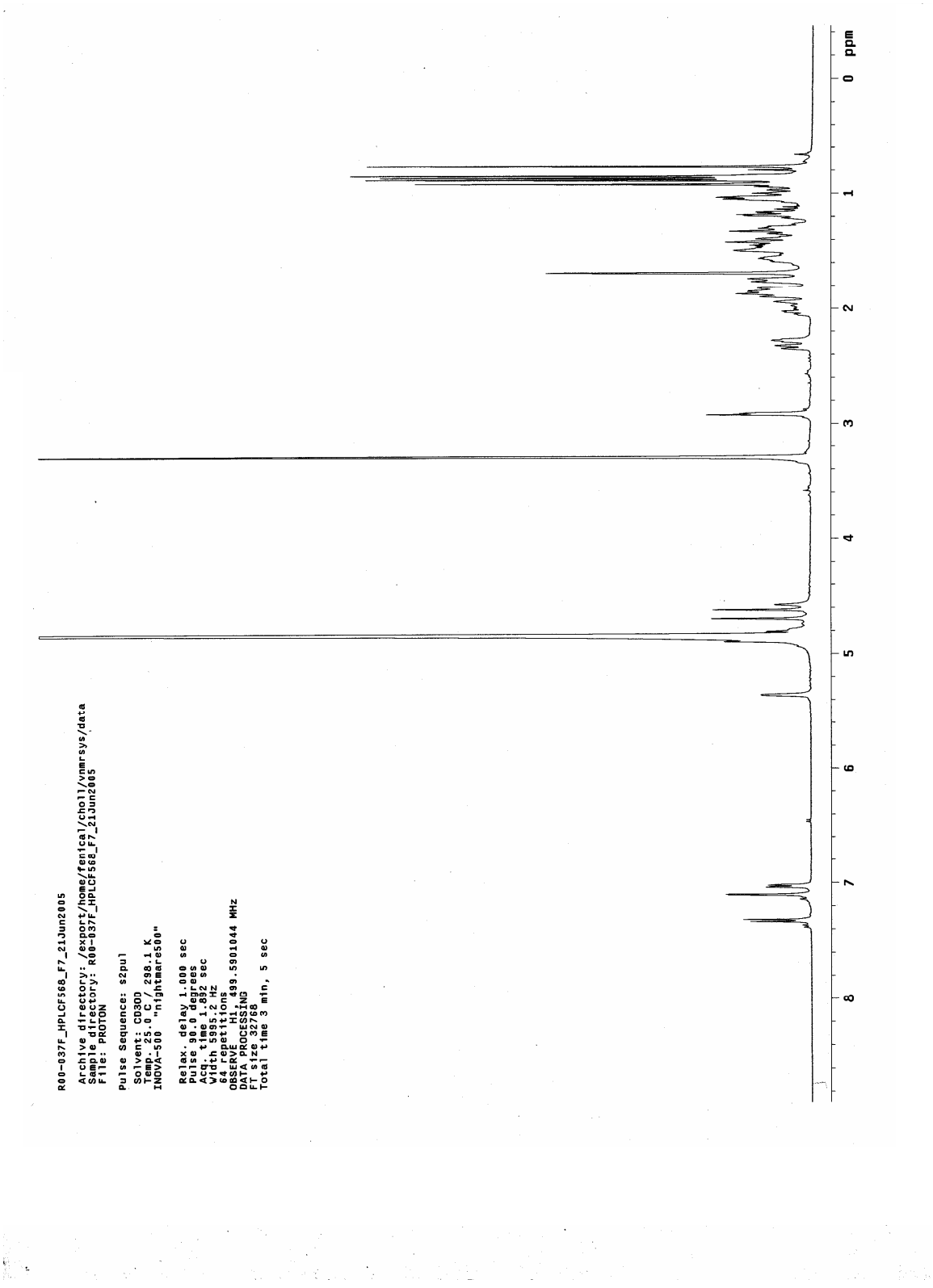

Figure II.3.3. ^{1}H NMR spectrum of adociasulfate 13 (**1**) (500 MHz, CD_3OD)

Table II.3.1. ^{1}H, ^{13}C, COSY, HMBC and ROESY NMR spectroscopic data (500 MHz, MeOH-d_4) for adociasulfate 13 (**1**)

C#	δ_C		δ_H	*J* (Hz)	COSY	HMBC	ROESY
1	25.1	CH_2	2.92 brd	6.5	2	C-1′, C-2′, C-2, C-3, C-6′, C-7	6′, 8a, 25a, 26
2	57.4	CH	2.28 brt	6.5	1	C-1′, C-1, C-3, C-7, C-25, C-26	4b, 6, 6′
3	149.1	C					
4a	39.4	CH_2	2.34 brtd	12.5	4b, 5b	C-2, C-5	5a, 5b, 25b
b			2.03 brd	5, 12.5	4a, 5a	C-3, C-5, C-25	2, 6
5a	25.5	CH_2	1.76 m		4b, 5b	C-6, C-7	4a, 27
b			1.43 m		4a, 5a, 6	C-6, C-4	4a, 26
6	59.1	CH	1.33 m		5b	C-5, C-7, C-10, C-26	2, 4b, 27
7	41.1	C					
8a	40.4	CH_2	1.88 m		8b		1
b			1.29 m		8a	C-26	2
9	20.6	CH_2	1.49 m				10b, 26
10a	38.5	CH_2	1.74 m		10b	C-8, C-27	
b			1.03 m		10a	C-12	9
11	38.3	C					
12a	37.1	CH_2	1.86 m		12b, 13a	C-27	26
b			1.04 m		12a	C-27	14
13a	22.9	CH_2	1.35 m		12a, 13b	C-12, C-14	20a, 27, 29
b			1.06 m		13a, 14		28, 29
14	57.3	CH	1.49 m		13b		12b, 18, 20b
15	136.5	C					
16	123.0	CH	5.36 m		17a, 28		17a, 28
17a	24.9	CH_2	1.95 m		16, 17b, 18		16, 18, 30
b			1.87 m		17a, 18		24, 29
18	51.6	CH	1.18 m		17a, 17b	C-14, C-17, C-19, C-23, C-24, C-29, C-30	14, 20b, 30
19	38.2	C					
20a	40.4	CH_2	1.83 m		20b		13a
b			0.97 m		20a	C-29	14, 18, 22b
21	19.8	CH_2	1.44 m				
22a	43.5	CH_2	1.41 m		22b	C-18, C-23	
b			1.19 m		22a	C-24	20b
23	33.9	C					
24	22.3	CH_3	0.89 s			C-18, C-22, C-23, C-30	17b, 29
25a	108.8	CH_2	4.62 brs			C-2, C-3, C-4	1, 6′
b			4.70 brs			C-2, C-4	4a
26	16.1	CH_3	0.87 s			C-2, C-6, C-7, C-8	1, 5b, 9, 12a, 28
27	29.9	CH_3	0.92 s			C-6, C-10, C-11, C-12	5a, 6, 13a
28	22.6	CH_3	1.69 s		16	C-14, C-15, C-16	13b, 16, 26
29	14.1	CH_3	0.77 s			C-14, C-18, C-19, C-20	13a, 17b, 20a, 24
30	33.7	CH_3	0.85 s			C-18, C-22, C-23, C-24	17a, 18
1′	137.6	C					
2′	149.0	C					
3′	123.1	CH	7.33 d	8.5	4′	C-1′, C-2′, C-5′	4′
4′	119.8	CH	7.03 dd	8.5, 2.5	3′	C-2′, C-5′, C-6′	3′
5′	150.5	C					
6′	123.4	CH	7.11 d	2.5		C-1, C-2′, C-4′, C-5′	1, 2, 25a

The ^{1}H NMR spectrum of adociasulfate 13 (**1**) measured in CD_3OD (Figure II.3.3) illustrated three aromatic proton signals at δ 7.33 (1H, d, *J* = 8.5 Hz), 7.11 (1H, d, *J* = 2.5 Hz) and 7.03 (1H, dd, *J* = 8.5, 2.5 Hz) that corresponded to HSQC correlations of aromatic carbon signals at δ 123.4 (C-6′), 123.1 (C-3′) and δ 119.8 (C-4′), respectively. The position of the sulfate ester groups at C-2′ and C-5′ was assigned by analysis of COSY and HMBC NMR spectral data. HMBC correlations (Figure II.3.4) of the aromatic proton signals to the carbons at δ 150.5 (C-5′), 149.0 (C-2′), 137.6 (C-1′), 123.4 (C-6′), 123.1 (C-3′) and δ 119.8 (C-4′), defined the substitution pattern of the aromatic ring to be 1-alkyl-2,5-disulfate. The methylene proton H-1 (δ 2.92) showed HMBC correlations to C-1′, C-2′, and C-6′, which confirmed the alkyl substitution at C-1′.

The framework of the C/D decalin ring system and its connection to the aromatic moiety were established by HMBC, COSY and TOCSY correlations. HMBC correlations from two methyl signals, Me-26 (δ 0.87) to C-2, C-6, C-7, C-8, and Me-27 (δ 0.92) to C-6, C-10, C-11, were used to assemble a major part of the C/D rings. The exocyclic olefinic methylene protons (H-25) at δ 4.62 and 4.70 showed correlations to C-2, C-3, and C-4. The connection of methylene signal at δ 2.92 to the methine carbon at C-2 was confirmed by a COSY correlation between H-1 (δ 2.92) and H-2 (δ 2.28). A three-bond HMBC correlation from the methine signal at H-2 to C-1′, further supported the connection from methylene carbon at C-1 to C-1′ position on the aromatic ring. The ethyl linkage that connected the A/B and C/D decalin ring

systems was established from COSY correlations of methylene group between H-12/H-13, and H-13/H-14, as well as from HMBC correlations from Me-27 to C-12.

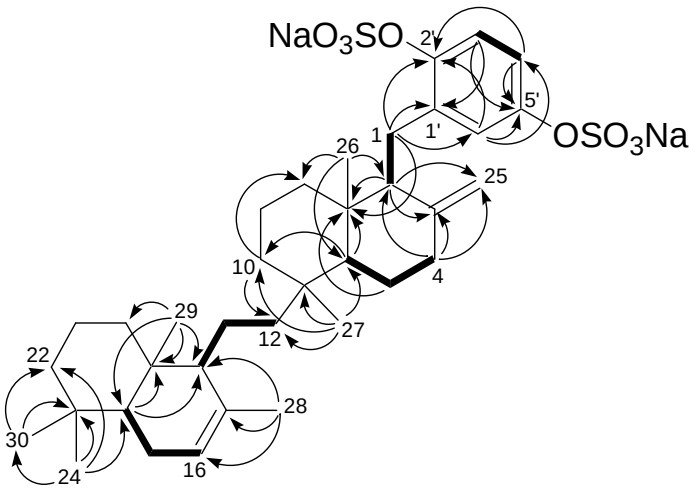

Figure II.3.4. Selected COSY (bold lines) and HMBC (arrows) correlations observed in the NMR spectra for **1**.

Likewise, HMBC and COSY correlations allow the major portion of the A/B decalin ring system, including the trisubstituted double bond, to be established. The planar structure of the A/B rings was defined using HMBC correlations from Me-28 (δ 1.69) to C-14, C-15, and C-16, from Me-29 (δ 0.77) to C-14, C-18, C-19, and C-20, as well as from Me-24 (δ 0.89) and Me-30 (δ 0.85) to C-18, C-22, and C-23. The location of double bond was confirmed by COSY correlations between H-16 and H-17, and from HMBC correlations of Me-28 to the quaternary carbon at C-15 (δ 136.5) and olefinic methine carbon at C-16 (δ 123.0). TOCSY correlations were used to

confirm the connectivity of C-5/C-6/C-7 and C-20/C-21/C-22, thus allowing the complete assignment of both decalin rings.

The relative stereochemistry of adociasulfate 13 (**1**) was determined by interpretation of ROESY NMR data that showed correlations as indicated in Figure II.3.5. The benzyl chain and Me-27 were found to be in equatorial positions, while the ethyl bridge that linked the two decalin ring systems was attached in an axial position to the C ring. This geometry was confirmed by ROESY correlations from the axial Me-26 to H-1, H-5b, H-9, and H-12a, and also from methine signal at H-6 (δ 1.33) to Me-27, H-2, and H-4b. These correlations suggested the C/D rings were *trans*-fused. The exocyclic olefinic methylene protons at δ 4.62 showed ROESY correlations to an aromatic proton at δ 7.11 and a methylene proton at δ 2.92, providing further evidence that the benzyl chain was positioned in an equatorial position.

In a similar way, the *trans*-fused nature of the A/B ring system was established by ROESY correlations from Me-29 to Me-24 and H-17b, and from H-18 (δ 1.18) to Me-30 and H-20b. The ethyl linkage C-12/C-13 was placed in an equatorial position next to C-14 on the basis of a ROESY correlation between Me-29 and H-13a. The *cis*-configuration of double bond at C-15–C-16 was determined by ROESY correlations between H-16 and Me-28. The assignment of relative stereochemistry was quite difficult due to highly overlapped signals of aliphatic protons, in particular, the signals between two decalin rings system A/B and C/D. Nevertheless, the observed ROESY correlations from the methine proton at H-14 to H-12b, and from Me-26 to Me-28 and H-12a, allow the relative stereochemistry between two decalin rings to be established.

The relative stereochemistry of adociasulfate 13 (**1**) can therefore be assigned as (2*R**, 6*S**, 7*S**, 11*R**, 14*S**, 18*S**, 19*S**).

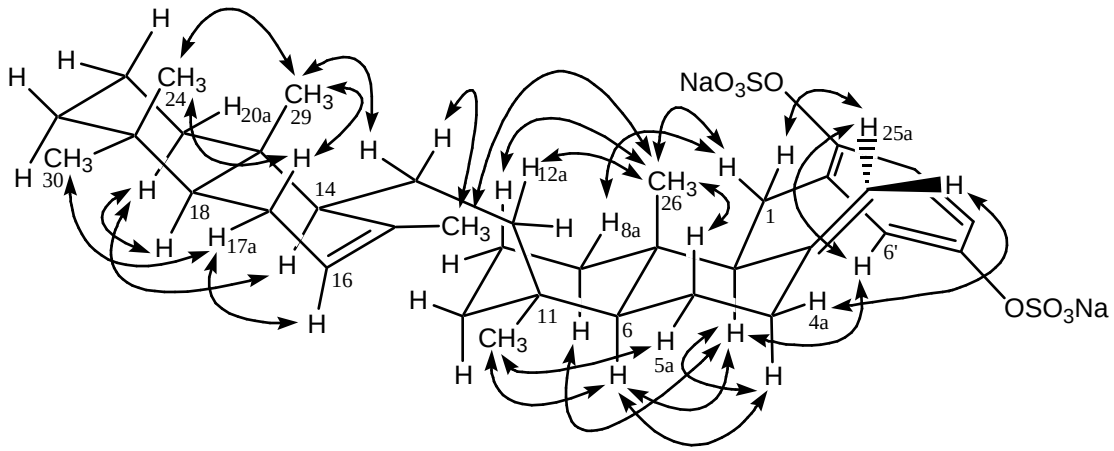

Figure II.3.5. Assigned relative stereochemistry of **1** established by selected ROESY correlations.

In addition to the previously reported bioactivities of the adociasulfates, the newly derived adociasulfate 13 (**1**), along with three known adociasulfates 2, 5, and 6, are reported here to possess antifungal activities against the pathogenic fungus, *C. albicans*. In this study, all isolated adociasulfates were evaluated for their inhibitions against both wild-type and amphotericin B-resistant strains of *C. albicans.* Cytotoxic activities against the HCT-116 human colon tumor cell line were also determined. The results are illustrated in Table II.3.2.

Table II.3.2. Antifungal and Cytotoxic Activities of **1-4**

compound	HCT-116 inhibition IC_{50} (μg/mL)	*C. albicans* (WT) MIC (μg/mL)	*C. albicans* (AmBR) MIC (μg/mL)
1	> 39.5	3.1	3.1
2	> 78	31.3	31.3
3	> 78	250	250
4	16.2	250	250

Among all derived adociasulfates, the newly isolated adociasulfate 13 (**1**) was found to exhibit the most potent antifungal activity against *C. albicans* at 3.1 μg/mL (4.3 μM). Despite structural similarities between adociasulfates 2 and 6, they exhibited different biological activities. Adociasulfate 2 (**2**) was more active in fungal inhibition with a moderate MIC value of 31.3 μg/mL, while the compound was much less cytotoxic in the HCT-116 assay. The presence of a hydroxyl group instead of a sulfate ester in adociasulfate 6 (**4**) seemed to drastically decrease inhibitory activities in the antifungal assay. Adociasulfate 5 (**3**) and 6, both of which possess a single sulfate group, showed very weak inhibition of *C. albicans* with MIC values of 250 μg/mL. According to the results from HCT-116 assays, all isolated adociasulfates exhibited weak or insignificant cytotoxic activities, hence, the selectivitiy of adociasulfate 13 (**1**) toward fungal inhibition has been demonstrated.

Most active antifungal metabolites isolated from marine invertebrates are found to express a similar level of cytotoxic activities in the mammalian cancer cell, HCT-116 assay. Adociasulfate 13 (**1**), however, is one of very few marine natural products that possess potent antifungal activities with negligible cytotoxicity.

Experimental Section

General Experimental Procedures. Optical rotations were measured on a Rudolph Autopol III polarimeter. UV spectra were obtained using Varian Cary 50 Bio UV-Visible spectrophotometer. Infrared spectra were recorded on a Nicolet IR100 FT-IR spectrometer. ^{1}H, ^{13}C, COSY, HSQC, HMBC, and ROESY NMR spectra were recorded on a Varian INOVA 500 MHz spectrometer. High-resolution mass measurements were obtained on Agilent ESI-TOF instruments at the Scripps Research Institute, La Jolla. All solvents were distilled prior to being used.

Biological material. The sponge *Haliclona* sp. was collected by hand using scuba at Red Sea, in 2000. The specimen was immediately frozen after collection and stored at –20 °C until extracted. The color in life is purple and the sponge was assigned as *Haliclona* sp. (order Haplosclerida, family Chalinidae). The sponge, which was identified by Mary Kay Harper, was previously known as an *Adocia* sp. A voucher specimen has been deposited at the University of Utah, Sponge Voucher Collection.

Extraction and isolation. The sponge (213.1g wet weight) was extracted with methanol (4 × 500 mL) for 24 h. The pale yellow extracts were combined and dried *in vacuo* to obtain a crude brown extract, which was fractionated by HP20SS column chromatography (acetone/water) to yield nine fractions. All nine fractions were concentrated to dryness and tested in a standard microdilution antifungal assay. The fraction eluted with 80% acetone-water (617 mg) was found to possess promising antifungal activity (MIC = 12.5 μg/mL), and was subjected to further purification on

reversed-phase HPLC (Dynamax C_{18} semi-preparative, 3 mL/min; 70–80% MeOH/H_2O over 25 min, 80–100% MeOH/H_2O over 15 min) to yield, in order of elution, adociasulfate 2 (**2**, 1.5 mg), adociasulfate 5 (**3**, 21 mg), adociasulfate 6 (**4**, 4.2 mg), and adociasulfate 13 (**1**, 5.4 mg, 2.5×10^{-3} % wet weight).

Adociasulfate 13 (**1**): white amorphous solid; $[\alpha]_D$ – 6.0 (*c* 0.07, MeOH); UV (MeOH) λ_{max} (log ε) 270 nm (2.05); IR ν_{max} (KBr) 2923, 1732, 1648, 1269, 1042, 849 cm^{-1}; NMR data, see Table II.3.1 ; EIMS $[M+Na]^+$ *m*/*z* 745; HRESITOFMS $[M+Na]^+$ *m*/*z* 745.2794 (calcd for $C_{36}H_{52}O_8S_2Na_3$, 745.2797), $[M–Na]^–$ *m*/*z* 699.2998 (calcd for $C_{36}H_{52}O_8S_2Na$, 699.3001).

Antifungal assay with *C. albicans*. The *C. albicans* strains ATCC 32354 (wild type) and ATCC 90873 (amphotericin B-resistant) were purchased from the American Type Culture Collection (ATCC). Inhibitory activity was determined by a standard microdilution liquid antifungal assay. *C. albicans* was incubated overnight at 37 °C in RPMI 1640 media (GibcoBRL) and aliquots transferred to 96-well plates the next day. The indicator Alamar Blue was added to the *C. albicans* culture before they were transferred to the plates. Samples were added along with Amphotericin B (Sigma) and DMSO (solvent) as positive and negative controls respectively, and serially diluted. The plates were then incubated overnight for 14-16 h. Minimum inhibitory concentration (MIC) values were determined by the change in color from blue to pink of the media according to the indicator.

Human colon tumor (HCT-116) cytotoxicity assay. Aliquot samples of HCT-116 human colon adenocarcinoma cells were transferred to 96-well plates and incubated overnight at 37 °C in 5% CO_2/air. Test compounds were added to the plates in DMSO and serially diluted. The plates were then further incubated for another 72 h, and at the end of this period, a CellTiter 96 Aq_{ueous} non-radioactive cell proliferation assay (Promega) was used to assess cell viability. Inhibition concentration (IC_{50}) values were deduced from the bioreduction of MTS/PMS by living cells into a formazan product. MTS/PMS was first applied to the sample wells, followed by incubation for 3 h. Etoposide (Sigma) and DMSO (solvent) were used as the positive and negative controls in this assay. The quantity of the formazan product (in proportion to the number of living cells) in each well was determined by the Molecular Devices Emax microplate reader set to 490 nm wavelength. IC_{50} values were calculated using the analysis program, SOFTMax.

References

(1) Fukami, A.; Ikeda, Y.; Kondo, S.; Naganawa, H.; Takeuchi, T.; Furuya, S.; Hirabayashi, Y.; Shimoike, K.; Hosaka, S.; Watanabe, Y.; Umezawa, K. *Tetrahedron Lett*. **1997**, *38*, 1201-1202.

(2) Issacs, S.; Kashman, Y. *Tetrahedron Lett*. **1992**, *33*, 2227-2230.

(3) Issacs, S.; Hizi, A.; Kashman, Y. *Tetrahedron* **1993**, *49*, 4275-4282.

(4) Loya, S.; Tal, R.; Hizi, A.; Issacs, S.; Kashman, Y.; Loya, Y. *J. Nat. Prod*. **1993**, *56*, 2120-2125.

(5) Blackburn, C. L.; Hopmann, C.; Sakowicz, R.; Berdelis, M. S.; Goldstein, L. S. B.; Faulkner, D. J. *J. Org. Chem.* **1999**, *64*, 5565-5570.

(6) Kalaitzis, J. A.; de Almeida Leone, P.; Harris, L.; Butler, M. S.; Ngo, A.; Hooper, J. N. A.; Quinn, R. J. *J. Org. Chem*. **1999**, *64*, 5571-5574.

(7) Kalaitzis, J. A.; Quinn, R. J. *J. Nat. Prod*. **1999**, *62*, 1682-1684.

(8) Blackburn, C. L.; Faulkner, D. J. *Tetrahedron* **2000**, *56*, 8429-8432.

(9) Sakowicz, R.; Berdelis, M. S.; Ray, K.; Blackburn, C. L.; Hopmann, C.; Faulkner, D. J.; Goldstein, L. S. B. *Science* **1998**, *280*, 292-295.

(10) West, L. M.; Faulkner, D. J. *J. Nat. Prod*. **2006**, *69*, 1001-1004.

Acknowledgements

The text of II.3, in full, is the manuscript to be submitted to an academic journal as it appears in Boonlarppradab, C.; Faulkner, D. J. Adociasulfate 13, an antifungal merotriterpenoid from the Red Sea sponge *Haliclona* (aka *Adocia*) sp. The dissertation author was the primary author and directed and supervised the research, which forms the basis for this chapter.

II.4

Eurysterols A and B, cytotoxic and antifungal steroidal sulfates from a marine sponge of the genus *Euryspongia*

Abstract

Two new steroidal sulfates, eurysterols A (**1**) and B (**2**), were isolated from an undescribed marine sponge of the genus *Euryspongia* collected by Faulkner group members in Palau. The structures of the new compounds were assigned by NMR spectroscopic data interpretation. Compounds **1** and **2** showed cytotoxicity against human colon carcinoma (HCT-116) cells with IC_{50} values of 2.9 μg/mL and 14.3 μg/mL, respectively, and exhibited antifungal activity against amphotericin B-resistant and wild-type strains of *Candida albicans* with MIC values, in turn, of 15.6 μg/mL and 62.5 μg/mL.

Introduction

Sponges of the genus *Euryspongia* (order Dictyoceratida, family Dysideidae) have been shown to contain various types of secondary metabolites, including secosteroids,[1] hydroquinones,[2] sesquiterpene quinones,[3] and furanoterpenoids.[4,5] As part of an interest in the discovery of antifungal and cytotoxic natural products, we examined a cytotoxic crude methanol extract of a previously undescribed sponge of the genus *Euryspongia* collected in Palau. Using cytotoxicity against HCT-116 human colon carcinoma cells as a guide, two new moderately cytotoxic steroidal sulfates, eurysterols A (**1**) and B (**2**), were isolated. In this paper, we describe the isolation, structure elucidation, and biological activities of these new steroidal sulfates.

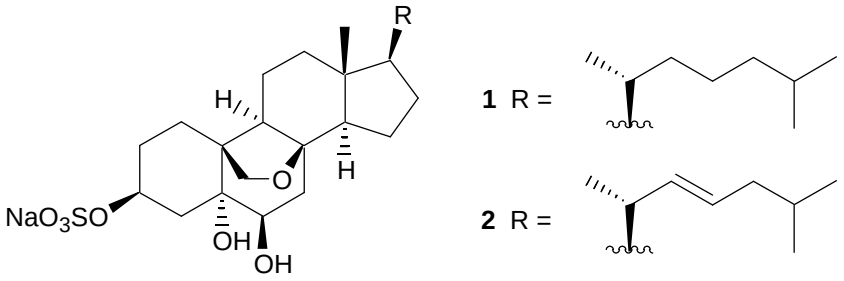

Figure II.4.1. The structures of eurysterols A (**1**) and B (**2**)

Results and Discussion

The *Euryspongia* sp. sponge was collected by hand using scuba at a depth of 37 m from a reef slope, west of the lighthouse at Koror, Palau. The frozen sample (187.6 g) was defrosted and extracted exhaustively with MeOH. The MeOH extract was then dried *in vacuo* and the extract was fractionated by partition on HP20SS resin, subsequently eluting with acetone/water mixtures to obtain 20%, 40%, 60%, 80%, and 100% acetone fractions. The 60% acetone fraction (64.1 mg), which contained all of the antifungal and cytotoxic activity, was further fractionated by reversed-phase C_{18} HPLC to yield eurysterols A (**1**, 5.5 mg) and B (**2**, 2.1 mg).

The molecular formula for eurysterol A (**1**) was determined as $C_{27}H_{45}O_7SNa$ by high-resolution MALDIFTMS (*m*/*z* 559.2688, $[M+Na]^+$) and from its NMR data. The LRMS spectra showed ions that analyzed for $[M–Na]^–$ and $[2M–Na]^–$ at *m*/*z* 513 and 1049, which suggested the presence of Na in this polar compound. Initial analysis by ^1H and ^{13}C NMR methods, including interpretation of the DEPT and HSQC spectroscopic data, revealed that the molecule **1** is steroidal. Analysis of the IR spectroscopic data showed a broad absorption bands at 1216 cm^{-1} and 1072 cm^{-1}, both of which suggested the presence of a sulfate group.[6]

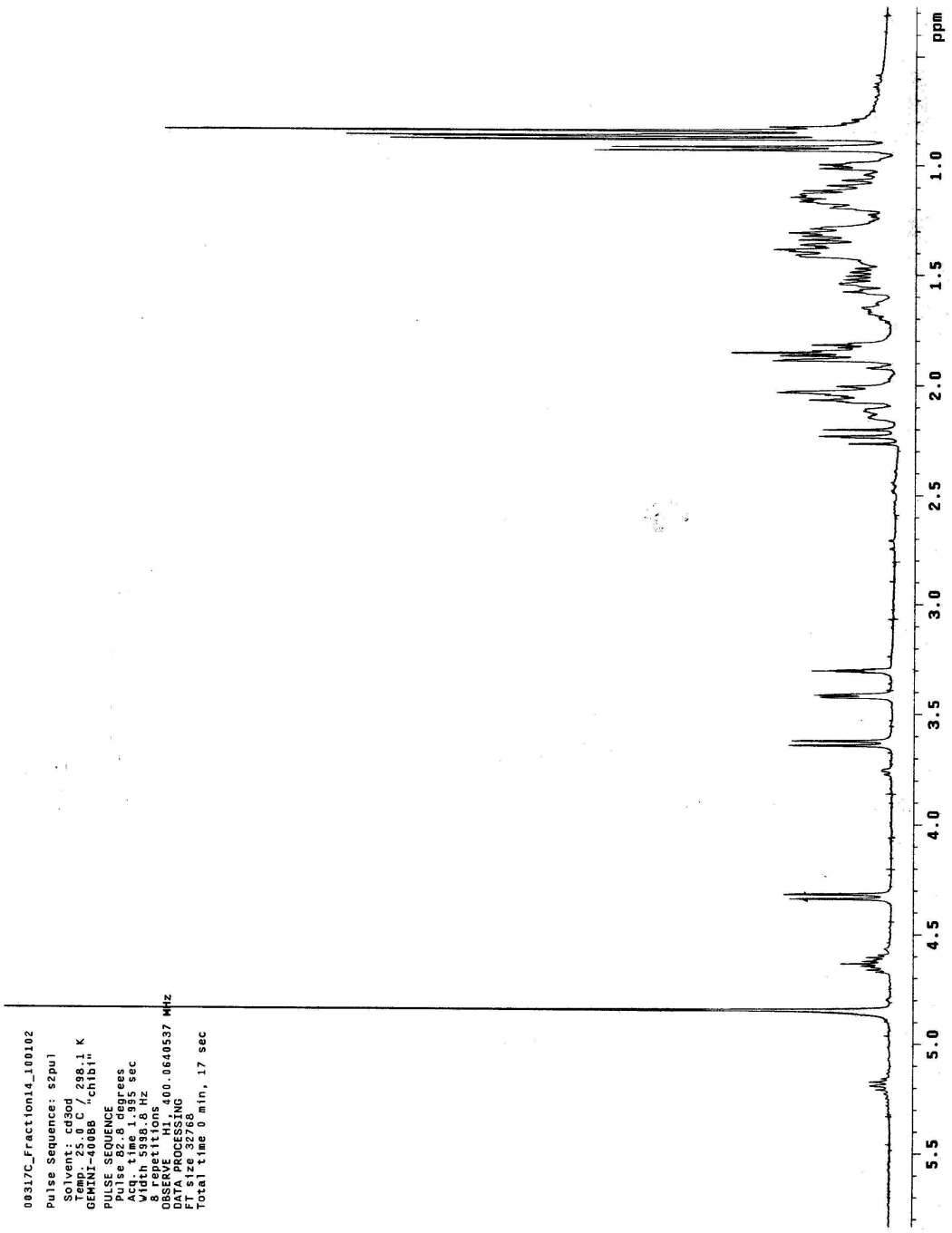

Figure II.4.2. ^{1}H NMR spectrum of eurysterol A (**1**) (500 MHz, CD_3OD)

Table II.4.1. ^{1}H, ^{13}C, COSY and HMBC NMR spectroscopic data (CD_3OD) for eurysterol A (**1**)

C#	δ_C		δ_H	*J* (Hz)	COSY	HMBC
1α	26.4	CH_2	1.85 m		2α, 2β	C-2, C-5, C-10
β			1.56 m		2α, 2β	C-2
2α	31.8	CH_2	2.13 m		1α, 1β, 3	C-10
β			1.18 m		1β	C-4
3	76.6	CH	4.63 tt	11.6, 4.4	2α, 4α, 4β	
4α	39.9	CH_2	2.05 m		3	C-2, C-3, C-10
β			2.23 dd	13.6, 11.6	3	C-2, C-3
5	77.3	C				
6	75.6	CH	3.42 dd	4.0	7α, 7β	C-5, C-7, C-8, C-10
7α	42.6	CH_2	1.87 m		6	C-5, C-6, C-8, C-9
β			1.87 m		6	C-5, C-6, C-8, C-9
8	85.5	C				
9	46.5	CH	2.03 m		11α, 11β	C-10, C-11, C-19
10	50.3	C				
11α	21.6	CH_2	1.39 m		9, 12α, 12β	C-10
β			1.41 m		9, 12α, 12β	C-8, C-9
12α	40.0	CH_2	1.14 m		11α, 11β	C-11
β			2.04 m		11α, 11β	C-9, C-14
13	42.8	C				
14	54.8	CH	1.32 m		15α, 15β	C-8, C-13, C-18
15α	21.6	CH_2	1.66 m		14, 16β	C-13, C-14, C-16
β			1.49 m		14, 16α	C-8, C-14
16α	28.8	CH_2	1.87 m		15β	C-14, C-15
β			1.30 m		15α, 17	C-15, C-17
17	57.8	CH	1.09 m		16β, 20	C-12, C-13, C-18, C-20
18	12.6	CH_3	0.84 s			C-12, C-13, C-14, C-17
19a	72.2	CH_2	3.63 d	8.4		C-1, C-5, C-10
b			4.33 d	8.4		C-5, C-8, C-9, C-10
20	36.7	CH	1.39 m		17, 21	C-21, C-22
21	19.3	CH_3	0.92 d	6.4	20	C-17, C-20, C-22
22	37.2	CH_2	1.01 m		23	C-17
23	25.0	CH_2	1.37 m		22, 24	C-22
24	40.7	CH_2	1.14 m		23, 25	C-26, C-27
25	29.2	CH	1.52 m		26, 27	C-23, C-24, C-26, C-27
26	23.0	CH_3	0.87 d	6.4	25	C-24, C-25, C-27
27	23.2	CH_3	0.87 d	6.4	25	C-24, C-25, C-26

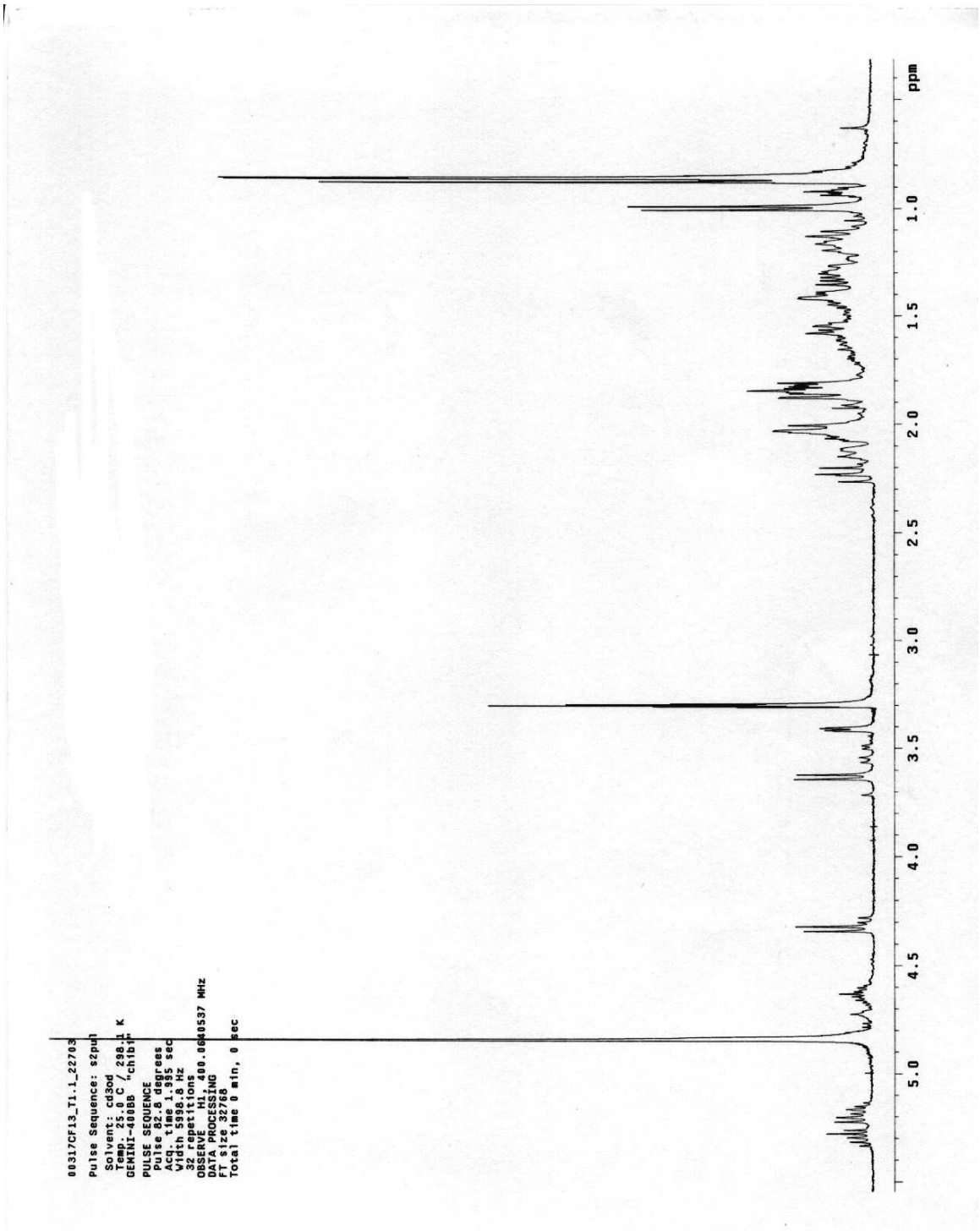

Figure II.4.3. ^{1}H NMR spectrum of eurysterol B (**2**) (500 MHz, CD_3OD)

Table II.4.2. ^{1}H, ^{13}C, COSY and HMBC NMR spectroscopic data (CD_3OD) for eurysterol B (**2**)

C#	δ_C		δ_H		COSY	HMBC
1α	26.4	CH_2	1.86 m		2α, 2β	C-5, C-10
β			1.56 m		2α, 2β	
2α	31.8	CH_2	2.13 m		1α, 1β, 3	
β			1.18 m		1α, 1β	
3	76.6	CH	4.63 tt	11.6, 4.4	2α, 4α, 4β	
4α	39.9	CH_2	2.04 m		3	C-2, C-3
β			2.23 dd	13.6, 11.6	3	C-3
5	77.4	C				
6	75.6	CH	3.41 dd	4.0	7α, 7β	
7α	42.6	CH_2	1.87 m		6	C-5, C-6, C-8, C-9
β			1.87 m		6	C-5, C-6, C-8, C-9
8	85.5	C				
9	46.6	CH	2.02 m		11α, 11β	C-10, C-19
10	50.3	C				
11α	21.6	CH_2	1.39 m		9, 12α, 12β	C-12
β			1.42 m		9, 12α, 12β	C-12
12α	40.0	CH_2	1.17 m		11α, 11β	C-18
β			2.03 m		11α, 11β	
13	42.7	C				
14	54.9	CH	1.34 m		15α, 15β	C-13, C-15, C-18
15α	21.6	CH_2	1.62 m		14, 16β	C-13
β			1.49 m		14, 16α	
16α	29.3	CH_2	1.69 m		15β, 17	
β			1.27 m			C-17
17	57.6	CH	1.13 m		16α, 20	C-13
18	12.8	CH_3	0.85 s			C-12, C-13, C-14, C-17
19a	72.2	CH_2	3.63 d	8.4		C-1, C-5, C-10
b			4.33 d	8.4		C-5, C-8, C-9
20	41.2	CH	2.03		17, 21	
21	21.4	CH_3	1.00 d	6.8	20	C-17, C-20, C-22
22	139.1	CH	5.20 dd	15.2, 8.4	23	C-20, C-24
23	127.4	CH	5.30 dt	15.2, 6.8	22, 24	C-20, C-24
24	43.1	CH_2	1.83 m		23, 25	C-22, C-23, C-25, C-26, C-27
25	29.8	CH	1.57 m		24, 26, 27	C-26, C-27
26	22.7	CH_3	0.87 d	6.8	25	C-24, C-25, C-27
27	22.8	CH_3	0.87 d	6.8	25	C-24, C-25, C-26

The ^{1}H NMR spectrum of **1** (Figure II.4.2) measured in CD_3OD (Table II.4.1) demonstrated three methyl signals [δ 0.84 (3H, s), 0.87 (6H, d, *J* = 6.4 Hz), and 0.92 (3H, d, *J* = 6.4 Hz)]. A portion of the side chain of the molecule was assembled by analysis of HMBC correlations (Figure II.4.4) from two methyl signals at δ 0.87 and 0.92 (Me-21 to C-17, C-20, C-22; Me-26 and 27 to C-24, C-25). Oxygenation at C-3 (δ 76.6), C-5 (δ 77.3), and C-6 (δ 75.6) in rings A and B was deduced from the ^{13}C NMR chemical shifts, which were in the downfield region. A sulfate group was placed at C-3 on the basis of the low-field resonance of H-3 (δ 4.63) and C-3 (δ 76.6).

The major part of a tetracyclic steroidal backbone could be assembled through the interpretation of COSY, HMBC, and HSQC-TOCSY NMR correlations. Analysis of the COSY and HSQC-TOCSY data allowed the assignment of the C-1/C-2/C-3/C-4, C-6/C-7, C-9/C-11/C-12, and C-17/C-20/C-21/C-22/C-23/C-24/C-25/C-26/C-27 connectivities. Interpretation of the HSQC and HMBC NMR data suggested that an ether bridge was present involving the A-ring bridgehead methyl group and C-8. HMBC correlations from H-19a to C-1, C-5, C-10 and from H-19b to C-5, C-8, C-9, C-10 supported this assignment. The carbon ring skeleton borne by **1** was previously known from the literature. The main steroidal skeleton is similar to abscisterol D, which has been isolated from *Cryptosporiopsis abietina* and found to be useful as a herbicide.[7]

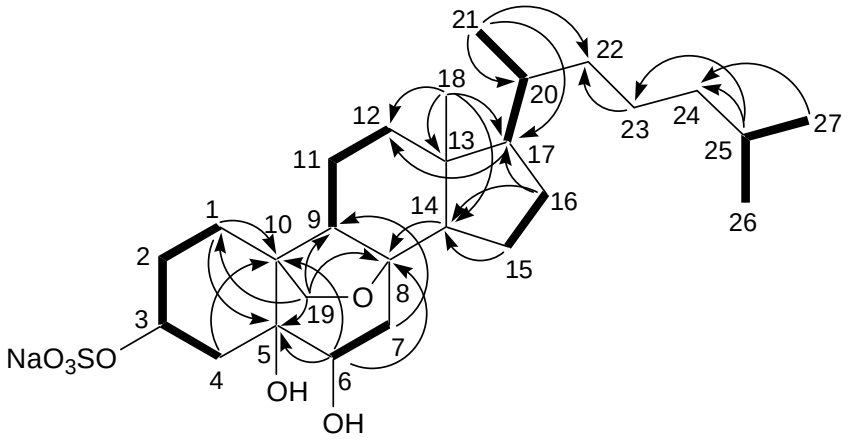

Figure II.4.4. Selected COSY (bold lines) and HMBC (arrows) NMR correlations observed for **1**.

The relative stereochemistry of the 3β-sulfate, 5α-hydroxyl, and 6β-hydroxyl groups in **1** was determined by interpretation of the ROESY NMR spectroscopic data and by analysis of vicinal coupling constants. Protons H-3α (δ 4.63) and H-4β (δ 2.23) were both placed in axial positions based upon their large vicinal coupling constant, $J_{3,4}$ = 11.6 Hz. This configuration was also confirmed by ROESY NMR spectroscopic correlations (Figure II.4.5) between H-3α and H-1α (δ 1.85), and between H-4β and H-19b (δ 4.33). The stereochemistry of the 6β-hydroxyl group was established by a ROESY correlation between H-6α (δ 3.42) and H-4α (δ 2.05). The assignment of stereochemistry at C-20 as *R** was indicated by ROESY correlations from Me-21 to H-12β and H-12α. Hence, the structure of eurysterol A (**1**) was elucidated as 5α-cholestan-8,19-epoxy-3β,5,6β-triol-3-sulfate.

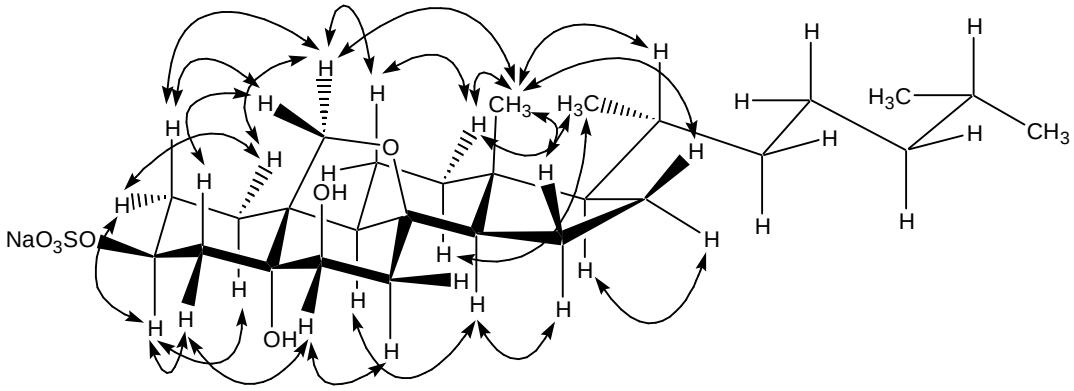

Figure II.4.5. Assigned relative stereochemistry of **1** from selected ROESY NMR correlations**.**

The structure of eurysterol B (**2**) was also elucidated on the basis of the interpretation of its 2D NMR data. The correlation patterns of the COSY and HMBC NMR spectroscopic data (Table II.4.2) were found to be similar to **1**. A molecular formula of $C_{27}H_{43}O_7SNa$ for **2** was established by HRESITOFMS (*m*/*z* 557.2523, $[M+Na]^+$) and only differed from **1** by having one additional degree of unsaturation. The ^1H NMR spectrum of **2** (Figure II.4.3) was almost superimposable on that of **1** except for the presence of the two additional olefinic proton signals at δ 5.20 and 5.30, respectively. The geometry of the double bond was established as *trans* on the basis of an observed vicinal coupling constant of 15.2 Hz. HSQC and HMBC NMR correlation data indicated the exact position of the double bond at C-22 and C-23 in the steroidal side chain. Therefore, eurysterol B (**2**) was defined as (22*E*)-5α-cholest-22-en-8,19-epoxy-3β,5,6β-triol-3-sulfate.

Marine organisms such as sponges and starfish are often found to contain sulfated secondary metabolites. Among these, a group of steroidal sulfates derived from marine sponges has been shown to exhibit diverse biological activities including anticancer,[8] antiviral,[9] antifungal,[10] antibacterial,[11] HIV-inhibition,[12] and antifouling effects.[13] Several of these compounds were also discovered to possess selective inhibitory activities against the specific cellular targets in significant cellular pathways, such as halistanol sulfate and sokostrasterol sulfate, which were identified as inhibitors of endoglucanase.[14]

Table II.4.3. Antifungal and cytotoxic activities of **1** and **2**

compound	HCT-116 inhibition IC_{50} (μg/mL)	*C. albicans* (WT) MIC (μg/mL)	*C. albicans* (AmBR) MIC (μg/mL)
1	2.9	15.6	15.6
2	14.3	62.5	62.5

The isolation of steroidal sulfates from marine sponges of the genus *Euryspongia* has not been reported previously. Eurysterols A (**1**) and B (**2**) were tested for their cytotoxic activities against the HCT-116 human colon tumor cell line and for inhibition against wild-type and amphotericin B-resistant strains of *C. albicans*. The results are shown in Table II.4.3. Despite their structural similarities, **1** and **2** showed somewhat different biological activities. Eurysterol A (**1**) was more active in both the cytotoxicity and fungal inhibition assays with an IC_{50} value of 2.9 μg/mL and MIC values of 15.6 μg/mL, respectively. The presence of the double bond in **2** reduced activities in both assays when compared to **1**.

Experimental Section

General Experimental Procedures. Optical rotations were measured using a Rudolph Autopol III polarimeter. UV spectra were obtained using Perkin-Elmer Lambda Bio-20 spectrometer. Infrared spectra were recorded on a Perkin-Elmer 1600 spectrophotometer. COSY, HMBC, ROESY, NOESY, HSQC-TOCSY, and HSQC NMR spectra were recorded on a Varian INOVA 300 MHz spectrometer, and ^{1}H, ^{13}C, and DEPT NMR spectra were recorded on a Varian Gemini 400 MHz spectrometer. High-resolution mass spectrometer measurements were obtained on IonSpec Ultima FTMS and Agilent ESI-TOF instruments at the Scripps Research Institute, La Jolla, CA. All solvents were distilled prior to being used.

Biological Material. The sponge, collection #00-317, was collected from a reef slope on Light House Reef, west of the lighthouse at Koror, Palau, from a depth of 37 m, in August 2000. It was kept frozen and stored at –20 °C until processed. In life, the sponge is composed of multiple conulose fingers, 12 cm tall, 10 mm diameter, that are fused at the base. The texture is firm but compressible, the sponge is elastic and tears quite easily, and the color is deep azure blue. The surface is closely conulose and granular. The skeleton is a reticulation of fine primary fibers that are packed with spicules and sand debris, and secondary reticulation of clear fibers with a granular pith region. The mesophyll has large eurpylous chambers. The sponge is an undescribed species of *Euryspongia* (order Dictyoceratida, family Dysideidae). A voucher specimen has been deposited at the Natural History Museum, London, UK (BMNH 2005.9.2.1).

Extraction and Purification. The sponge was lyophilized (22.2 g dry weight/ 187.6 g wet weight) before extraction with methanol (4 × 500 mL). The extracts were dried to obtain a dark green oil, which was fractionated by HP20SS column chromatography (acetone/water) to give five fractions. The fraction eluted with 60% acetone–water (64.1mg) was further purified by reversed-phase HPLC (Dynamax C_{18} semi-preparative, gradient from 40%-100% MeOH, 3mL/min) to obtain eurysterols A (**1**, 5.5 mg, 2.5×10^{-2} % dry weight) and B (**2**, 2.1 mg, 9.5×10^{-3} % dry weight).

Eurysterol A (**1**): colorless oil; $[\alpha]_D$ –15.4 (*c* 0.5, MeOH); UV (MeOH) λ_{max} (log ε) 258 nm (2.79); IR ν_{max} (KBr) 3449, 2952, 2868, 1216, 1072 cm^{-1}; NMR data, see Table II.4.1; EIMS $[M+Na]^+$ *m*/*z* 559; HRMALDIFTMS $[M+Na]^+$ *m*/*z* 559.2688 (calcd for $C_{27}H_{45}O_7SNa_2$, 559.2681).

Eurysterol B (**2**): colorless oil; $[\alpha]_D$ –19 (*c* 0.2, MeOH); UV (MeOH) λ_{max} (log ε) 258 nm (2.59); IR ν_{max} (KBr) 3449, 2952, 2868, 1212, 1071 cm^{-1}; NMR data, see Table II.4.2; EIMS $[M+Na]^+$ *m*/*z* 557; HRESITOFMS $[M+Na]^+$ *m*/*z* 557.2523 (calcd for $C_{27}H_{43}O_7SNa_2$, 557.2525).

HCT-116 Assay. HCT-116 human adenocarcinoma cells were plated in the 96-well plates and incubated overnight at 37 °C in 5% CO_2/air. Compounds were applied to the plates in DMSO and serially diluted, then the plates were further incubated for another 72 h. At the end of this period, a CellTiter 96 Aq_{ueous} non-radioactive cell proliferation assay (Promega) was used to assess cell viability. Inhibition

concentration (IC_{50}) values are determined from the bioreduction of MTS/PMS by living cells into a formazan product. MTS/PMS was first added to the sample wells, followed by incubation for 3 h. The positive and negative controls that were used in this assay consisted of etoposide (Sigma) and DMSO (solvent), respectively. The Molecular Devices Emax microplate reader, set to a 490 nm wavelength, was used to determine the quantity of the formazan product (in proportion to the number of living cells) in each well, and IC_{50} values were calculated by an analysis program, SOFTMax.

Antifungal Assay with *C. albicans*. The *C. albicans* strains ATCC 32354 (wild type) and ATCC 90873 (amphotericin B-resistant) were purchased from American Type Culture Collection (ATCC). Inhibitory activity was determined by a liquid antifungal assay. *C. albicans* was incubated overnight at 37 °C in RPMI media and transferred to a 96-well plates the following day. Compounds were added to the plates and serially diluted. The plates were then incubated for 14-16 h. Amphotericin B (Sigma) and DMSO (solvent) were used as positive and negative controls, respectively. Minimum inhibitory concentration (MIC) values were interpreted by the change in color from blue to pink of the media according to the indicator Alamar Blue.

References

(1) van Altena, I. A.; Butler, A. J.; Dunne, S. J. *J. Nat. Prod.* **1999**, *62*, 1154-1157.

(2) Hallock, Y. F.; Cardellina, J. H., II; Boyd, M. R. *Nat. Prod. Lett.* **1998**, *11*, 153-160.

(3) Urban, S.; Capon, R. J. *Aust. J. Chem.* **1996**, *49*, 611-615.

(4) van Altena, I. A.; Miller, D. A. *Aust. J. Chem.* **1989**, *42*, 2181-2190.

(5) Clark, R. J.; Garson, M. J.; Brereton, I. M.; Kennedy, J. A. *J. Nat. Prod.* **1999**, *62*, 915-916.

(6) Pretsch, E.; Simon, W.; Seibl, J.; Clerc, T. *Tables of Spectral Data for Structure Determination of Organic Compounds*; Springer-Verlag: Berlin, 1989; p I230.

(7) Yada, H.; Sato, H.; Ichihara, A. *Tetrahedron Lett.* **1995**, *36*, 7471-7474.

(8) Li, H.; Matsunaga, S.; Fusetani, N.; Fujiki, H.; Murphy, P. T.; Willis, R. H.; Baker, J. T. *Tetrahedron Lett.* **1993**, *34*, 5733-5736.

(9) Sun, H. H.; Cross, S. S.; Gunasekera, M.; Koehn, F. E. *Tetrahedron* **1991**, *47*, 1185-1190.

(10) Tsukamoto, S.; Matsunaga, S.; Fusetani, N.; van Soest, R. W. M. *J. Nat. Prod.* **1998**, *61*, 1374-1378.

(11) Nakatsu, T.; Walker, R. P.; Thompson, J. E.; Faulkner, D. J. *Experientia* **1983**, *39*, 759-761.

(12) Bifulco, G.; Bruno, I.; Minale, L.; Riccio, R. *J. Nat. Prod.* **1994**, *57*, 164-167.

(13) Tsukamoto, S.; Kato, H.; Hirota, H.; Fusetani, N. *Biofouling* **1997**, *11*, 283-291.

(14) Zvyagintseva, T. N.; Makar'eva, T. N.; Stonik, V. A.; Elyakova, L. A. *Khim. Prir. Soedin.* **1986**, 71-77.

Acknowledgements

The text of II.4, in full, is the manuscript submitted to *Journal of Natural Products* as it appears in Boonlarppradab, C.; Faulkner, D. J. Eurysterols A and B, Cytotoxic and Antifungal Steroidal Sulfates from a Marine Sponge of the Genus *Euryspongia*. *J. Nat. Prod*. **2007**, *70*, 846-848. The dissertation author was the primary author and directed and supervised the research, which forms the basis for this chapter.

II.5

Sagitol B, a cytotoxic pyridoacridine alkaloid from the palaun ascidian of the genus *Eudistoma*

Abstract

A new pyridoacridine alkaloid, sagitol B, was isolated from a purple ascidian of the genus *Eudistoma* collected in Palau. The structure of the new compound was assigned using spectroscopic data emphasizing on the interpretation of 2D NMR. Sagitol B showed cytotoxicity against human colon carcinoma (HCT-116) cells with IC_{50} values of 2.2 μg/mL, while it did not exhibit any inhibition against both amphotericin B-resistant and wild-type strains of *Candida albicans*. The known derivatives, sagitol, and kuanoniamine B-D, were also obtained from this marine ascidian.

Introduction

Marine ascidians of the genus *Eudistoma* have been intensely studied and investigated in both biological and chemical aspects. A large number of biologically active alkaloids, including eudistomins A-T,[1-4] eudistomidins A-F,[5-7] eudistalbins A-B,[8] isoeudistomins[9], eilatin[10], eudistones A-B[11], and segoline A[12] have been isolated from various *Eudistoma* species. Several of these chemical metabolites were reported to exhibit potent cytotoxic, antimicrobial or antiviral activities. Due to their interesting bioactivities and challenging structures, many of these alkaloids have been chosen as excellent targets in the chemical synthetic studies, in particular, for the development as therapeutic agents.

During the cytotoxicity bioassay screening of marine invertebrate collection, the extract of a purple marine tunicate from *Eudistoma* sp. was shown to possess potent cytotoxic activity. Bioassay-guided fractionation of the crude extract, using HCT-116 human colon carcinoma cells as a screening method, has led to the isolation of a new cytotoxic pyridoacridine alkaloid sagitol B (**1**), and several known isomers including sagitol[13] (**2**), and kuanoniamines B-D[14] (**3-5**). In this chapter, the isolation, structure elucidation, and biological activity of this new pyridoacridine alkaloid is described.

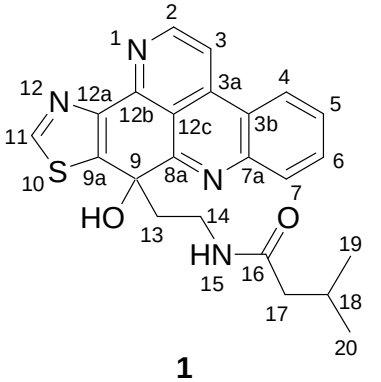

1

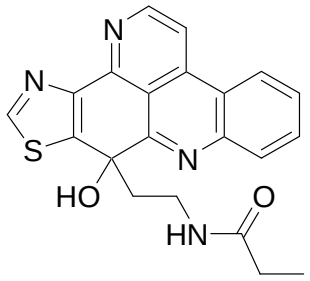

2

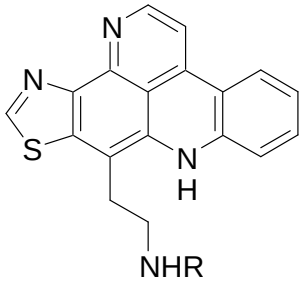

3 R =

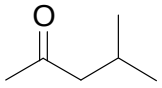

4 R =

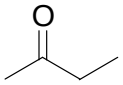

5 R =

Figure II.5.1. The structures of sagitol B (**1**), sagitol (**2**), and kuanoniamines B-D (**3**-**5**)

Results and Discussion

The ascidian of the genus *Eudistoma*, designated 00-341, was collected by hand using scuba at a depth of 5 to10 m from Palau in 2000. This purple ascidian (334.3 g, wet weight) was chopped into small pieces and extracted exhaustively with methanol overnight. The crude extract (deep red purple) was dried *in vacuo* and further separated by HP20SS column chromatography. The column was eluted with 25%, 50%, 75% and 100% acetone-water. HCT-116 cytotoxic activity was observed in the first three fractions (25% to 75%). The 50% acetone fraction (202 mg) was shown to possess the highest cytotoxicity with IC_{50} values less than 0.1 μg/mL, thus the fraction was subjected to purification by reversed-phase PRP-1 HPLC to yield fractions with the previously isolated bioactive pyridoacridine alkaloids, sagitol (**2**), and kuanoniamines B-D (**3-5**). The new isomer of these pyridoacridine alkaloids, sagitol B (**1**, 4.2 mg), which exhibit IC_{50} value of 1.22 μg/mL, was also isolated by reversed-phase PRP-1 HPLC from the 75% acetone fraction (346.5 mg).

Sagitol B (**1**) was obtained as amorphous yellow solid. The molecular formula was determined as $C_{23}H_{22}N_4O_2S$ by high-resolution MALDIFTMS (*m*/*z* 441.1365, $[M+Na]^+$) and from its NMR spectroscopic data (Table II.5.1). The LRMS spectra showed ions that analyzed for $[M–H]^–$ and $[2M+Na]^–$ at *m*/*z* 417 and 859. The molecular formula implied that there were fifteen degrees of unsaturation. The analysis of DEPT and ^{13}C NMR spectrum indicated a high degree of unsaturation as most carbon resonances, including seven methine carbons, were downfield of 100 ppm, and revealed the nature of this compound to be of heteroaromatic system.

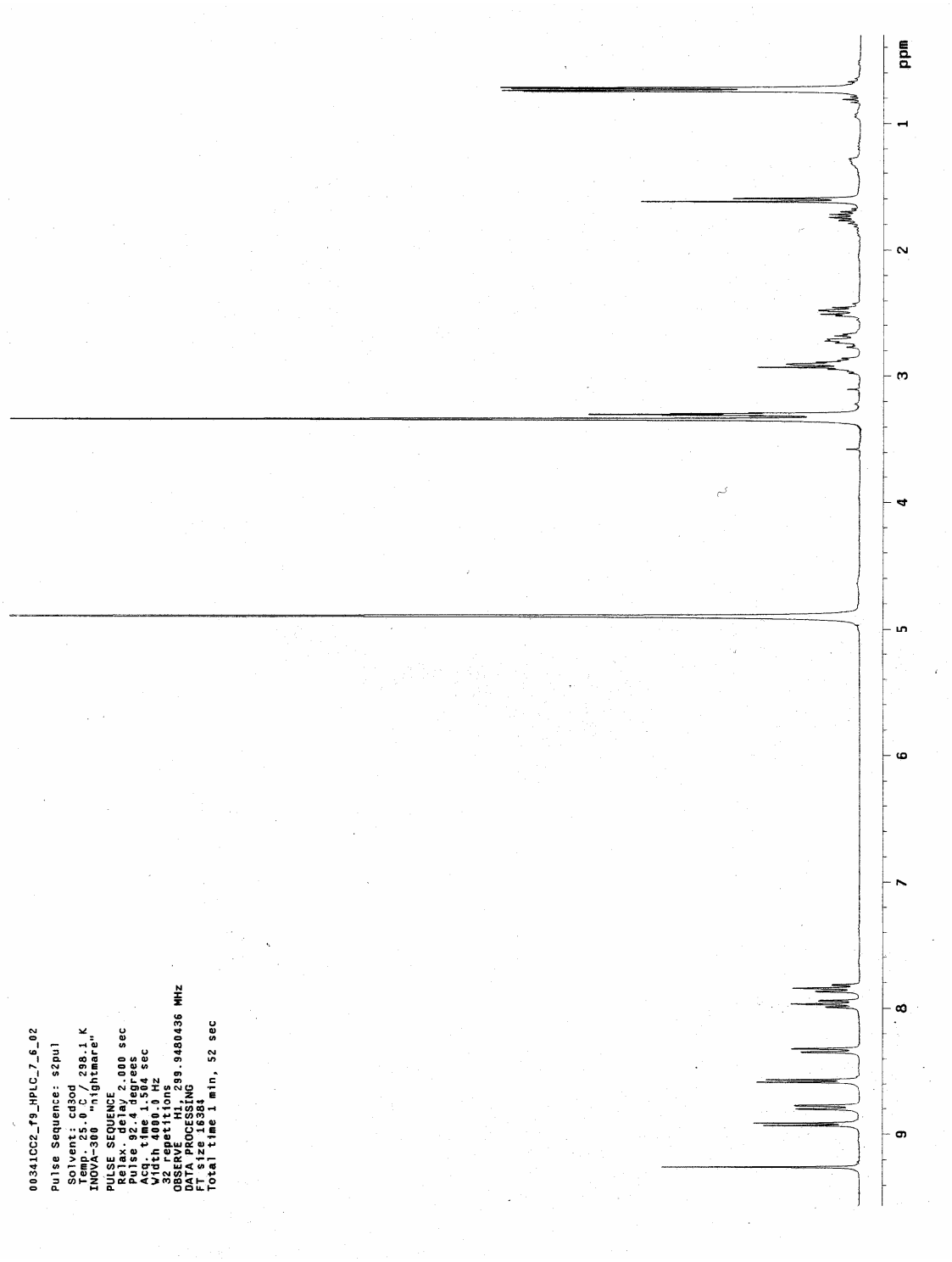

Figure II.5.2. ^{1}H NMR spectrum of Sagitol B (**1**) (300 MHz, CD_3OD)

Table II.5.1. ^{1}H, ^{13}C, COSY, HSQC, and HMBC NMR spectroscopic data (CD_3OD) for sagitol B (**1**)

C#	δ_C		δ_H	*J* (Hz)	COSY	HMBC
2	149.2	CH	8.92 d	6.0	3	C-3, C-3a, C-12b
3	116.7	CH	8.58 d	6.0	2	C-2, C-3b, C-12c,
3a	139.6	C				
3b	122.9	C				
4	124.3	CH	8.79 d	8.4	5	C-3a, C-6, C-7a
5	129.4	CH	7.84 t	8.4	4, 6	C-3b, C-7
6	132.5	CH	7.96 t	8.4	5, 7	C-4, C-7a
7	130.9	CH	8.33 d	8.1	6	C-3b, C-5
7a	146.7	C				
8a	162.3	C				
9	73.9	C				
9a	145.9	C				
11	156.9	CH	9.26 s			C-9a, C-12a
12a	149.1	C				
12b	150.0	C				
12c	115.9	C				
13	47.3	CH_2	2.48 m		14	C-8a, C-9
			2.90 m		14	C-14
14	35.9	CH_2	2.72 m		13	C-13
			2.90 m		13	C-9
16	174.7	C				
17	46.0	CH_2	1.61 d	6.6	18	C-16, C-18, C-19, C-20
18	27.1	CH	1.73 m	6.9	17, 19, 20	C-19, C-20
19	22.6	CH_3	0.73 d	6.9	18	C-17, C-18, C-20
20	22.6	CH_3	0.73 d	6.9	18	C-17, C-18, C-19

The ^{1}H NMR spectrum of **1** (Figure II.5.2) measured in CD_3OD demonstrated seven aromatic protons. The COSY correlations showed that four aromatic protons, H-4 (δ 8.79), H-5 (δ 7.84), H-6 (δ 7.96) and H-7 (δ 8.33), were on contiguous atoms of an aromatic ring. The isolated vicinal proton pair (δ 8.92 and δ 8.58) at C-2 (δ 149.2) and C-3 (δ 116.7), could be assigned as α- and β-pyridine protons due to their homonuclear coupling constant (J = 6 Hz). The remaining singlet aromatic proton at H-11 (δ 9.26) was likely to be positioned between two heteroatoms as suggested by the downfield chemical shift of C-11 at δ 156.9. In addition, the ^{1}H NMR also contained few signals in the upfield region including three methylene, two equivalent methyl, and one methine proton.

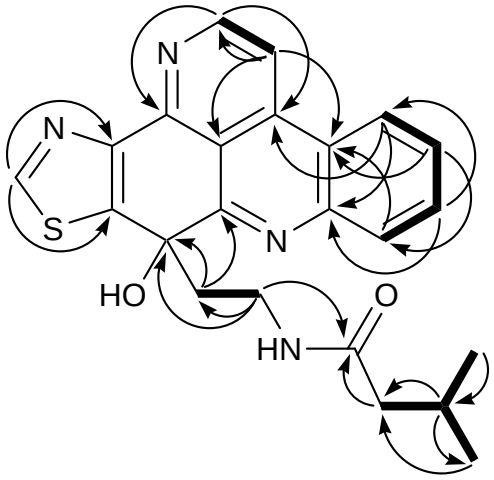

Figure II.5.3. Selected COSY (bold lines) and HMBC (arrows) NMR correlations observed for **1**.

Both COSY and HMBC spectroscopic data (Figure II.5.3) were used to establish the skeletal framework of the main heteroaromatic rings system. The HMBC correlations of four connective aromatic protons, from H-4 to C-3a, C-6 and C-7a, H-5 to C-3b and C-7, H-6 to C-4 and C-7a, H-7 to C-3b and C-5, confirmed the presence of a benzene ring (C-3b to C-7a). The downfield chemical shift of C-7a (δ 146.7) indicated that it might be attached to one of the aromatic nitrogen atoms. The observed HMBC correlations from H-2 to C-3a and C-12b, and from H-3 to C-12c suggested the presence of a pyridine ring, with nitrogen being placed between C-2 (δ 149.2) and C-12b (δ 150.0) due to their low field resonances. The bond between C-3a and C-3b was confirmed by HMBC correlations from H-3 to C-3b, and H-4 to C-3a. The singlet proton at C-11 showed only correlations to C-9a and C-12a, thus, suggesting an isolated system away from the other aromatic protons. This isolated ring system was deduced to be a thiazole ring as supported by the significantly downfield chemical shift of proton (δ 9.26) at C-11.

The comparison between the NMR data of **1** with the previously reported metabolites, indicated that heteroaromatic ring system in this compound is similar to the known pyridoacridine alkaloid, sagitol (**2**), isolated from the marine sponge *Oceanapia sagittaria*.[13] Sagitol is a pyridoacridine alkaloid that is closely related to kuanoniamine C (**4**) (aka dercitamide) with a quite similar structure, except for the addition of one more oxygen. More importantly, sagitol was reported to be the first pyridoacridine alkaloid from marine sponge whose aromatic ring system has been disrupted. CD measurements, however, proved that sagitol was not an artifact.[13]

In the case of sagitol B (**1**), its molecular formula ($C_{23}H_{22}N_4O_2S$) contained one more oxygen atom than that of kuanoniamine B (**3**), and from the comparison of both ^1H and ^{13}C NMR data to those of sagitol, the structure of **1** can be assigned. The disrupted aromatic system with the presence of a tertiary alcohol at C-9 was supported by the IR spectrum with a broad absorption bands at 3283 cm^{-1}, and a ^{13}C NMR signal of C-9 at δ 73.9. The side chain attached to the aromatic ring system at C-9 was found to be similar to that from kuanoniamine B. The HMBC correlations from H-13 and H-14 to C-9 also served to confirm the position of the side chain. The rest of the side chain was assembled through interpretation of both COSY and HMBC correlations.

In addition to sagitol B (**1**), another new derivative of sagitol was observed from another HPLC fraction. According to its ^1H NMR data and mass spectrum, this compound was predicted to contain a similar heteroaromatic ring system like sagitol, but possessed a side chain that was identical to that of kuanoniamine D. The LRMS spectra showed ions that analyzed for $[M+Na]^+$ at *m*/*z* 399, which agreed with this prediction. The ^1H NMR spectra was almost identical to that of **1**, except the presence of a singlet methyl signal instead of di-methyl, one methylene and one methine proton. Unfortunately, the newly obtained metabolite was isolated in very low yield (less than 0.5 mg) thus a full data set of NMR experiments could not be acquired.

Biological Activity

Among marine-derived alkaloids, pyridoacridines appear to be the largest group that has been isolated. There are over 50 alkaloids that contain pyridoacridine skeleton isolated from various marine organisms, including marine sponges, ascidians, mollusk

and cnidarian.[15] Pyridoacridine alkaloids usually possess interesting biological activity, and distinct heterocyclic structures that make them a good target for synthetic studies and development of future generation of therapeutic agents. These alkaloids have excellent biological activities including in vitro and in vivo cytotoxicity against several tumor cell lines, inhibition against topoisomerases I and II, and DNA intercalation.[15]

Kuanoniamines B-D demonstrated moderate cytotoxicity against KB (human pharyngeal cancer) cell lines in vitro at IC_{50} of >10 μg/mL for **3**, and 5 μg/mL for **5**.[14] The newly isolated sagitol B (**1**) was evaluated in both the cytotoxicity assay against HCT-116 human colon tumor cell line, and in the antifungal assay for inhibition against wild-type and amphotericin B-resistant strains of *C. albicans*. Sagitol B (**1**) exhibited moderate cytotoxic activity with IC_{50} of 2.2 μg/mL in HCT-116 assay, whereas the inhibition against both strains of *C. albicans* was not observed (MIC > 250 μg/mL).

Experimental Section

General Experimental Procedures. UV spectra were obtained using Varian Cary 50 Bio UV-Visible spectrophotometer. Infrared spectra were recorded on a Perkin-Elmer 1600 spectrophotometer. ^{1}H, COSY, HMBC, and HSQC NMR spectra were recorded on a Varian INOVA 300 MHz spectrometer, and ^{13}C, and DEPT NMR spectra were recorded on a Varian Gemini 400 MHz spectrometer. High-resolution mass spectrometer measurements were obtained on IonSpec Ultima FTMS

instruments at the Scripps Research Institute, La Jolla, CA. All solvents were distilled prior to being used.

Biological material. The marine ascidian *Eudistoma* sp. was collected by hand using scuba at the depth of 5-10 m from Palau, in 2000. The specimen was immediately frozen after collection and stored at –20 °C until processed. The color in life is dark purple and the ascidian was assigned as *Eudistoma* sp. The taxonomic identification was not officially confirmed but the initial examination by Catherine Sincich suggested that this ascidian might be identified as *Eudistoma Reginum* sp. A voucher specimen has been deposited in the SIO Benthic Invertebrate Collection.

Extraction and isolation. The marine ascidian (334.3 g wet weight) was extracted with methanol (3 × 500 mL) for 24 h. The crude extracts were combined and dried *in vacuo* to obtain a deep red purple extract, which was fractionated by HP20SS column chromatography (acetone/water) to yield 25%, 50%, 75% and 100% fractions. All four fractions were concentrated to dryness and tested in HCT-116 assay. The first three fractions eluted with 25%, 50% and 75% acetone-water were found to possess potent cytotoxic activity (IC_{50} = 1.98, 0.08, and 1.22, respectively). The 50% acetone fraction was subjected to further purification on reversed-phase HPLC (Hamilton PRP-1 semi-preparative, 2 mL/min; 10–70% ACN/H_2O with 0.1% TFA over 60 min, 70–100% ACN/H_2O over 15 min) to yield sagitol (**2**, 0.8 mg), kuanoniamines C (**4**, 2.6 mg) and D (**5**, 3.7 mg). Using similar approach, the 75% acetone fraction was also purified by reversed-phase HPLC (Hamilton PRP-1 semi-preparative, 2 mL/min; 20–

70% ACN/H_2O with 0.1% TFA over 60 min, 70–100% ACN/H_2O over 15 min) to yield kuanoniamine B (**3**, 0.9 mg), and the new derivative of sagitol, sagitol B (**1**, 4.2 mg, 1.3×10^{-3} % wet weight).

Sagitol B (**1**): yellow amorphous solid; UV (MeOH) λ_{max} (log ε) 354 nm (3.99), 337 nm (4.12), 262 nm (4.51); IR ν_{max} (KBr) 3283, 2355, 1631, 1596, 1561, 1455 cm^{-1}; NMR data, see Table II.5.1 ; EIMS $[M–H]^+$ *m*/*z* 417; HRMALDIFTMS $[M+Na]^+$ *m*/*z* 441.1365 (calcd for $C_{23}H_{22}N_4O_2SNa$, 441.1361).

References

(1) Rinehart, K. L., Jr.; Kobayashi, J.; Harbour, G. C.; Hughes, R. G., Jr.; Mizask, S. A.; Scahill, T. A. *J. Am. Chem. Soc.* **1984**, *106*, 1524-1526.

(2) Kobayashi, J.; Harbour, G. C.; Gilmore, J.; Rinehart Jr., K. L. *J. Am. Chem. Soc.* **1984**, *106*, 1526-1528.

(3) Rinehart, K. L., Jr.; Kobayashi, J.; Harbour, G. C.; Gilmore, J.; Mascal, M.; Holt, T. G.; Shield, L. S.; Lafargue, F. *J. Am. Chem. Soc.* **1987**, *109*, 3378-3387.

(4) Kinzer, K. F.; Cardellina, J. H., II. *Tetrahedron Lett.* **1987**, *28*, 925-926.

(5) Kobayashi, J.; Nakamura, H.; Ohizumi, Y.; Hirata, Y. *Tetrahedron Lett*. **1986**, *27*, 1191-1194.

(6) Kobayashi, J.; Cheng, J.; Ohta, T.; Nozoe, S.; Ohizumi, Y.; Sasaki, T. *J. Org. Chem.* **1990**, *55*, 3666-3670.

(7) Murata, O.; Shigemori, H.; Ishibashi, K. S.; Hayashi, K.; Kobayashi, J. *Tetrahedron Lett.* **1991**, *32*, 3539-3542.

(8) Adesanya, S. A.; Chbani, M.; Païs, M.; Debitus, C. *J. Nat. Prod.* **1992**, *55*, 525-527.

(9) Kang, H.; Fenical. W. *Nat. Prod. Lett.* **1996**, *9*, 7-12.

(10) Rudi, A.; Benayahu, Y.; Goldberg, I.; Kashman, Y. *Tetrahedron Lett.* **1988**, *29*, 6655-6656.

(11) He, H. Y.; Faulkner, D. J. *J. Org. Chem.* **1991**, *56*, 5369-5371.

(12) Rudi, A.; Benayahu, Y.; Goldberg, I.; Kashman, Y. *Tetrahedron Lett.* **1988**, *29*, 3861-3862.

(13) Salomon, C. E.; Faulkner, D. J. *Tetrahedron Lett.* **1996**, *37*, 9147-9148.

(14) Carroll, A. R.; Scheuer, P. J. *J. Org. Chem.* **1990**, *55*, 4426-4431.

(15) Delfourne, E.; Bastide, J. *Med. Res. Rev.* **2003**, *23*, 234-252.

III

New secondary metabolites from marine actinomycetes

Chapter III describes several marine microbial projects that yield different types of bioactive secondary metabolites, all of which were isolated by bioassay-guided fractionation. The major focus of this chapter is the investigation of marine actinomycete bacteria for their potential production of bioactive compounds that may prove to be efficient therapeutic agents for the treatment of cancer and fungal diseases. Chapter III.1 provides the details of the screening of a marine actinomycete collection using the standard liquid antifungal susceptibility test.

Chapter III.2 reports a study of the non-traditional actinomycete, strain CNJ787 collected in Palau. This chapter discusses an unexpected problem encountered utilizing the liquid antifungal assay. The compounds isolated are proven to possess significant antifungal activity, but they are siderophores and express their antifungal activities via the complexation of iron.

In chapter III.3, two new quinoline alkaloids are described as a result of a screening effort utilizing the extracts of marine actinomycetes. The new metabolites possess interesting structures although they do not exhibit significant antifungal activity against *C. albicans*.

Chapter III.4 discusses a modification of the liquid antifungal assay, which was required in order to overcome the pitfall that was discovered in project CNJ787. The adjustment was necessary to eliminate undesired antifungal activity from known siderophore metabolites. The results from the second screening of marine actinomycetes after the adjustment was made to the assay is presented.

Chapter III.5 describes the isolation and structure elucidation of an uncommon bacterial sesterterpenoid, and two novel cytotoxic macrolides from the MAR3 clade, a new group of marine-derived actinomycetes collected from coastal waters in San Diego. The active metabolite possesses very unique and distinct chemical skeleton with potent cytotoxic activity as demonstrated by screening results utilizing the HCT-116 human colon carcinoma assay.

III.1

Antifungal bioassay-guided screening of marine actinomycetes

III. 1. Antifungal bioassay-guided screening of marine actinomycetes

Introduction

Actinomycetes are known to be the most prolific source of microbial secondary metabolites, and historically provided a significant resource for drug discovery research.[1] By the 1980s, the actinomycetes accounted for nearly 70% of the world's naturally occurring antibiotics.[2] Still, the rate of discovery of useful microbial metabolites declined progressively after 1970, while the rate of dereplication of known compounds has increased.[3] Hence, it is critical to examine new groups of microbes from unexplored habitats that may serve as potential sources for novel therapeutic agents.

The ocean, which covers more than 70% of the earth's surface, is composed of highly complex microbial communities with typical bacterial abundances of 10^6 cells per ml in seawater, and up to 10^9 cells per ml in ocean-bottom sediments.[4] The great diversity of these unique marine microbes remains largely unexplored in both chemical and biological aspects. Despite the fact that terrestrial actinomycetes have been thoroughly studied during the past 60 years, the investigation of marine actinomycetes has recently emerged as a potential source for pharmaceutical development. It has been speculated that numerous secondary metabolites with clinically relevant bioactivities and novel skeletal structures are waiting to be discovered from these microbial communities.

Since marine invertebrates have been exhaustively investigated and the continued discovery of new metabolites with unprecedented skeletons has become extremely difficult, actinomycetes from the marine environment are judged to be the next promising candidate for the Fenical group screening program. An obvious benefit of microbial discovery programs over examining invertebrates is that the supply problem can be resolved by cultivating the organism to obtain more secondary metabolites.

Antifungal Susceptibility Tests and Results

Because of the uncertainty of the disc diffusion method, the liquid dilution antifungal bioassay method was employed. This is based upon my previous antifungal screening of marine invertebrate extracts, the results of which demonstrated that almost half of the test samples that showed activity from the disc diffusion method seemed to lack activity in the antifungal liquid assay. The difference may stem from compound degradation, but there are also chances that the metabolites with antifungal activity may not exhibit zone of inhibition in the disc diffusion method due to their poor diffusivities in agar. For that reason, the disc diffusion method was discarded in favor of the more reliable liquid antifungal assay in the screening process. The major pathogenic fungal target still focused on *C. albicans* wild type (ATCC32354) and the amphotericin B resistant strains (ATCC90873) as the standard test for overall screening of crude extracts in order to identify promising marine microbial projects.

There is a considerably large marine microbial collection from Fenical research group that can be evaluated for both cytotoxic and antifungal activities. This includes marine fungi, and marine bacteria such as actinomycetes of the *Salinospora* genus[5]

and members of the MAR2-13 groups. Crude extracts of cultured actinomycete strains, produced under different media conditions, are stored in 96-well plate formats, each of which contains about 80 samples of bacterial crude extracts. For the first screening, the liquid antifungal assay against an amphotericin B resistant strain of *C. albicans* was performed on ten randomly chosen 96-well plates (Box #120-129). The extracts in this plate were primarily from actinomycete strains.

The initial screening of crude extracts for antifungal active agents was carried out at a single concentration of 150 μg/mL. Approximately 800 crude extracts were tested in the first screening. Unexpectedly, the screening results were shown to exhibit a hit rate over 50% (466 active extracts), which is much higher than that observed from the marine invertebrates (10% or less). It is possible that this difference may arise from the use of different type of antifungal assays. Nevertheless, it is undeniable that the hit rate of antifungal active metabolites from marine microbes is still much greater than that of marine invertebrates. As there were too many candidates for the selection process, the serial dilution method of liquid antifungal assay, that can establish a specific MIC value, was used to narrow down the number of these active microbial extracts.

In addition, I imposed an antifungal selectivity criterion by comparing the results from the HCT-116 human colon carcinoma cytotoxicity assay with results from the liquid dilution antifungal assay. The crude microbial extracts with at least 50% survival in the HCT-116 assay and MIC $\leq$ 150 μg/mL in the liquid antifungal assay were chosen for further investigation. Selectivity is one of the important factors that

determine whether the active metabolites will be suitable candidates for drug development. Factors for choosing projects are that the compound should be effective against pathogenic fungi but non-cytotoxic to human cells. It is important to note that even though the result from the HCT-116 assay may show non-significant cytotoxic activity, it is possible that tests against other cell lines may exhibit higher levels of cytotoxicity. Basing upon the above selective criteria, 183 extracts from a total of approximately 800 samples were found to meet these criteria.

To further refine the sample pool, a serial dilution liquid antifungal assay was performed with samples at the concentration of 25 μg/mL, to assign the specific MIC value of each selective strain. The result of the screening program is shown in Figure III.1.1. From 183 samples, approximately 75% of the test extracts showed moderate to weak growth inhibition of *C. albicans* with MIC values over 20 μg/mL. The remaining 36 strains were found to exhibit the highest antifungal activity with MIC values $\leq$ 9.8 μg/mL. These strains were retested in the liquid antifungal assay at 5 μg/mL in order to select even further and obtain a more accurate inhibition concentration. The results of antifungal screening for the 36 most active marine actinomycete strains compared with the reported percent survival from the HCT-116 assay are illustrated in Table III.1.1. In addition, 40 marine bacterial extracts that possessed moderate antifungal activity with MIC values between 20 and 40 μg/mL are also shown in Table III.1.2.

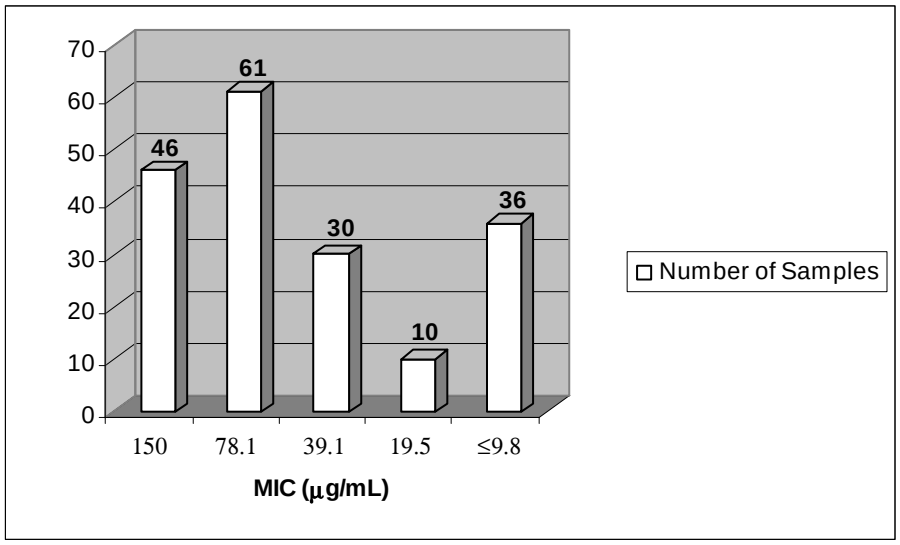

Figure III.1.1. Screening results of 183 samples of marine microbial extracts using the liquid dilution antifungal assay against *C. albicans* (AMBR).

The 36 samples with the most potent antifungal activity and negligible cytotoxicity were found to share some unexpected similarities. These 35 strains of marine microbes were discovered to have been cultured using the same media condition (TCG media). This result is very interesting as it may suggest that the media somehow influences the production of antifungal compounds. On the other hand, there is also a possibility that the active metabolites may be derived from the growth media itself. In order to confirm that the active compounds were indeed produced by the microorganism, the media itself was extracted, and tested in both antifungal and HCT-116 assays. The media extracts showed no significant antifungal and cytotoxic activity, thus indicating that the antifungal compounds are not derived from the growth medium.

Table III.1.1. The results of antifungal screening against *C. albicans* (AMBR) for 36 of the most active marine actinomycete strains showing MIC ≤ 9.8 μg/mL.

Box #	Extract #	Strain #	Media	HCT-116 (% Survival)	*C. albicans* (AMBR) MIC (μg/mL)
120	1386	CNQ803	TCG	105	3.9
120	1426	CNQ877	TCG	60	3.9
121	1470	CNQ917	TCG	69	≤1.95
121	1490	CNQ949	TCG	129	3.9
121	1556	CNR026	AlBFe-C	60	3.9
121	1550	CNR016	TCG	115	≤1.95
121	1558	CNR026	TCG	87	3.9
122	1618	CNR079	TCG	70	3.9
124	1686	CNQ857	TCG	65	3.9
125	1858	CNQ695	TCG	81	7.8
125	1902	CNR530	TCG	96	7.8
126	1850	CNQ435	TCG	52	7.8
126	1854	CNQ554	TCG	72	3.9
126	1918	CNQ702	TCG	75	3.9
126	1986	CNR381	TCG	67	≤1.95
126	1922	CNQ749	TCG	83	7.8
126	1958	CNR165	TCG	85	≤1.95
127	2046	CNP853	TCG	82	≤1.95
127	2062	CNP943	TCG	79	3.9
127	2074	CNP947	TCG	60	7.8
127	2098	CNP962	TCG	68	3.9
128	2078	CNP948	TCG	70	≤1.95
128	2082	CNP949	TCG	91	3.9
128	2194	CNP956	TCG	65	3.9
128	2066	CNP944	TCG	70	3.9
128	2210	CNP967	TCG	71	3.9
128	2218	CNP971	TCG	82	7.8
129	2242	CNP961	TCG	76	3.9
129	2262	CNP973	TCG	139	7.8
129	2266	CNP975	TCG	139	≤1.95
129	2286	CNP989	TCG	81	7.8
129	2302	CNP995	TCG	69	≤1.95
129	2342	CNQ024	TCG	93	7.8
129	2314	CNP998	TCG	65	7.8
129	2322	CNQ001	TCG	64	≤1.95
129	2338	CNQ023	TCG	61	≤1.95

Table III.1.2. The results of antifungal screening against *C. albicans* (AMBR) of 40 active marine actinomycete extracts with MIC values ≤ 39.1 μg/mL but ≥ 19.5 μg/mL.

Box #	Extract #	Strain #	Media	HCT-116 (% Survival)	*C. albicans* (AMBR) MIC (μg/mL)
120	1434	CNQ894	TCG	81	19.5
122	1614	CNR078	TCG	80	19.5
123	1590	CNR014	TCG	66	19.5
123	1598	CNR043	TCG	80	19.5
125	1851	CNQ435	AlBFe+C	81	19.5
126	1938	CNQ989	TCG	78	19.5
127	2022	CNP847	TCG	88	19.5
128	2226	CNP977	TCG	59	19.5
129	2278	CNP987	TCG	84	19.5
129	2326	CNQ002	TCG	72	19.5
120	1478	CNQ932	TCG	92	39.1
120	1382	CNQ802	TCG	97	39.1
120	1410	CNQ822	TCG	51	39.1
120	1422	CNQ868	TCG	77	39.1
122	1582	CNR004	TCG	65	39.1
123	1755	CNR157	AlBFe+C	60	39.1
124	1706	CNR106	TCG	71	39.1
124	1674	CNQ732	TCG	82	39.1
124	1806	CNR266	TCG	80	39.1
125	1635	CNR091	AlBFe+C	72	39.1
125	1699	CNR094	AlBFe+C	66	39.1
125	1727	CNR135	AlBFe+C	72	39.1
125	1759	CNR158	AlBFe+C	67	39.1
125	1836	CNR363	AlBFe-C	89	39.1
125	1888	CNR382	AlBFe-C	73	39.1
125	1896	CNR431	AlBFe-C	79	39.1
125	1903	CNR530	AlBFe+C	71	39.1
126	1659	CNQ445	AlBFe+C	66	39.1
126	1912	CNQ685	AlBFe-C	56	39.1
126	1928	CNQ936	AlBFe-C	94	39.1
126	1940	CNQ995	AlBFe-C	69	39.1
126	1950	CNR049	TCG	50	39.1
126	1954	CNR143	TCG	60	39.1
127	2042	CNP852	TCG	96	39.1
128	2084	CNP952	AlBFe-C	90	39.1
128	2080	CNP949	AlBFe-C	73	39.1
129	2241	CNP961	Mar2DPh	62	39.1
129	2296	CNP994	AlBFe-C	68	39.1
129	2290	CNP992	TCG	91	39.1
129	2298	CNP994	TCG	75	39.1

After several rounds of the antifungal screening of the crude extracts, 24 projects were selected from 36 promising candidates that exhibit MIC ≤ 9.8 μg/mL. To confirm activity on these strains, 24 bacterial strains were recultured in 1L scale and the extracs were rescreened for antifungal activity. The results of this retest are provided in Table III.1.3. Unfortunately, 11 strains of the regrowth did not retest positive and showed significantly less activity with MIC values over 60 μg/mL. The rest of the test extracts retained their antifungal activities, however several were less active with recorded MIC values at much higher concentrations. This is not uncommon when working with microbial cultures since it frequently occurs that microbes may not sustain their abilities to produce the active compounds from different cultivations. The remaining 13 projects were under investigation selected for isolation and identification of the antifungal active compounds.

The crude acetone extracts derived from the 1L second cultures of the 13 bacterial strains were fractionated by HP20SS column chromatography. The column was eluted with 20%, 40%, 60%, 80% and 100% acetone-water gradient to yield five fractions for each strain extract. The fractions obtained were dried *in vacuo* and tested in the liquid antifungal assay to assess if they had survived chromatography. Table III.1.4 lists these promising 13 microbial strains with their corresponded HP20SS fractions and antifungal activities. Analysis of the active fractions by both LCMS and ^{1}H NMR spectroscopy allowed these projects to be prioritized. The strain producing fractions with unique UV absorbing metabolites, and interesting ^{1}H NMR spectral data was given a higher priority for investigation.

Table III.1.3. Antifungal screening results of the regrowth culture extracts of 24 marine bacterial strains against *C. albicans* (AMBR).

Strain #	Samples from Mother Plates		Regrowth in 1L Cultures	
	C. albicans (AMBR) MIC (μg/mL)	HCT-116 (%Survival)	*C. albicans* (AMBR) MIC (μg/mL)	HCT-116 IC_{50} (μg/mL)
CNP853	≤ 1.95	82	≤ 3.9	NSA
CNP948	≤ 1.95	70	≤ 3.9	78
CNP975	≤ 1.95	139	15.6	NSA
CNP995	≤ 1.95	69	250	NSA
CNQ001	≤ 1.95	64	3.9	78
CNQ023	≤ 1.95	61	3.9	NSA
CNQ917	≤ 1.95	69	7.8	NSA
CNR165	≤ 1.95	85	62.5	NSA
CNP962	3.9	68	7.8	56
CNP944	3.9	70	62.5	NSA
CNP956	3.9	65	≤ 3.9	NSA
CNP961	3.9	76	500	NSA
CNP967	3.9	71	7.8	NSA
CNQ803	3.9	105	15.6	NSA
CNQ877	3.9	60	7.8	NSA
CNR026	3.9	60	500	NSA
CNR079	3.9	70	62.5	78
CNP949	3.9	91	≤ 3.9	21.3
CNP973	7.8	139	250	NSA
CNP989	7.8	81	62.5	NSA
CNP998	7.8	65	62.5	78
CNQ024	7.8	93	500	78
CNQ749	7.8	83	62.5	48
CNP971	7.8	82	7.8	78

Table III.1.4. Antifungal screening results of HP20SS fractions from the regrowth culture extracts of 13 marine actinomycete strains.

CNP853	MIC (µg/mL)	HCT-116 (IC_{50})	Mass (mg)
20%	31.3	NSA	48.5
40%	≤ 3.9	48.2	37.8
60%	15.6	NSA	5.4
80%	62.5	NSA	6.4
100%	500	NSA	9.5

CNP948	MIC (µg/mL)	HCT-116 (IC_{50})	Mass (mg)
20%	62.5	NSA	25.7
40%	≤ 3.9	NSA	50.1
60%	15.6	NSA	21.8
80%	31.3	NSA	5.7
100%	125	NSA	16.3

CNP949	MIC (µg/mL)	HCT-116 (IC_{50})	Mass (mg)
20%	500	NSA	35.7
40%	≤ 3.9	31.6	24.5
60%	≤ 3.9	67.9	24.8
80%	≤ 3.9	70.2	26.2
100%	≤ 3.9	NSA	21.5

CNP956	MIC (µg/mL)	HCT-116 (IC_{50})	Mass (mg)
20%	125	NSA	44.5
40%	≤ 3.9	NSA	52.8
60%	7.8	73.6	13.1
80%	31.3	NSA	8.2
100%	250	NSA	13.7

CNP962	MIC (µg/mL)	HCT-116 (IC_{50})	Mass (mg)
20%	7.8	NSA	24
40%	≤ 3.9	NSA	30.9
60%	7.8	NSA	16
80%	31.3	65.3	21.1
100%	62.5	NSA	7.6

CNP967	MIC (µg/mL)	HCT-116 (IC_{50})	Mass (mg)
20%	125	NSA	100.5
40%	7.8	NSA	34.1
60%	≤ 3.9	NSA	47
80%	≤ 3.9	NSA	19.8
100%	≤ 3.9	NSA	22

CNP971	MIC (µg/mL)	HCT-116 (IC_{50})	Mass (mg)
20%	31.3	NSA	51.1
40%	≤ 3.9	42.4	34.3
60%	7.8	NSA	10.5
80%	15.6	52.1	15.7
100%	62.5	NSA	21.1

CNP975	MIC (µg/mL)	HCT-116 (IC_{50})	Mass (mg)
20%	250	NSA	22
40%	500	NSA	18.3
60%	15.6	NSA	21.7
80%	≤ 3.9	NSA	20.9
100%	7.8	NSA	43.5

CNQ001	MIC (µg/mL)	HCT-116 (IC_{50})	Mass (mg)
20%	31.3	NSA	49.5
40%	≤ 3.9	NSA	41.1
60%	15.6	NSA	7.2
80%	31.3	NSA	12.2
100%	250	NSA	15

CNQ023	MIC (µg/mL)	HCT-116 (IC_{50})	Mass (mg)
20%	7.8	NSA	62
40%	≤ 3.9	75.03	35.9
60%	≤ 3.9	NSA	14.6
80%	7.8	NSA	7.6
100%	15.6	NSA	11.3

CNQ803	MIC (µg/mL)	HCT-116 (IC_{50})	Mass (mg)
20%	500	NSA	28.7
40%	7.8	NSA	26
60%	31.3	NSA	18.6
80%	31.3	NSA	11.5
100%	125	NSA	7.2

CNQ877	MIC (µg/mL)	HCT-116 (IC_{50})	Mass (mg)
20%	250	NSA	16.2
40%	125	NSA	20.6
60%	15.6	NSA	37.4
80%	≤ 3.9	NSA	12.1
100%	62.5	NSA	37.3

CNQ917	MIC (µg/mL)	HCT-116 (IC_{50})	Mass (mg)
20%	500	NSA	75.5
40%	15.6	NSA	17
60%	≤ 3.9	NSA	26.2
80%	≤ 3.9	25.1	7.5
100%	15.6	NSA	26

References

(1) Berdy, J. *J. Antibiotic*. **2005**, *58*, 1-26.

(2) Okami. Y; Hotta, K. Search and discovery of new antibiotics. In *Actinomycetes in biotechnology*, edited by Goodfellow, M.; William, S. T.; Mordarski, M. New York: Academic Press, **1988**, pp. 33-67.

(3) Challis, G. L.; Hopwood, D. A. *Proc. Natl. Acad. Sci.* **2003**, *100*, 14555-14561.

(4) Jensen, P. R.; Fenical, W. *Nat. Chem. Biol*. **2006**, *2*, 666-673.

(5) (a) Mincer, T. J.; Jensen, P. R.; Kauffman, C. A.; Fenical, W. *Appl. Environ. Microbiol*. **2002**, *68*, 5005-5011. (b) Jensen, P. R.; Gontang, E.; Mafnas, C.; Mincer, T. J.; Fenical, W. *Environ. Microbiol*. **2005**, *7*, 1039-1048. (c) Maldonado, L. A.; Fenical, W.; Jensen, P. R.; Kauffman, C. A.; Mincer, T. J.; Ward, A. C.; Bull, A. T.; Goodfellow, M. *Int. J. Syst. Evol. Microbiol*. **2005**, *55*, 1759-1766.

III.2

Isolation of desferrioxamine E, a known siderophore from the non-traditional actinomycete CNJ787 (genus *Kocuria*) from Palau. Identification of an inherent problem in the liquid antifungal bioassay-guided screening

Introduction

The research in the field of marine natural products chemistry from bacterial sources is mostly concentrated on the actinomycetes, whose members have an excellent ability to produce diverse secondary metabolites with remarkable biological activity. In fact, as terrestrial actinomycetes continue to yield unacceptably high numbers of previously described compounds, the search for novel species of marine microbes is emerging to the forefront as a new focus in pharmaceutical research programs.[1]

Despite the fact that major understanding of marine microbial diversity has been largely derived from the intensive studies of bacterioplankton, which are mostly gram-negative bacteria, there is evidence suggesting that gram-positive bacteria may account for a significant proportion of complex marine microbial communities, particularly those in marine sediments.[2]

An investigation of 1,624 gram-positive bacteria isolated from Palaun marine sediments by Erin Gontang, has revealed several isolates that represented new taxa.[2] In particular, the distinct unicellular strains that were designated as “non-traditional actinomycetes” (non-filamentous forms) are being evaluated as a potential source for novel secondary metabolites. Chemical investigations of these bacterial strains is just beginning and many aspects of these organisms remain largely unexplored. Since little is known about these actinomycete strains, studies of the compounds they produce may prove to provide a better understanding of these microbes.

.

Antifungal screening of "non-traditional" actinomycetes

The liquid antifungal assay, using *C. albicans* (AMBR), was performed on samples from four mother plates (Boxes #165-168) of non-traditional actinomycete strains. The initial screening of crude extracts was carried out at a single concentration which would yield MIC values ≤ 10 μg/mL. Instead of using the single concentration of 150 μg/mL, the test concentration was lowered due to the large number of active strains derived from the first screening as illustrated in chapter III.1.

From the total of approximately 320 bacterial extracts from four microbial extract mother plates, only 8 strains (2.5%) showed inhibition against *C. albicans* (AMBR) at MIC values ≤ 10 μg/mL. Table III.2.1 shows the list of antifungal active non-traditional actinomycete strains with their most closely related genera derived by Erin Gontang through comparison of partial 16S rRNA gene sequences.[2]

Table III.2.1. The list of active crude extracts from the antifungal assay screening on the non-traditional actinomycete collection isolated from marine sediments collected in Palau.

Strain #	Closely related genera	*C. albicans* (AMBR) MIC (μg/mL)
CNJ752	*Gordonia*	≤ 10
CNJ754	*Gordonia*	≤ 10
CNJ786	*Gordonia*	≤ 10
CNJ770	*Kocuria*	≤ 10
CNJ787	*Kocuria*	≤ 10
CNJ736	*Micrococcus*	≤ 10
CNJ811	*Micrococcus*	≤ 10
CNR872	MAR2	≤ 10

From 8 promising candidates, 4 strains of non-traditional actinomycetes were chosen for 1L recultivations. The crude acetone extracts, obtained using XAD-7 resin, were tested in the liquid antifungal assay against *C. albicans* (AMBR) to yield the exact MIC value for each strain. The results of antifungal assay along those of the complementary HCT-116 cytotoxicity assay are shown in Table III.2.2.

Table III.2.2. Antifungal screening results against *C. albicans* (AMBR) of the extracts of regrows of 4 non-traditional actinomycete strains.

Strain #	*C. albicans* (AMBR) MIC (μg/mL)	HCT-116 IC_{50} (μg/mL)
CNJ770	≤ 3.9	NSA
CNJ787	15.6	NSA
CNJ736	125	NSA
CNJ811	15.6	NSA

Out of 4 promising projects, the results of antifungal assay after the regrowth of 1L cultures showed that only 3 of them retained antifungal activity. These three active strains, including CNJ770, CNJ787, and CNJ811, were selected to be carefully investigated for the antifungal metabolites. Strain CNJ787 was chosen to be examined first because it yielded the largest amount of culture extract, thus facilitating chemical examination.

Chemical investigation of strain CNJ787 (*Kocuria* sp.)

The crude acetone extract from the 1L regrow of CNJ787 was fractionated by partition on HP20SS resin, and subsequent elution with acetone/water mixtures to obtain 20%, 40%, 60%, 80% and 100% acetone fractions. The fractions were dried *in vacuo* and tested in the liquid antifungal assay against *C. albicans* (AMBR). The screening results (Table III.2.3) showed that the 40% (B2) and 60% (C1) acetone mixtures exhibited the most potent antifungal activity with an MIC value of $\leq$ 0.39 μg/mL.

Table III.2.3. Antifungal screening results of HP20SS extract fractions from strain CNJ787 against *C. albicans* (AMBR).

Fraction #	% Acetone/Water	*C. albicans* (AMBR) MIC (μg/mL)
A1	20	250
A2	20	125
B1	40	7.8
B2	40	$\leq$ 0.39
C1	60	$\leq$ 0.39
C2	60	31.3
D1	80	125
D2	80	125
E1	100	125
E2	100	500

The 40% (B2, 15.4 mg) and 60% (C1, 6.3 mg) acetone fractions were subjected to further purification by gradient reversed-phase C_{18} HPLC (Dynamax C_{18} semi-preparative, 3 mL/min; 40% MeOH/H_2O over 25 min, 40–60% MeOH/H_2O over 30 min) to yield a major metabolite identified as desferrioxamine E. This compound was

identified by comparison of its spectral data (^{1}H NMR (Figure III.2.1), COSY and HRMS data) to that in the literature.[3] This known compound, desferrioxamine E, was evaluated in both liquid antifungal test and HCT-116 assay. Desferrioxamine E exhibited very potent antifungal activity against *C. albicans* (AMBR) at an MIC value of 0.31 μg/mL, whereas the IC_{50} observed in the HCT-116 assay is 18.4 μg/mL. Apart from the fact that this metabolite has been previously reported, it appeared to match with the selective criteria for an antifungal drug candidate very well. This molecule possessed a high potency of antifungal activity while showed non-significant cytotoxicity.

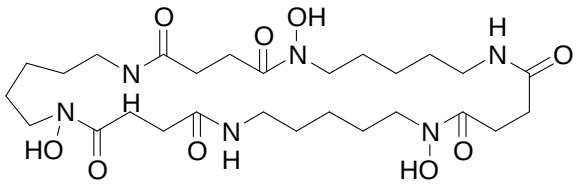

Desferrioxamine E

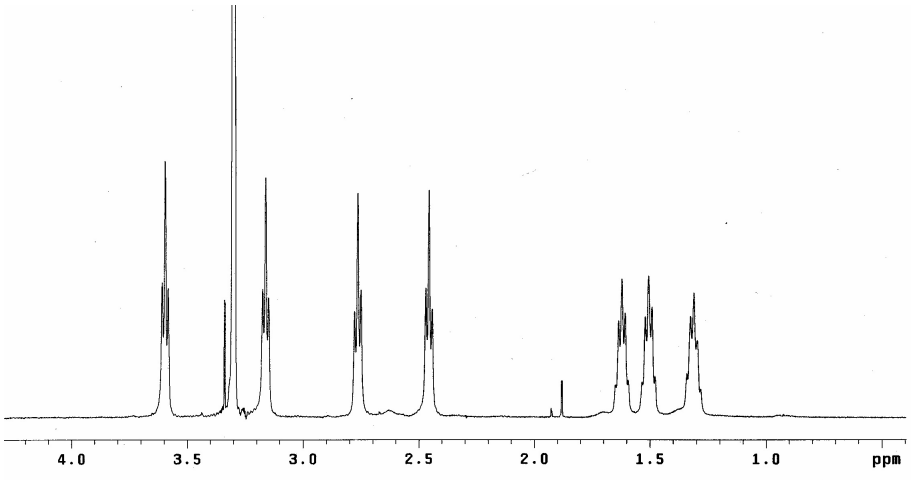

Figure III.2.1. ^{1}H NMR spectrum of desferrioxamine E (500 MHz, CD_3OD)

The presence of desferrioxamine E also raises questions regarding its antifungal activity and what impact this compound may have on the antifungal screening of the marine bacterial collection. Desferrioxamines are a structurally related family of tris-hydroxamate siderophores that form strong complexes with ferric iron. Given the condition of the liquid antifungal assay that was performed, there is a high possibility that these siderophores are likely to inhibit the growth of *C. albicans* by iron limitation. In fact, desferrioxamine is known to be used as pharmaceutical agent in the treatment of iron overload in the patients.[4,5]

Therefore, to categorize desferrioxamine as antifungal compound may not be correct since they do not interact directly with fungal cells. Rather, these metabolites prevent cell growth by uptake of available iron which is necessary for the proliferation of *C. albicans*.[6] Iron is an essential nutrient for *C. albicans*, and iron uptake may play a special role in promoting virulent infections.[7] If the above hypothesis is true, then the supply of an excess iron along with desferrioxamine to the liquid antifungal assay should result in no growth inhibition.

After discussion with Dr. Kathy Barbeau at SIO, ferric citrate was suggested as a source of excess iron to be applied to the liquid antifungal assay. Ferric citrate was added to the *C. albicans* cultures in the liquid antifungal assay with desferrioxamine E in 1:1 and 2:1 mol ratio. The result of this antifungal test is shown in Table III.2.4.

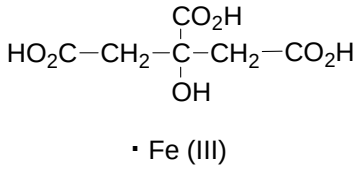

Ferric citrate

Table III.2.4. Antifungal evaluation of desferrioxamine E with added ferric citrate against *C. albicans* (AMBR).

Test Samples	*C. albicans* (AMBR) MIC (μg/mL)
Desferrioxamine E	0.31
Desferrioxamine E with ferric citrate (1:1)	NSA
Desferrioxamine E with ferric citrate (2:1)	NSA
Ferric citrate	NSA

The results indicated that the hypothesis regarding the mechanism of fungal inhibition by iron uptake from siderophores is indeed correct. With excess ferric ion, provided from the added ferric citrate, desferrioxamine E no longer shows inhibition of *C. albicans* (AMBR). This outcome confirms that desferrioxamine E exhibits highly potent antifungal activity in the liquid assay because of its ability to form strong complexes with free iron in the media, and consequently leads to the iron deficient condition which prevents the growth of *C. albicans*.

It has come to our attention that these siderophores may cause a difficult problem in the antifungal screening of marine actinomycete collection. Unlike marine inverterbrates, marine bacteria often produce desferrioxamines as their common metabolites. Since this type of siderophore appears to be non-cytotoxic and exhibit

very potent activity in the liquid antifungal assay, using the selective criteria that were mentioned earlier for choosing promising candidates will likely result in numerous strains that contain these siderophores.

This critical complication will need to be solved. As the reported antifungal activity from the chosen active projects may all derive from the presence of desferrioxamines, the modification of liquid antifungal assay is very crucial in order to remove the unwanted activity caused by this group of compounds. Modification of the assay will be discussed in a later chapter.

References

(1) Mincer, T. J.; Jensen, P. R.; Kauffman, C. A.; Fenical, W. *Appl. Environ. Microbiol.* **2002**, *68*, 5005-5011.

(2) Gontang, E. A.; Fenical, W.; Jensen, P. R. *Appl. Environ. Microbiol.* **2007**, *73*, 3272-3282.

(3) Berner, I.; Konetschny-Rapp, S.; Jung, G.; Winkelmann, G. *Biol. Met.* **1988**, *1*, 51-56.

(4) Cohen, A. R. *Hematology* **2006**, *1*, 42-47.

(5) Barton, J. C. *Curr. Gastroenterol. Rep.* **2007**, *9*, 74-82.

(6) Lee, J. H.; Han, Y. *Arch. Pharm. Res*. **2006**, *29*, 249-255.

(7) Ramanan, N.; Wang, Y. *Science*. **2000**, *288*, 1062-1064.

III.3

Actinoquinolines A and B, new quinoline alkaloids produced by the marine actinomycete CNP975

Introduction

The quinoline skeleton is a bicyclic aromatic compound that contains a nitrogen atom in a place of a carbon adjacent to the ring fusion; it is also a weak tertiary base.[1] Quinoline and isoquinoline alkaloids are one of the largest groups of alkaloids (the other being indole alkaloids and their derivatives), and they have been isolated from various sources including, plants, cyanobacteria, fungi, marine invertebrates, marine microbes, and amphibians.[2-5] Quinoline alkaloids have also been widely used in medical applications and in the chemical industry.[2]

As part of my interest to identify selective antifungal metabolites, actinomycete strains isolated from marine sediments collected from various locations were investigated carefully. From the results from the first antifungal screening of the marine microbial collection (Chapter III.1), marine actinomycete strain CNP975 was one of the 13 promising projects that was chosen from approximately 800 crude extracts to be further examined. This project was found to be active in the antifungal assay against *C. albicans*, while exhibited negligible cytotoxicity in the HCT-116 colon carcinoma cytotoxicity assay. This project was selected over the other 12 strains because the "active" chromatography fractions yielded interesting ^{1}H NMR spectra and unique UV spectral data (Figure III.3.2). In this chapter, we describe the isolation, purification and structural elucidation of two new quinoline alkaloids, actinoquinolines A (**1**) and B (**2**) from marine actinomycete strain CNP975.

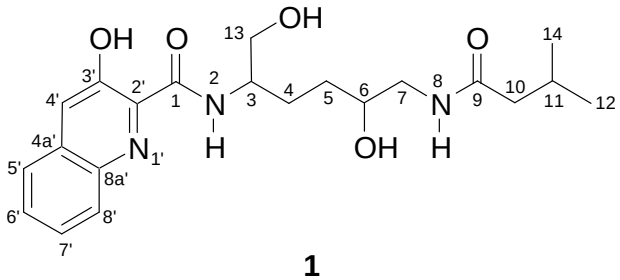

1

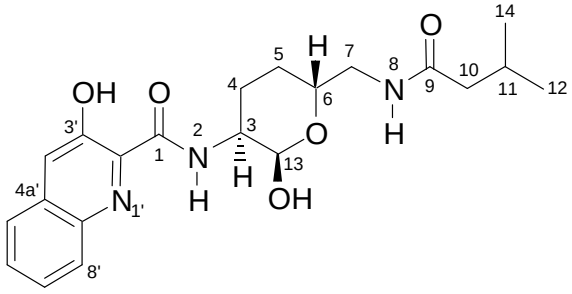

2

Figure III.3.1. The structures of actinoquinolines A (**1**) and B (**2**)

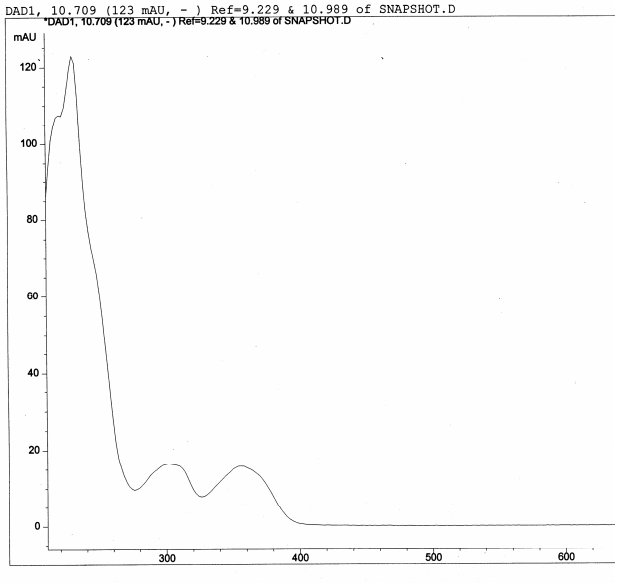

Figure III.3.2. The UV spectrum of actinoquinoline A

Results and Discussion

Marine actinomycete strain CNP975 was isolated from marine sediments collected from La Jolla, San Diego. The study of this strain began with the chemical investigation of a 1L culture, as mentioned in chapter III.1 (Table III.1.4). The crude acetone extracts were partitioned by HP20SS column chromatography into 5 fractions eluted with 20%, 40%, 60%, 80% and 100% acetone-water mixtures. The most active fraction with the lowest MIC from the result of antifungal assay against *C. albicans* (AMBR) was the 80% acetone fraction (MIC $\leq$ 3.9 μg/mL). This partially purified material was further separated on reversed-phase C_{18} HPLC to yield the potentially new metabolite with antifungal activity at MIC of 7.8 μg/mL. Unfortunately, the yield of the target compound was extremely low, less than 0.3 mg, which is insufficient for NMR analysis.

Consequently, a 35L regrow of strain CNP975 provided enough crude extract facilitating the isolation and structure elucidation of the target compounds. The crude acetone extract was fractionated using HP20SS resin, subsequently eluting 9 fractions with 20% to 100% acetone-water mixtures. The 80% acetone fraction, which was found to exhibit the most potent antifungal activity (MIC $\leq$ 3.9 μg/mL), was subjected to further purification by reversed-phase gradient C_{18} HPLC to yield actinoquinolines A (**1**, 4.6 mg) and B (**2**, 1.1 mg).

Actinoquinoline A (**1**) was isolated as an amorphous green oil, which analyzed for the molecular formula $C_{21}H_{29}N_3O_5$ by analysis of NMR spectroscopic data (Table III.3.1) and high-resolution ESITOFMS data ($[M+H]^+$ m/z = 404.2183). The molecular formula of **1** required nine degrees of unsaturation. Initial analysis of ^{13}C NMR data revealed 10 aliphatic, 9 aromatic/olefinic, and possibly 2 quaternary carbonyl carbons. On the basis of the molecular formula, and interpretation of NMR data, those nine degrees of unsaturation were suggested to be assigned to a heteroaromatic ring and two unsaturations from carbonyl groups.

The ^1H NMR spectrum of actinoquinoline A (**1**) measured in acetone-d_6 (Figure III.3.3) illustrated five aromatic proton signals at δ 7.74 (1H, s), 7.87 (1H, m), 7.60 (1H, m), 7.60 (1H, m) and 7.98 (1H, m) that corresponded by HSQC NMR correlation spectroscopy to aromatic carbon signals at δ 120.6 (C-4′), 127.3 (C-5′), 129.4 (C-6′), 128.1 (C-7′) and δ 130.2 (C-8′), respectively. The carbon framework of the quinoline ring was established by analysis of COSY and HMBC NMR spectral data (Figure III.3.4). The connectivity of four aromatic protons (δ 7.87, δ 7.60, δ 7.60 and δ 7.98) was assembled by the interpretation of COSY NMR correlations, while the last singlet aromatic proton at δ 7.74 (s) appeared to be isolated from the others. HMBC NMR correlations from H-6′ to C-4a′, H-7′ to C-8a′, H-5′ to C-4′ and C-4a′, H-8′ to C-8a′, H-4′ to C-2′, C-3′, and C-8a′ were used to establish the quinoline ring structure. The position of nitrogen between C-2′ and C-8a′ was also supported by the ^{13}C chemical shifts of the carbons observed at δ 136.1 and δ 142.1, respectively.

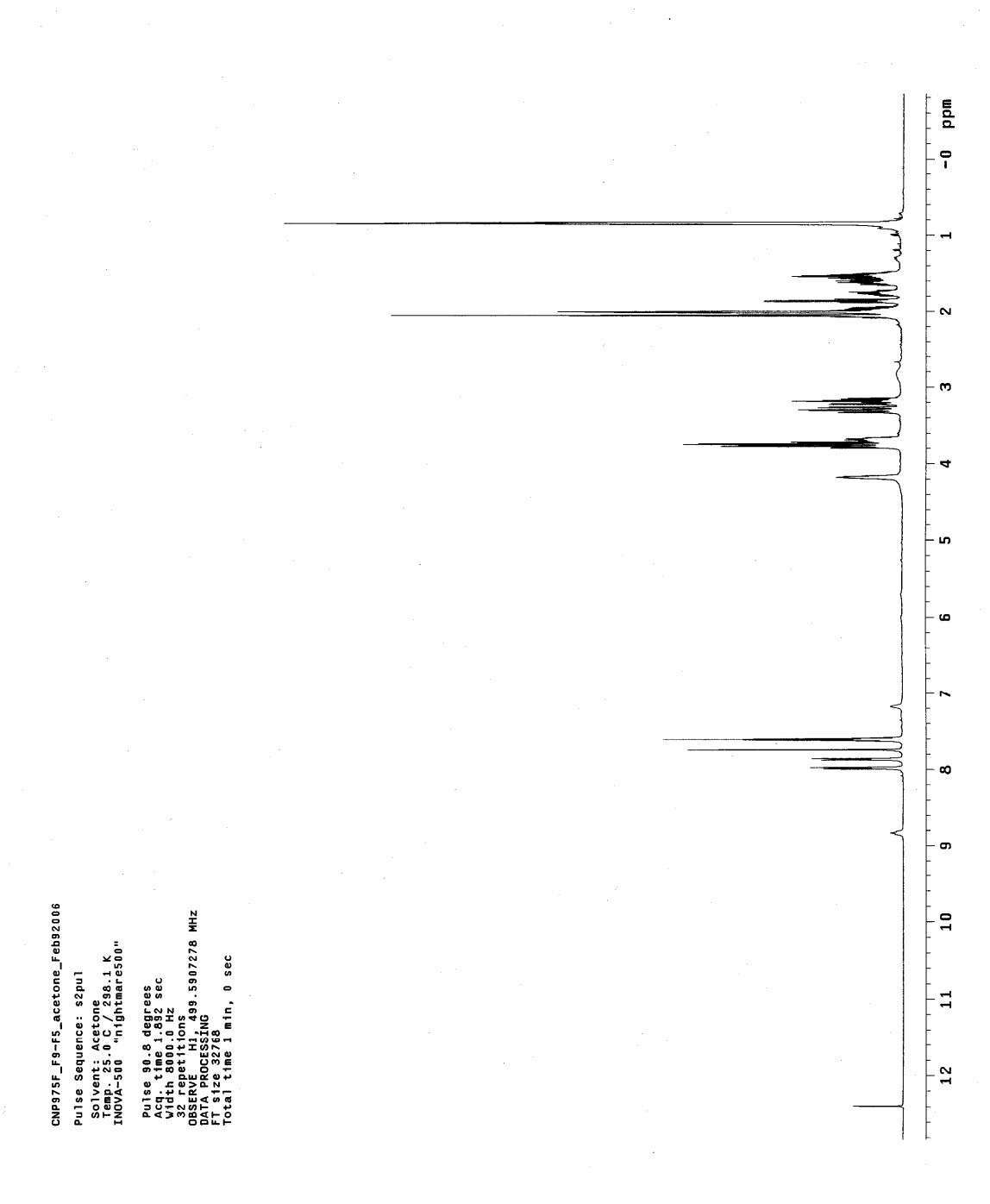

Figure III.3.3. ^{1}H NMR spectrum of actinoquinoline A (**1**) (500 MHz, acetone-d_6)

Table III.3.1. ^{1}H, ^{13}C, COSY, HSQC and HMBC spectroscopic data (500 MHz, acetone-d_6) for actinoquinoline A (**1**)

Position #	δ_C		δ_H	*J* (Hz)	COSY	HMBC
1	169.1	C				
2-NH			8.83 m	10.0	3	
3	52.5	CH	4.17 m		2, 4, 13	C-1, C-4, C-5, C-13
	52.1*	CH	4.17*m		2, 4, 13	C-1, C-4, C-5, C-13
4	28.0	CH_2	1.76 m		3, 5	C-3, C-5, C-6, C-13
			1.97 m		3, 5	C-3, C-5, C-6, C-13
	27.9*	CH_2	1.86* q	8.0	3, 5	C-3, C-5, C-6, C-13
5	32.1	CH_2	1.61 m		4, 6	C-3, C-4, C-6, C-7
	31.9*	CH_2	1.54*m		4, 6	C-3, C-4, C-6, C-7
6	71.6	CH	3.68 m		5, 7	C-4
	71.2*	CH	3.68*m		5, 7	C-4
7	46.1	CH_2	3.18 m	6.0	6, 8	C-5, C-6, C-9
			3.29 m	5.0	6, 8	C-5, C-6, C-9
8-NH			7.18 m		7	
9	173.6	C				
10	45.8	CH_2	2.01 m			C-9, C-11, C-12, C-14
11	26.6	CH	2.01 m		12, 14	C-9, C-10, C-12, C-14
12	22.6	CH_3	0.84 m		11	C-10, C-11, C-14
13	64.2	CH_2	3.75 qd	5.0, 11.5	3	C-3, C-4
14	22.6	CH_3	0.84 m		11	C-10, C-11, C-12
1′						
2′	136.1	C				
3′	154.7	C				
4′	120.6	CH	7.74 s			C-2′, C-3′, C-5′, C-8a′
4a′	132.9	C				
5′	127.3	CH	7.87 m		6′	C-4′, C-4a′, C-6′, C-7′, C-8a′
6′	129.4	CH	7.60 m		5′, 7′	C-4a′, C-8′
7′	128.1	CH	7.60 m		6′, 8′	C-5′, C-8a′
8′	130.2	CH	7.98 m		7′	C-4a′, C-6′, C-8a′
8a′	142.1	C				
3′-OH			12.39 s			C-2′, C-3′, C-4′

***** The chemical shifts of an amide rotamer of actinoquinoline A

The HMBC correlations from hydroxyl proton at δ 12.39 to C-2′, C-3′, and C-4′ indicated the position of OH group in the ring and confirmed the presence of 3-hydroxyquinaldic acid as an aromatic chromophore.[6-7] The side chain was attached to the quinoline ring at C-2′ by the interpretation of both COSY and HMBC correlations. The major portion of the side chain was assigned by COSY correlations from H-2 to H-8 to confirm the connectivity of N-2/C-3/C-4/C-5/C-6/C-7/N-8. The location of carbonyl groups was assigned by HMBC correlations of H-7 and H-11 to C-9, and from H-3 to C-1.

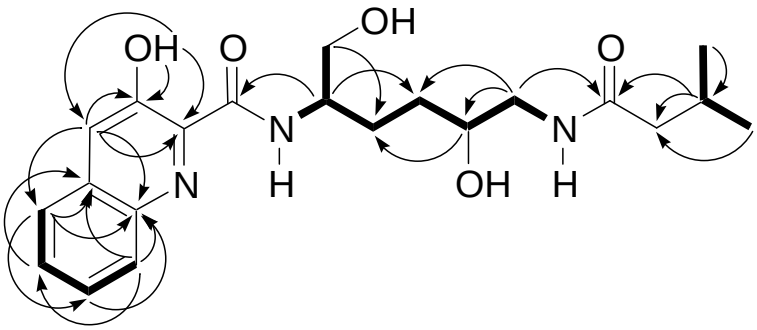

Figure III.3.4. Selected COSY (bold lines) and HMBC (arrows) correlations observed in the NMR spectra for **1**.

The isolation and structure assignment of actinoquinoline A (**1**) was complicated by the fact that the isolated metabolite was observed as a mixture of two amide rotamers. This rotameric mixture, presumable derived by isomers about the C-1 – N-2 bond, was observed in both the HSQC and ^{13}C NMR spectroscopic data. The carbon signals from C-3 to C-6 and their corresponded protons were split into two sets as illustrated in Table III.3.1. Unfortunately, these rotamers could not be stabilized, hence the structure determination had to contend with these spectral complexities.

Actinoquinoline B (**2**) was obtained as a viscous oil that showed a molecular ion at *m*/*z* 400.1887 ($[M–H]^-$) by the high-resolution ESITOFMS. This minor compound was obtained in a very low yield in comparison to actinoquinoline A (**1**). In fact, there were three missing quaternary carbon signals whose peaks were too small to be seen in ^{13}C NMR data. Nevertheless, UV and ^{1}H NMR data (Figure III.3.5) provided obvious evidence that this compound had a similar aromatic chromophore as in **1**. The chemical shifts of five aromatic protons (δ 7.76, δ 7.87, δ 7.62, δ 7.62 and δ 7.99) from ^{1}H NMR in acetone-d_6 were almost exactly identical. The only difference between actinoquinoline A and B was seen in the side chain.

COSY and HMBC NMR correlation data (Figure III.3.6) allowed the major portion of the side chain of this molecule to be assembled. The side chain of actinoquinoline B was almost similar to **1** except that it formed a six member cyclic ether ring instead of the linear chain. Two methyl signals at δ 0.96 (H-12 and H-14) showed HMBC correlations to methylene and methine carbons at C-10 and C-11, respectively.

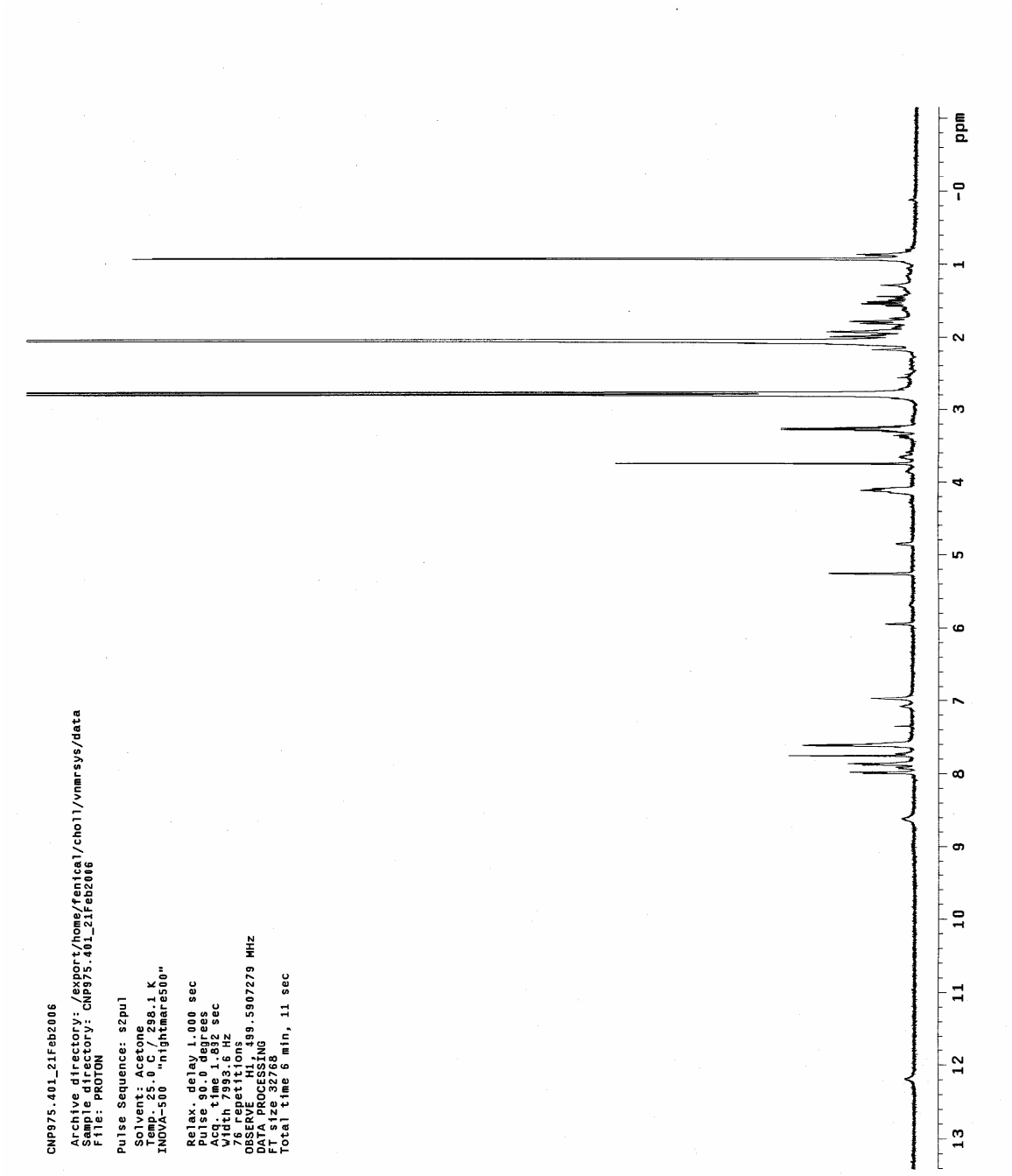

Figure III.3.5. ^{1}H NMR spectrum of actinoquinoline B (**2**) (500 MHz, Acetone-d_6)

Table III.3.2. ^{1}H, ^{13}C, COSY, HSQC and HMBC NMR spectroscopic data (500 MHz, methanol-d_4) for actinoquinoline B (**2**)

Position #	δ_C		δ_H	*J* (Hz)	COSY	HMBC
1		C				
2-NH						
3	50.1	CH	4.16 m		4, 13	
4	24.8	CH_2	1.92 m		3, 5	
			2.00 m			
5	29.2	CH_2	1.51 m		4, 6	C-4, C-6
			1.76 m		4, 6	
6	67.8	CH	4.09 m		5, 7	
7	44.7	CH_2	3.24 m		6	C-5, C-6, C-9
			3.32 m		6	C-5, C-6, C-9
8-NH						
9	175.7	C				
10	46.3	CH_2	2.08 m			C-9, C-11, C-12, C-14
11	27.4	CH	2.07 m		12, 14	C-9, C-10, C-12, C-14
12	22.8	CH_3	0.96 d	6.5	11	C-10, C-11, C-14
13	92.1	CH	5.21 d	3.5	3	C-4, C-6
14	22.8	CH_3	0.96 d	6.5	11	C-10, C-11, C-12
1′						
2′		C				
3′		C				
4′	121.8	CH	7.56 s			C-8a′
4a′	133.7	C				
5′	126.9	CH	7.69 m		6′	C-7′, C-8a′
6′	129.2	CH	7.47 m		5′, 7′	
7′	127.2	CH	7.47 m		6′, 8′	
8′	130.4	CH	7.97 m		7′	C-4a′, C-6′
8a′	142.1	C				
3′-OH						

The framework of an ether ring was established by COSY correlations which defined the connectivity of the carbon skeleton as C-13/C-3/C-4/C-5/C-6. A three-bond HMBC correlation from the methine signal at H-13 (δ 5.21) to C-6, further supported the presence of an ether ring. The position of oxygen was placed between C-6 (δ 67.8) and C-13 (δ 92.1), which was consistent with their chemical shifts.

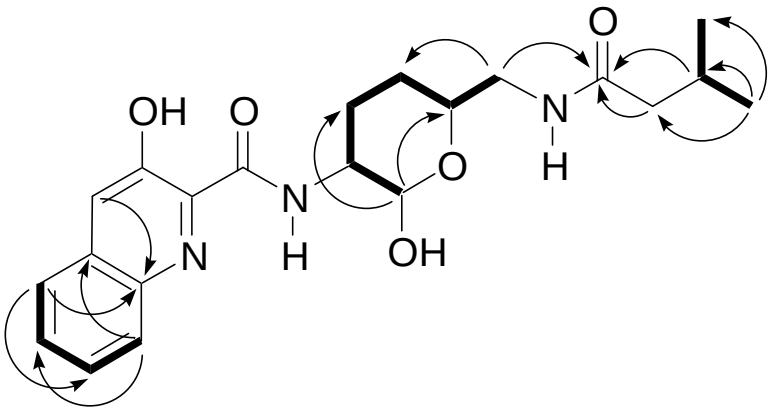

Figure III.3.6. Selected COSY (bold lines) and HMBC (arrows) correlations observed in the NMR spectra for **2**.

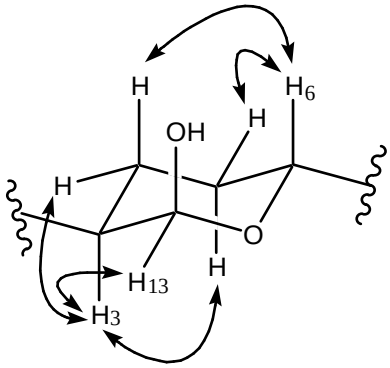

Figure III.3.7. Assigned relative stereochemistry of **2** established by selected ROESY correlations.

The relative stereochemistry of actinoquinoline B (**2**) was determined by interpretation of ROESY experimental data that illustrated key correlations forming the chair pyranose ring (Figure III.3.7.). The ROESY correlations between H-3 (δ 4.16) and H13 (δ 5.21) confirmed that both proton signals were on the same side of the ring. H-3 was also found to show ROESY correlations to H-4 (δ 1.92) and H-5 (δ 1.51). In contrast, a ROESY correlation between H-6 (δ 4.09) and H-13 was not observed, while H-6 showed correlations to H-4 (δ 2.00) and H-5 (δ 1.76). According to these ROESY NMR data, it can be deduced that H-3 and H-13 are on the same side of the cyclic ether ring while H-6 was on the opposite side.

Since the ^{13}C NMR data of **2** were incomplete, the structure assigned was established based only on the available data. Therefore, the proposed structure of **2** must be considered unconfirmed.

Biological Activity

In this study, actinoquinolines A (**1**) and B (**2**) were evaluated for their capability to inhibit both wild-type and amphotericin B-resistant strains of *C. albicans*. Cytotoxic activities against the HCT-116 human colon tumor cell line were also tested. Actinoquinolines were initially thought to be potent antifungal compounds. However, after the purification process by the reversed phase HPLC, both **1** and **2** were discovered to be no longer active in the liquid antifungal assay against both strains of *C. albicans*. The careful inspection of LCMS and ^{1}H NMR spectral data indicated that the partially purified fraction that was tested in the beginning, contained desferrioxamines which were likely to be the metabolites that caused the antifungal activity. These two quinoline alkaloids were also evaluated in the cytotoxicity assay but they did not exhibit any cytotoxicity against HCT-116 colon carcinoma.

This, again, provides an excellent example of how siderophores can affect the screening results. Even if there is only a very small amount of these contaminates, it can easily result in the misinterpretation of the antifungal potency of the test samples. Despite the fact that the biological activity of these quinoline alkaloids has yet to be defined, it appears that this group of metabolites may be common among certain species of actinomycetes. According to their distinct UV spectrum and ^{1}H NMR, these quinoline alkaloids were rather easy to distinguish. Out of 13 promising projects from the first screening, other derivatives of these quinoline alkaloids have also been found in the other actinomycete strains including CNP962 and CNP967. This discovery suggests that this group of quinoline alkaloids may share a similar functionality or common role among marine actinomycetes.

Experimental Section

General Experimental Procedures. Optical rotations were measured on a Rudolph Autopol III polarimeter. UV spectra were obtained using Varian Cary 50 Bio UV-Visible spectrophotometer. Infrared spectra were recorded on a Nicolet IR100 FT-IR spectrometer. ^{1}H, ^{13}C, COSY, HSQC, HMBC and ROESY NMR spectra were recorded on a Varian INOVA 500 MHz spectrometer. High-resolution mass measurements were obtained on Agilent ESI-TOF instruments at the Scripps Research Institute, La Jolla. All solvents were distilled prior to being used.

Collection and Phylogenetic Analysis of strain CNP975. The marine actinomycete, designated CNP975, was isolated from marine sediment sample, collected in La Jolla, San Diego by Alejandra Davo Prieto. Phylogenetic analysis has not been performed on this strain, hence no confident taxonomic assignment can be made.

Fermentation and Extraction. Strain CNP975 was cultured at 27 ^{o}C with shaking at 250 rpm in 35 x 2.8-L Fernbach flasks each containing 1 L of TCG medium. After 6 days, the organic constituents from a 35 L culture were extracted by a solid-phase extraction method using Amberlite XAD-7 resin. The crude extract was prepared by washing the resin with acetone and concentrated by rotary evaporation.

Isolation and Purification. The crude acetone extract (17 g) from 35L cultures of CNP975 was dried *in vacuo* to obtain a sticky brown substance, which was

fractionated by HP20SS column chromatography (acetone/water) to yield nine fractions (20%, 30%, 40%, 50%, 60%, 70%, 80%, 90%, and 100% acetone mixtures). All nine fractions were concentrated to dryness and tested in a standard microdilution antifungal assay. The fraction eluted with 90% acetone-water (1 g) was found to possess very potent antifungal activity (MIC ≤ 3.9 μg/mL), and was subjected to further purification by reversed-phase HPLC (Dynamax C_{18} semi-preparative, 3 mL/min; 30% ACN/H_2O over 30 min, 30–40% ACN/H_2O over 10 min, 40–100% ACN/H_2O over 20 min) to yield, actinoquinolines A (**1**, 4.6 mg) and B (**2**, 1.1 mg).

Actinoquinoline A (**1**): green oil; $[\alpha]_D$ +3.5 (*c* 0.2, MeOH); UV (MeOH) λ_{max} (log ε) 356 nm (3.69), 298.1 (3.69), 231 (4.58), 220 (4.53); IR ν_{max} (KBr) 3343, 2957, 2872, 1655, 1538, 1445, 1334, 735 cm^{-1}; NMR data, see Table III.3.1; EIMS $[M+H]^+$ *m*/*z* 404; HRESITOFMS $[M+H]^+$ *m*/*z* 404.2183 (calcd for $C_{21}H_{30}N_3O_5$, 404.2185)

Actinoquinoline B (**2**): green oil; $[\alpha]_D$ +16.7 (*c* 0.03, MeOH); UV (MeOH) λ_{max} (log ε) 357.1 nm (3.59), 298.1 (3.61), 231 (4.48), 220 (4.43); IR ν_{max} (KBr) 3326, 2957, 1656, 1532, 1445, 1334, 1069, 750 cm^{-1}; NMR data, see Table III.3.2 ; EIMS $[M+Na]^+$ *m*/*z* 424; HRESITOFMS $[M–H]^-$ *m*/*z* 400.1887 (calcd for $C_{21}H_{26}N_3O_5$, 400.1872)

References

(1) Dembitsky, V. M. *Lipids* **2005**, *40*, 1081-1105.

(2) Michael, J. P. *Nat. Prod. Rep.* **2004**, *21*, 650-668.

(3) Von Nussbaum, F. *Angew. Chem. Int. Ed. Engl.* **2003**, *42*, 3068-3071.

(4) Daly, J. W.; Noimai, N.; Kongkathip, B.; Kongkathip, N.; Wilham, J. M.; Garraffo, H. M.; Kaneko, T.; Spande, T.F., Nimit, Y.; Nabhitabhata, J. *et al*. *Toxicon* **2004**, *44*, 805-815.

(5) Orjala, J.; Gerwick, W. H. *Phytochemistry* **1997**, *45*, 1087-1090.

(6) Konishi, M.; Ohkuma, H.; Sakai, F.; Tsuno, T.; Koshiyama, H.; Naito, T.; Kawaguchi, H. *J. Antibiot.* **1981**, *34*, 148-159.

(7) Perez Baz, J.; Canedo, L. M.; Fernandez Puentes, J. L.; Silva Elipe, M. V. *J. Antibiot.* **1997**, *50*, 738-741.

III.4

Antifungal bioassay-guided screening of marine actinomycetes using the modified liquid antifungal assay

Introduction

The liquid dilution antifungal assay was chosen as the standard method for the bioassay-guided screening of marine microbial extracts due to the accuracy of the results obtained. However, it was discovered that there was an unexpected pitfall regarding the use of this liquid assay that could consequently become a big obstacle in conducting screening for new antifungal compounds. As it was demonstrated in chapter III.2, given the selective criteria for good antifungal but low HCT-116 cytotoxic activity, the selection of the promising bacterial strains led to the isolation of a known metabolite, desferrioxamine E[1]. Desferrioxamines are iron-chelating compounds that are produced and secreted by many actinomycetes including species of *Streptomyces*, *Nocardia*, and *Micromonospora*.[2] This group of siderophores is considered to be common among actinomycetes and is usually found to be produced in significant amounts.

The problem regarding this type of siderophores is that even trace quantities can exhibit extremely potent antifungal activity (MIC < 1 μg/mL) in the liquid assay due to their abilities to uptake iron, eventually leading to the inhibition of fungal cell growth. Hence, all actinomycete strains that produce these siderophores will show up as promising candidates in the antifungal screening. In the worst situation, all of the chosen active strains may exhibit antifungal activity because of the presence of these and perhaps other siderophore molecules. As a result, the modification of the liquid antifungal assay to remove the undesired effect from these siderophores was considered a crucial component of this thesis research.

The modification of the liquid antifungal assay

Since it has been shown that desferrioxamines inhibit *C. albicans* growth by means of iron limitation, the best way to modify liquid antifungal assay is to provide excess iron to the media so that it can counteract the effect of siderophores. Ferric citrate appears to be an appropriate candidate for the ferric ion source as it does not interfere with cell proliferation. However, it was, nonetheless important to test ferric citrate in the liquid assay at different concentrations to examine its impact on the growth of *C. albicans*. It is also important to determine that ferric citrate addition will not alter the antifungal activity of other possible active metabolites. Consequently, several experiments were performed to confirm that ferric citrate will be suitable to use in the modified assay.

In the first experiment, 5 μl of ferric citrate solution at concentrations of 10 mg/mL, 20 mg/mL, and 40 mg/mL, were added to the liquid antifungal assay. The ferric citrate solution was prepared by dissolving the ferric citrate powder in DMSO or DI water. The serial dilution bioassay was performed with added ferric citrate and the results showed no inhibition of *Candida* growth. This test indicated that the addition of ferric citrate can be tolerated in the *C. albicans* bioassay.

As shown in chapter III.2, the addition of ferric citrate with desferrioxamine E can suppress fungal inhibition caused by the iron limitation. In addition to desferrioxamine E, ferric citrate has also been tested with another derivative, desferrioxamine B^3, and the results were the same. Without an addition of ferric citrate, desferrrioxamine B exhibited MIC value at less than 1 μg/mL, however, after the addition of free iron, inhibition against *C. albicans* was not observed. Hence, it is

confirmed that the additional supply of iron from ferric citrate can cancel the inhibitory effect by desferrioxamines and, perhaps, other siderophores.

As for the final test, ferric citrate was added to the liquid antifungal assay in the presence of the known antifungal drug amphotericin B. The MIC value of amphotericin B derived from this bioassay was identical without added ferric citrate. The similar outcomes were also obtained when ferric citrate was added to the assay with the previously tested crude extracts that contained antifungal active metabolites, which were not siderophores. Therefore, it can be assumed that ferric citrate will probably not interfere with the other antifungal active compounds or alter the potency in fungal inhibition.

After several trials of the liquid antifungal assay with ferric citrate, it was decided that the amount of ferric citrate to be added for each sample will depend on the concentration of the test materials. For example, for crude extracts tested at a concentration of 10 mg/mL, additional ferric citrate with at least the same concentration will be required.

Antifungal screening of marine actinomycetes by the modified liquid assay

After the modified antifungal assay had been tested and functioning properly, it is crucial to retest the previously selected projects that were discussed in chapter III.1. The results of the first screening of the microbial collection gave 13 promising bacterial strains that were discovered to exhibit very potent antifungal activity with negligible cytotoxicity. The crude extract from the regrowth of 1L culture for each strain had already been partitioned using HP20SS column chromatography and tested

in the regular liquid antifungal assay. (Figure III.1.4) At this time, the active fractions from those 13 marine actinomycete strains were reevaluated with the newly modified liquid antifungal assay.

The results of the antifungal screening using the iron-modified method proved to be very disappointing. All of the chosen active fractions from 13 microbial strains were discovered to be inactive after an addition of ferric citrate to the antifungal assay. None exhibited antifungal activity, which can only mean that the metabolites that cause inhibition against *C. albicans* from those 13 projects are likely to be siderophores. The inspection by LCMS and ^{1}H NMR has led to the same conclusion. As a result, it was necessary to go back and rescreen the microbial collection again using the newly developed method in order to search for a better antifungal project whose activity does not come from siderophores.

The second screening of marine microbial collection

Two random mother plates (Box #136 and #148) that contained crude microbial extracts were chosen for screening with the modified liquid antifungal assays. The initial screening of crude extracts for antifungal active metabolites was carried out at a single concentration screening at MIC $\leq$ 150μg/mL. Out of the total of 160 test samples, 76 of them (48%) exhibited antifungal activity at this concentration.

The serial dilution method of the modified liquid antifungal assay was performed with these 76 samples at the concentration of 4 mg/mL, to determine the MIC value of each selective strain. The result of this modified antifungal screening was illustrated in Figure III.4.1.

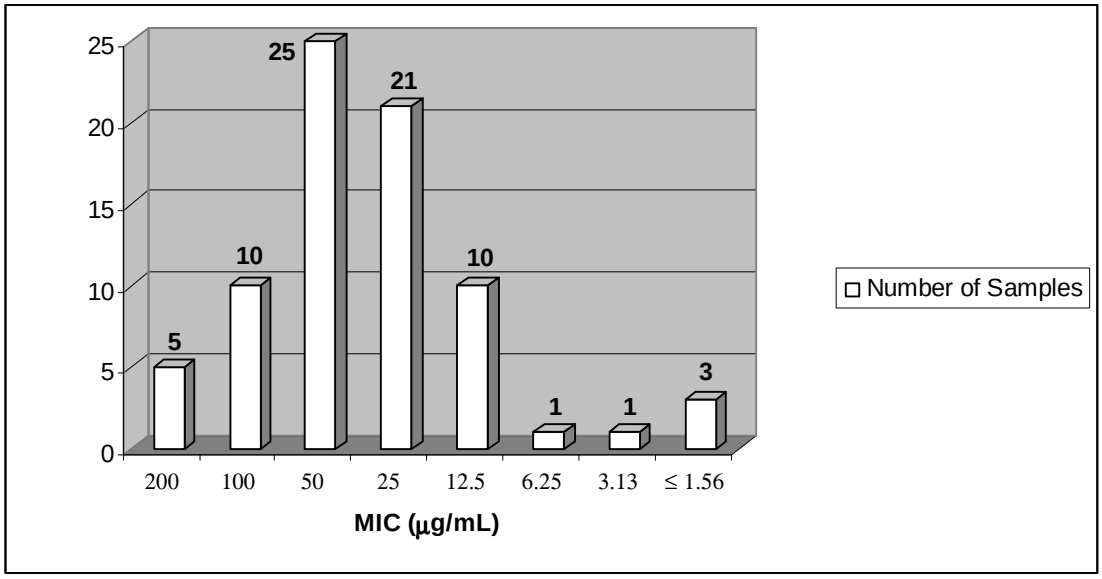

Figure III.4.1. Screening results of 76 marine microbial extracts from a modified liquid antifungal assay against *C. albicans* (AMBR).

Of the 76 active samples that were evaluated in the liquid antifungal assay, only 5 bacterial extracts (7%) exhibited potent antifungal activity against *C. albicans* with MIC value less than 7 μg/mL. These results included both cytotoxic and non-cytotoxic bacterial strains, and yet the number of active crude extracts was very low. The remaining 71 samples were found to exhibit moderate to weak antifungal activity with MIC > 12 μg/mL. In fact, approximately 53% of the total extracts showed weak inhibition against *C. albicans* with MIC values over 50 μg/mL. Since the antifungal hit rate was much lower in the modified liquid assay, the promising candidates that were chosen for further investigation included both cytotoxic and non-cytotoxic strains.

Table III.4.1. The details of antifungal screening results of the chosen marine actinomycete strains for the regrowth of 1L cultures.

Box #	Strain #	Media	HCT-116 (% Survival)	*C. albicans* (AMBR) MIC (µg/mL)
136	CNQ040	TCG	71	25
136	CNQ041	TCG	100	50
136	CNQ041	AlBFe-C	3	25
136	CNQ041	AlBFe+C	19	50
136	CNQ045	AlBFe-C	26	50
136	CNQ045	AlBFe+C	13	25
136	CNQ087	AlBFe-C	4	≤ 1.56
136	CNQ089	TCG	17	12.5
136	CNQ089	AlBFe-C	3	12.5
136	CNQ091	AlBFe-C	20	50
136	CNQ094	TCG	47	50
136	CNQ094	AlBFe-C	85	100
136	CNQ095	AlBFe-C	4	50
136	CNQ095	TCG	1	25
136	CNQ095	AlBFe+C	2	25
136	CNQ097	TCG	2	12.5
136	CNQ097	AlBFe-C	1	12.5
136	CNQ100	TCG	2	25
136	CNQ100	AlBFe+C	100	50
136	CNQ104	AlBFe+C	3	12.5
136	CNQ110	AlBFe+C	57	25
136	CNQ111	AlBFe+C	1	25
136	CNQ111	AlBFe-C	2	12.5
136	CNR292	TCG	40	25
148	CNQ449	AlBFe+C	78	50
148	CNQ450	AlBFe+C	84	50
148	CNQ456	TCG	88	50
148	CNQ456	AlBFe-C	98	50
148	CNQ456	Mar2DPh	92	25
148	CNQ461	TCG	88	50
148	CNQ506	TCG	85	50
148	CNQ506	AlBFe+C	99	100
148	CNQ551	TCG	13	3.13
148	CNQ551	AlBFe-C	11	≤ 1.56
148	CNQ598	AlBFe-C	93	50
148	CNQ617	Mar2DPh	74	25
148	CNQ617	AlBFe-C	97	50
148	CNQ625	AlBFe-C	71	25

After several antifungal screenings, 23 promising actinomycete strains (Table III.4.1) from 76 active extracts were chosen to be regrown in 1L culture volumes. The crude acetone extracts derived from the regrowth of 1L recultures from these bacterial strains were partitioned by HP20SS column chromatography. The column was eluted with 20%, 40%, 60%, 80% and 100% acetone-water gradient to yield five fractions for each selective strain. The partially purified fractions were dried *in vacuo* and evaluated in the modified liquid antifungal assay. Table III.4.2 demonstrates the screening details of these promising bacterial strains with their corresponding HP20SS fractions and antifungal activities. Analysis of these active fractions by both LCMS and ^{1}H NMR methods data gave better insight to determine which project should be given higher priority for investigation.

Unfortunately, the majority of the selective strains exhibited very weak antifungal activity, even after the fractionation of crude materials by HP20SS column. A few of the cultures did not retain antifungal activity after the regrowth, while most of the others still showed antifungal activity but at much weaker levels. This result suggested that the number of marine actinomycete strains that produced potent antifungal active metabolites is in fact very small, and it will require a great effort to find both chemically novel and therapeutically effective compounds. Hence, in order to find a promising project with potent antifungal activity may require a lot more screening of microbial collections as the modified assay proved that the number of antifungal active strains after removing the inhibitory effect by siderophores is much lower than it was expected.

Table III.4.2. Antifungal screening results of HP20SS fractions from extracts of the regrowth of 1L culture of 23 marine actinomycete strains.

CNQ040	MIC (μg/mL)	HCT-116 (IC_{50})
20%	NSA	NSA
40%	NSA	NSA
60%	250	NSA
80%	NSA	NSA
100%	NSA	NSA

CNQ041	MIC (μg/mL)	HCT-116 (IC_{50})
20%	NSA	NSA
40%	NSA	NSA
60%	62.5	NSA
80%	125	NSA
100%	NSA	NSA

CNQ045	MIC (μg/mL)	HCT-116 (IC_{50})
20%	NSA	NSA
40%	NSA	NSA
60%	250	NSA
80%	250	62.5
100%	NSA	NSA

CNQ087	MIC (μg/mL)	HCT-116 (IC_{50})
20%	NSA	N/A
40%	NSA	N/A
60%	31.3	N/A
80%	≤ 3.9	N/A
100%	7.8	N/A

CNQ089	MIC (μg/mL)	HCT-116 (IC_{50})
20%	NSA	NSA
40%	250	86.4
60%	62.5	NSA
80%	125	NSA
100%	NSA	NSA

CNQ091	MIC (μg/mL)	HCT-116 (IC_{50})
20%	NSA	NSA
40%	NSA	NSA
60%	250	NSA
80%	NSA	NSA
100%	NSA	NSA

CNQ094	MIC (μg/mL)	HCT-116 (IC_{50})
20%	NSA	NSA
40%	NSA	NSA
60%	250	NSA
80%	250	NSA
100%	NSA	NSA

CNQ095	MIC (μg/mL)	HCT-116 (IC_{50})
20%	62.5	NSA
40%	15.6	NSA
60%	15.6	NSA
80%	15.6	NSA
100%	125	NSA

CNQ097	MIC (μg/mL)	HCT-116 (IC_{50})
20%	NSA	NSA
40%	NSA	NSA
60%	NSA	NSA
80%	62.5	NSA
100%	NSA	NSA

CNQ100	MIC (μg/mL)	HCT-116 (IC_{50})
20%	NSA	N/A
40%	NSA	N/A
60%	125	N/A
80%	31.3	N/A
100%	62.5	N/A

CNQ104	MIC (μg/mL)	HCT-116 (IC_{50})
20%	NSA	NSA
40%	NSA	NSA
60%	250	NSA
80%	250	NSA
100%	NSA	NSA

CNQ110	MIC (μg/mL)	HCT-116 (IC_{50})
20%	NSA	NSA
40%	NSA	NSA
60%	250	NSA
80%	250	NSA
100%	NSA	NSA

CNQ111	MIC (μg/mL)	HCT-116 (IC_{50})
20%	NSA	NSA
40%	NSA	NSA
60%	NSA	NSA
80%	250	NSA
100%	NSA	NSA

CNQ449	MIC (μg/mL)	HCT-116 (IC_{50})
20%	NSA	NSA
40%	NSA	NSA
60%	NSA	NSA
80%	NSA	NSA
100%	NSA	NSA

Table III.4.2. Continued.

CNQ450	MIC (μg/mL)	HCT-116 (IC_{50})
20%	NSA	NSA
40%	NSA	NSA
60%	NSA	NSA
80%	250	NSA
100%	31.3	NSA

CNQ456	MIC (μg/mL)	HCT-116 (IC_{50})
20%	NSA	NSA
40%	NSA	NSA
60%	250	67.2
80%	62.5	19.5
100%	NSA	75

CNQ461	MIC (μg/mL)	HCT-116 (IC_{50})
20%	NSA	NSA
40%	NSA	NSA
60%	NSA	NSA
80%	NSA	NSA
100%	NSA	NSA

CNQ506	MIC (μg/mL)	HCT-116 (IC_{50})
20%	250	NSA
40%	250	NSA
60%	7.8	NSA
80%	62.5	NSA
100%	NSA	NSA

CNQ551	MIC (μg/mL)	HCT-116 (IC_{50})
20%	NSA	N/A
40%	NSA	N/A
60%	25	N/A
80%	≤ 3.9	N/A
100%	0.78	N/A

CNQ598	MIC (μg/mL)	HCT-116 (IC_{50})
20%	NSA	NSA
40%	NSA	NSA
60%	31.3	NSA
80%	NSA	NSA
100%	NSA	NSA

CNQ625	MIC (μg/mL)	HCT-116 (IC_{50})
20%	NSA	NSA
40%	NSA	NSA
60%	NSA	NSA
80%	NSA	NSA
100%	NSA	NSA

CNR292	MIC (μg/mL)	HCT-116 (IC_{50})
20%	NSA	NSA
40%	NSA	NSA
60%	125	NSA
80%	250	NSA
100%	250	NSA

CNQ617	MIC (μg/mL)	HCT-116 (IC_{50})
20%	NSA	NSA
40%	NSA	NSA
60%	NSA	NSA
60%	125	14.2
80%	250	12.9
80%	NSA	0.75
80%	NSA	18.7
100%	NSA	NSA

Basing upon the obtained results, an initial investigation using LCMS and ^{1}H NMR spectroscopy has been performed on these active fractions. Two most promising actinomycete strains CNQ087 and CNQ551, which exhibited the highest antifungal activities with MIC values less than 3.9 μg/mL, were discovered to possess a previously reported anticancer metabolite, staurosporine which was originally isolated in 1977 from the bacterium *Streptomyces staurosporeus* by Omura et al.[4] Since staurosporine was also known to be very antifungal, these two projects were not

further pursued. Nevertheless, it has been proved that the modified antifungal assay successfully eliminated the antifungal projects with siderophores.

Despite the fact that most of the derived actinomycete strains exhibit rather weak antifungal activity, several projects including CNQ617, CNQ456 and CNQ506 appear to be interesting and have a high potential for the isolation of new metabolites on the basis of data analysis by LCMS and ^{1}H NMR spectroscopy. A project involving strain CNQ617 will be described in detail in the following chapter.

References

(1) Berner, I.; Konetschny-Rapp, S.; Jung, G.; Winkelmann, G. *Biol. Met.* **1988**, *1*, 51-56.

(2) Zahner, H.; Bachmann, E.; Hutter, R.; Nfuesch, J. *Pathol. Microbiol.* **1962**, *25*, 708-736.

(3) Bickel, H.; Bosshardt, R.; Gaumann, E.; Reusser, P.; Vischer, E.; Voser, W.; Wettstein, A.; Zahner, H. *Helv. Chim. Acta.* **1960**, *43*, 2119-2128.

(4) Omura, S.; Iwai, Y.; Hirano, A.; Nakagawa, A.; Awaya, J.; Tsuchiya, H.; Takahashi, Y.; Masuma, R. *J. Antibiot.* **1977**, *30*, 275-282.

III.5

Novel bioactive secondary metabolites from the marine actinomycete strain CNQ617 (a member of the new MAR 3 clade)

Abstract

Two novel cytotoxic macrocycles, marineosins A and B, along with an uncommon bacteria-derived sesterterpenoid, marinoquinoline A, have been isolated from the culture of a marine actinomycete CNQ617 (MAR3 clade) recovered from a sediment sample collected in San Diego. The structures of these new metabolites were assigned using spectroscopic data emphasizing the interpretation of 2D NMR experiments. Marineosin A exhibited very potent cytotoxicity against human colon carcinoma (HCT-116) cells with an IC_{50} value of 0.5 μM, while it did not show any antifungal activity against both amphotericin B-resistant and wild-type strains of *Candida albicans*.

Introduction

Marine actinomycetes have been perhaps the most prolific source of bioactive secondary metabolites, which have had a great impact in many areas, particularly in the field of pharmaceutical drug development.[1] Since the decline in the discovery of novel lead compounds from terrestrial actinomycetes, which began in the early 1990s, actinomycetes from marine sources have become a growing focus as a new source for bioactive agents.[2] The search for rare or novel actinomycete taxa has also gained importance as well as the development of various innovative bioassays to find unique metabolites. The first obligate marine actinomycete genus, *Salinispora*, which requires sea water for growth and is highly prolific in the production of secondary metabolites, has been recently discovered.[3] In addition to *Salinispora* sp., there are other taxonomically unique strains of marine actinomycetes that have remained largely unexplored both chemically and biologically. Among those is the phylogenetically distinct group, MAR3[4], which is part of the family Streptomycetaceae. Chemical studies of a member of this new taxon will be the main focus of this chapter.

As a result of the secondary screening of the marine microbial collection using the modified liquid dilution antifungal assay, strain CNQ617, a member of the MAR3 group, was chosen to be further investigated. Initial screening indicated that extracts of CNQ617 exhibited good antifungal activity with insignificant cytotoxic activity. Unfortunately, the obtained results on the second recultivation proved to be very different. Unexpectedly, the new crude extract of strain CNQ617 was found to be significantly cytotoxic (IC_{50} < 10 μg/mL) in the HCT-116 assay, while the antifungal

activity was shown to be extremely weak with MIC value over 100 μg/mL. Therefore, instead of pursuing the antifungal metabolite, the focus was changed toward the isolation of the cytotoxic compound. Bioassay-guided fractionation of the crude extract using HCT-116 human colon carcinoma cells as a screening method, led to the isolation of two novel cytotoxic macrocycles, marineosin A (**1**) and B (**2**). In addition, an uncommon bacterial sesterterpenoid, marinoquinoline A (**3**), has also been isolated from this same strain. In this chapter, the isolation, structure elucidation, and biological activities of these new metabolites will be described.

Results and Discussion

Marineosin A (**1**) was analyzed by EI high-resolution mass spectrometry for the molecular formula $C_{25}H_{35}N_3O_2$ ($[M]^+$ *m*/*z* 409.2726). The LRESIMS also showed ions that analyzed for $[M+H]^+$ at *m*/*z* 410. This molecular formula was further supported by ^1H and ^{13}C NMR spectral data (Table III.5.1). The obtained molecular formula implied that there were ten degrees of unsaturation. The initial analysis of DEPT and ^{13}C NMR spectrum indicated that the majority of proton signals are methylene protons. The ^1H NMR spectrum of **1** (Figure III.5.2) measured in acetone-d_6 also demonstrated five aromatic protons at δ 5.44 (t, *J* = 3 Hz), 5.68 (t, *J* = 3 Hz), 6.11 (dd, *J* = 2.5, 3.5 Hz), 6.37 (dd, *J* = 1.5, 3.5 Hz), and 6.97 (dd, *J* = 1.5, 2.5 Hz). NMR analysis by both COSY and HMBC methods, showed correlations (Figure III.5.3) which illustrated that these proton signals were parts of two pyrrole rings.

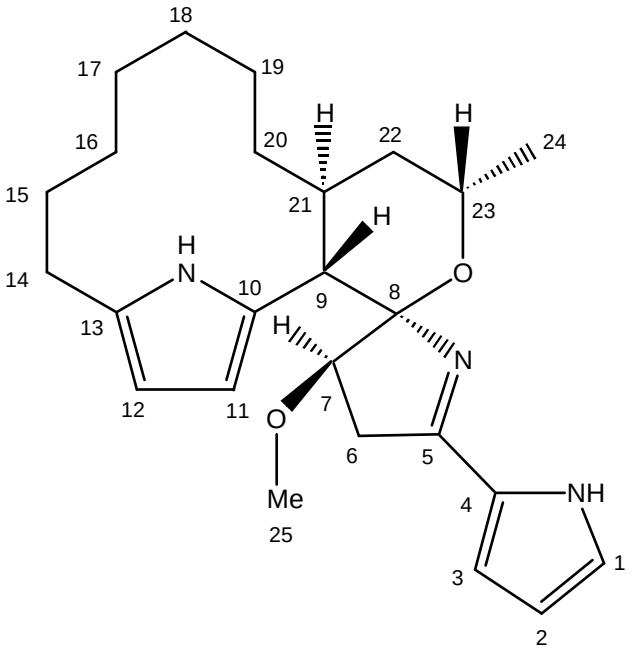

1

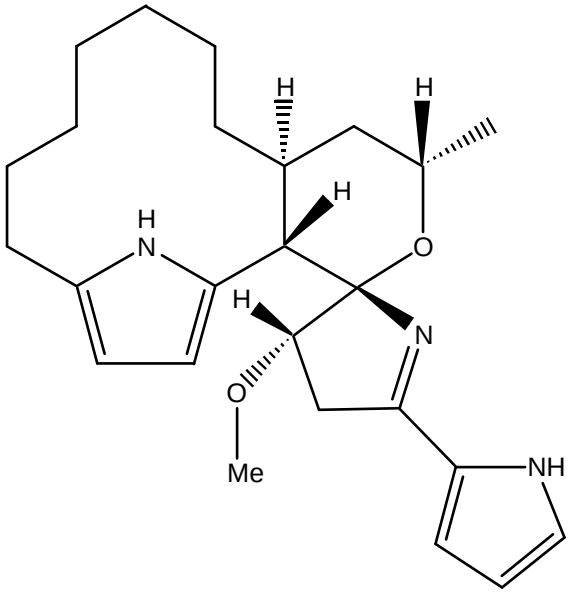

2

Figure III.5.1. The structures of marineosins A (**1**) and B (**2**)

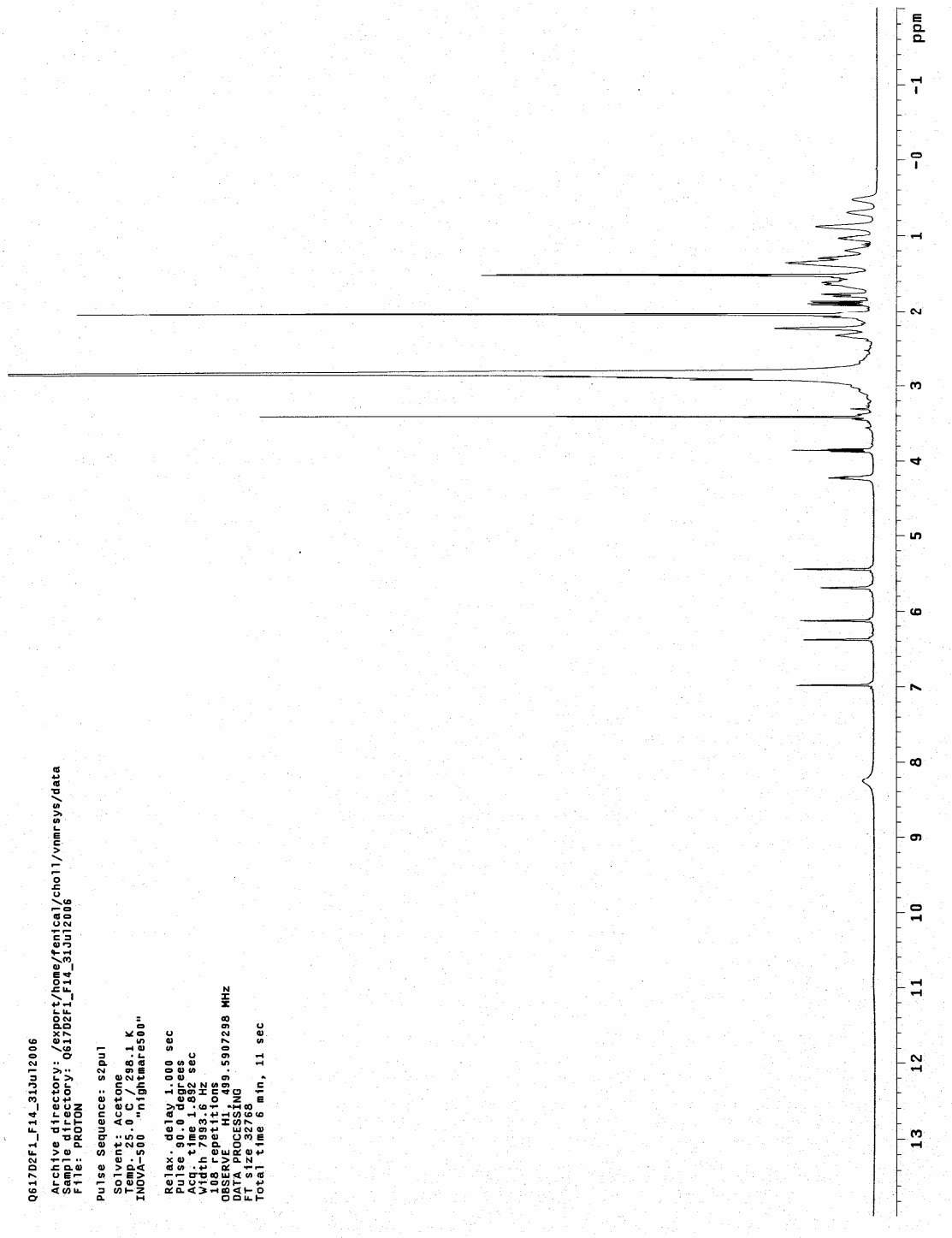

Figure III.5.2. ^{1}H NMR spectrum of marineosin A (**1**) (500 MHz, acetone-d_6)

Table III.5.1. ^{1}H, ^{13}C, COSY, HMBC, and ROESY NMR spectroscopic data (acetone-d_6) for marineosin A (**1**)

#	δ_C		δ_H	*J* (Hz)	COSY	HMBC	ROESY
1	122.5	CH	6.97 dd	1.5, 2.5	2	C-2, C-3, C-4	2
2	109.9	CH	6.11 dd	2.5, 3.5	1, 3	C-1, C-3, C-4	1, 3
3	113.5	CH	6.37 dd	1.5, 3.5	2	C-1, C-2, C-4	2, 6b
4	129.1	C					
5	164.4	C					
6 a	39.0	CH_2	1.88 dd	8.5, 16.0	7	C-5, C-7	
b			2.88 dd	8.5, 16.0	7	C-5, C-7, C-8	3
7	89.9	CH	3.85 t	8.5	6	C-6, C-8, C-25	9, 25
8	106.1	C					
9	45.9	CH	2.91 d	12.0	21	C-7, C-8, C-10, C-11, C-20, C-21, C-22	7, 11, 20b, 22a
10	129.9	C					
11	110.1	CH	5.68 t	3.0	12	C-10, C-12, C-13	9, 12
12	104.7	CH	5.44 t	3.0	11, 14	C-10, C-11, C-13	11, 14
13	131.6	C					
14	28.6	CH_2	2.23 m		12, 15	C-12, C-13, C-15, C-16	12
15 a	25.5	CH_2	1.37 m		14		
b			1.64 m		14		
16 a	28.0	CH_2	1.28 m		17	C-14, C-18	
b			1.34 m		17	C-14, C-18	
17 a	25.5	CH_2	0.52 m		16, 18		
b			0.69 m		16, 18		
18 a	25.7	CH_2	1.02 m		17, 19	C-16, C-17, C-20	
b			1.52 m		17, 19		10-NH
19 a	25.4	CH_2	0.88 m		18, 20		
b			1.18 m		18, 20		
20 a	32.0	CH_2	0.88 m		19, 21		
b			1.35 m		19, 21		9
21	29.6	CH	2.32 m		9, 20, 22		10-NH, 22b, 24
22 a	39.6	CH_2	1.61 td	6.5, 12.0	21, 23	C-9, C-20, C-21, C-23, C-24	9, 20a
b			1.77 m	12.0	21, 23	C-9, C-21	20a, 21
23	70.4	CH	4.23 m	6.5	22, 24	C-8, C-21, C-22, C-24	
24	22.8	CH_3	1.51 d	7.0	23	C-22, C-23	10-NH, 21
25	58.5	CH_3	3.40 s			C-7	7
1-NH			10.93 br				
10-NH			8.23 brs				14, 18b, 21, 24

COSY NMR correlations between H-11 (δ 5.68) and H-12 (δ 5.44), and HMBC correlations from H-11 to C-10, C-12 and C-13, H-12 to C-10, C-11 and C-13, suggested the presence of a 2,5-disubstituted pyrrole ring. The proton coupling constants of H-11 and H-12 (J = 3 Hz) also supported this substitution pattern. The remaining three aromatic proton signals showed COSY correlations between each of them that allowed the connectivity of C-1/C-2/C-3 to be established. The observed HMBC correlations from H-1 to C-3 and C-4, H-2 to C-4, and H-3 to C-1 and C-4 indicated that these olefinic protons could be assigned to a pyrrole ring with mono-substitution at C-4. The additional evidence, which confirmed the presence of this pyrrole ring, were the expected carbon chemical shifts and proton coupling constants of these three methine signals that matched with the other known pyrrole derivatives.[5]

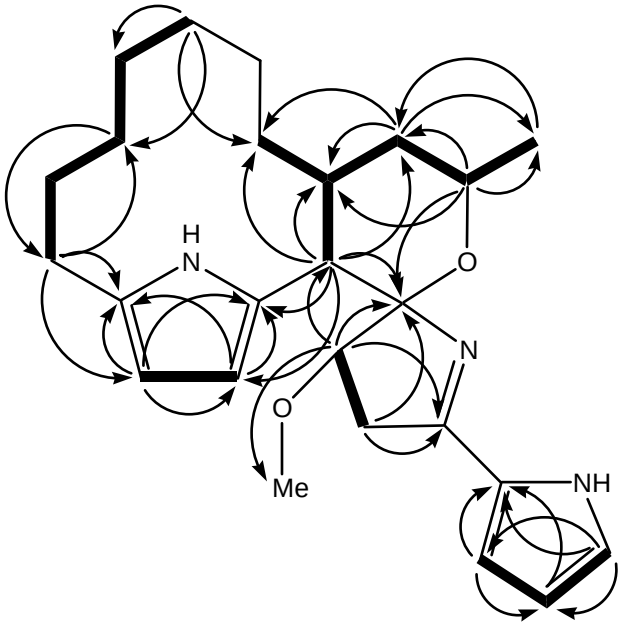

Figure III.5.3. Selected COSY (bold lines) and HMBC (arrows) NMR correlations observed for marineosin A (**1**).

The major portion of the macrocyclic skeleton framework, which is composed of mostly methylene carbons, could be assembled through the interpretation of COSY, HMBC, TOCSY and HSQC-TOCSY NMR correlations. Analysis of COSY, TOCSY and HSQC-TOCSY data allowed the establishment of C-14/C-15/C-16/C-17/C-18/C-19/C-20/C-21/C-22/C-23/C-24 connectivities. The alkyl chain was connected to a pyrrole ring at C-13 based on the HMBC correlations from H-14 to C-12 and C-13. On the other side of the alkyl chain, H-21 showed COSY correlation to the methine proton at C-9. HMBC correlations from H-9 to the pyrrole carbon at C-10 and C-11 established the 12-member macrocyclic ring. This part of the structure is somewhat remniscent to the macrocyclic ring of roseophilin, which is an antibiotic isolated from the terrestrial actinomycete *Streptomyces griseoviridis*.[6]

The H-9 and H-23 methine protons both demonstrated HMBC correlations to quaternary carbon at C-8, suggesting the presence of a 6-membered cyclic ether. Oxygen was placed between C-8 (δ 106.1) and C-23 (δ 70.4) on the basis of their appropriate carbon chemical shifts. HMBC correlations from the methylene protons at H-6 and the methine proton at H-7 to C-8 were observed. The methoxy group was connected to C-7 on the basis of HMBC correlation between H-25 and C-7. Both H-6 and H-7 also showed HMBC correlations to the quaternary carbon at C-5, which was initially thought to be a carbonyl group due to its chemical shift at δ 164.4. However, analysis by IR spectral data indicated a lack of carbonyl groups in this molecule. Based upon the molecular formula and the partial structural data defined above, C-5 was deduced to be attached to the other mono-substituted pyrrole ring at C-4, and formed a double bond with the nitrogen that was connected to C-8. This completed

construction of a five-membered ring with carbon C-8 forming a spiro center. This part of the structure, which includes two five-member rings is very similar to structural features of the common 4-methoxy-2,2′-bipyrrole chromophores from the marine-derived tambjamines[7] and the bacterial pigments of the prodigiosin family.[8] The only difference is that the methoxy group in **1** is attached to the pyrrole whose conjugated system has been disrupted.

Additional evidence that confirmed the structure of **1** came from the EIMS experiment that clearly illustrated fragment ions in support of the structure. Two major fragments, including the peak at *m*/*z* 189.2 and 231.3 are illustrated in Figure III.5.4 along with their corresponded partial structures. This result also supported the presence of a bipyrrole chromophore, as it appeared that the substructure fragmented in predictable ways in this experiment.

The assignment of the relative configuration of marineosin A (**1**), and confirmation of the overall structure, was achieved by interpretation of the ROESY NMR spectroscopic data (Figure III.5.5) and by analysis of vicinal coupling constants. The methine protons H-9 (δ 2.91) and H-21 (δ 2.32) were both placed in axial positions based upon their large vicinal coupling constant (J = 12 Hz). Me-24 (δ1.51) was also placed in an axial position on the same side of the ring with H-21 on the basis of a mutual ROESY correlation. This result suggested the six-member cyclic ether ring was in a chair configuration. The methine signal at H-9 also showed a ROESY correlation to the pyrrole proton at H-11, and therefore proved that both protons were on the same side of the molecule.

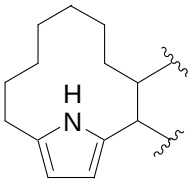

m/*z* 189.2

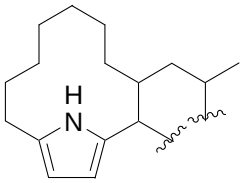

m/*z* 231.3

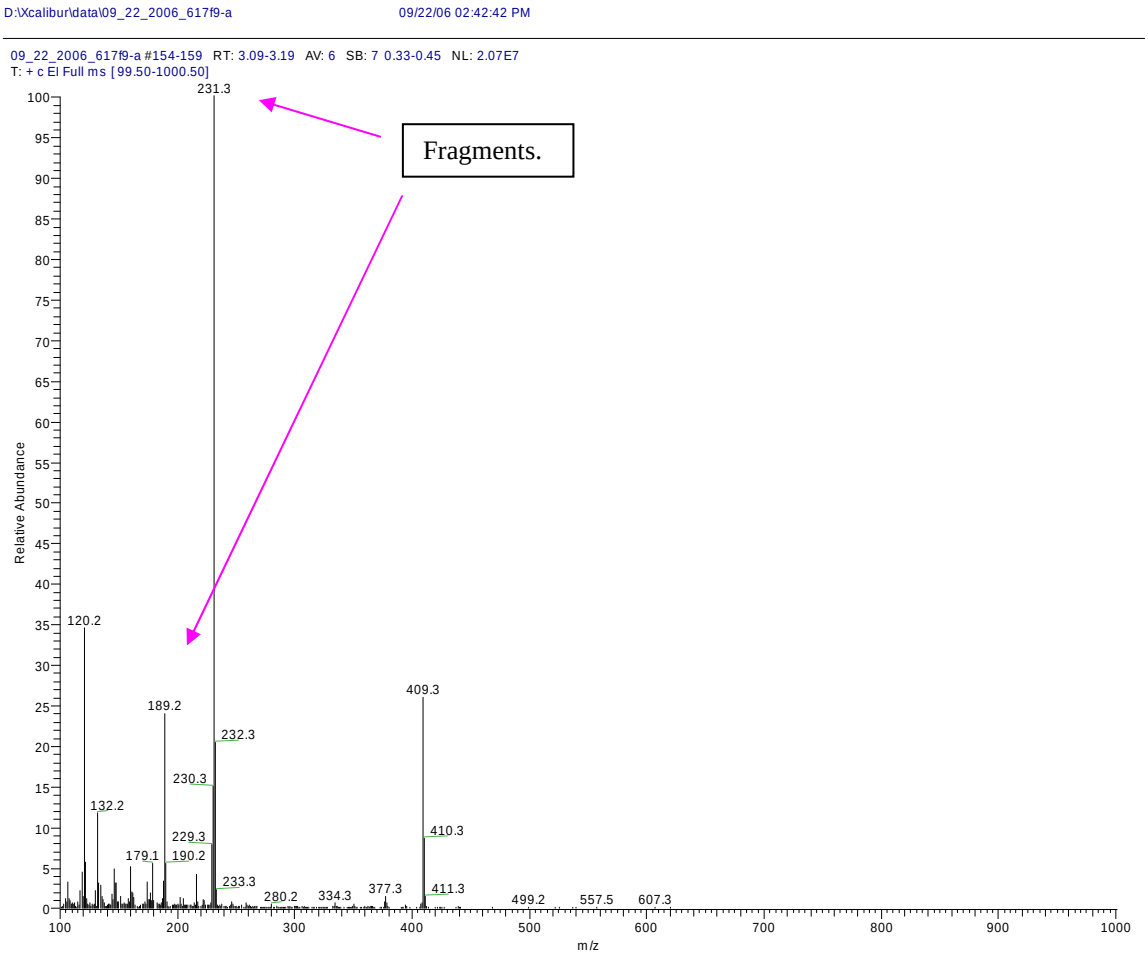

Figure III.5.4. Fragment ions observed in the EIMS experiment performed on marineosin A (**1**)

ROESY correlations observed from H-7 to H-9 and from H-6 to H-3 and H-11 confirmed the assignment of the spiro center placing nitrogen on the opposite side of the molecule from the H-9 methine proton. The 2,5-disubstitution pattern of the pyrrole ring was also supported by ROESY correlations observed between H-11 and H-12.

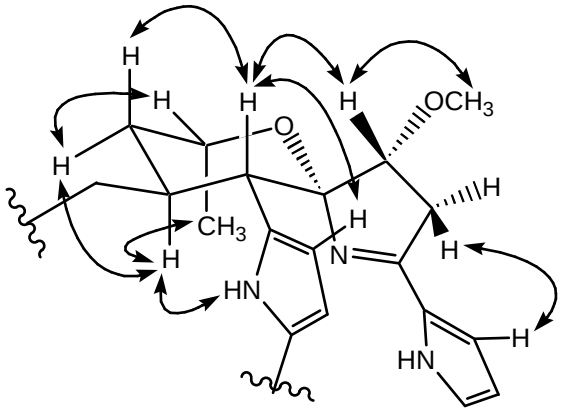

Figure III.5.5. Assigned relative configuration of **1** based upon selected ROESY NMR correlations**.**

The molecular formula for marineosin B (**2**), was assigned as $C_{25}H_{35}N_3O_2$, isomeric with **1**, by HRFABMS (*m*/*z* 410.2804, $[M+H]^+$) and from its NMR spectral data (Table III.5.2). Initial analysis of the ^1H NMR spectral data for **2** (Figure III.5.6) illustrated features very similar to those of **1**, although most chemical shifts were slightly different. From this observation, it was deduced that these molecules are very closely related and possibly share an epimeric relationship.

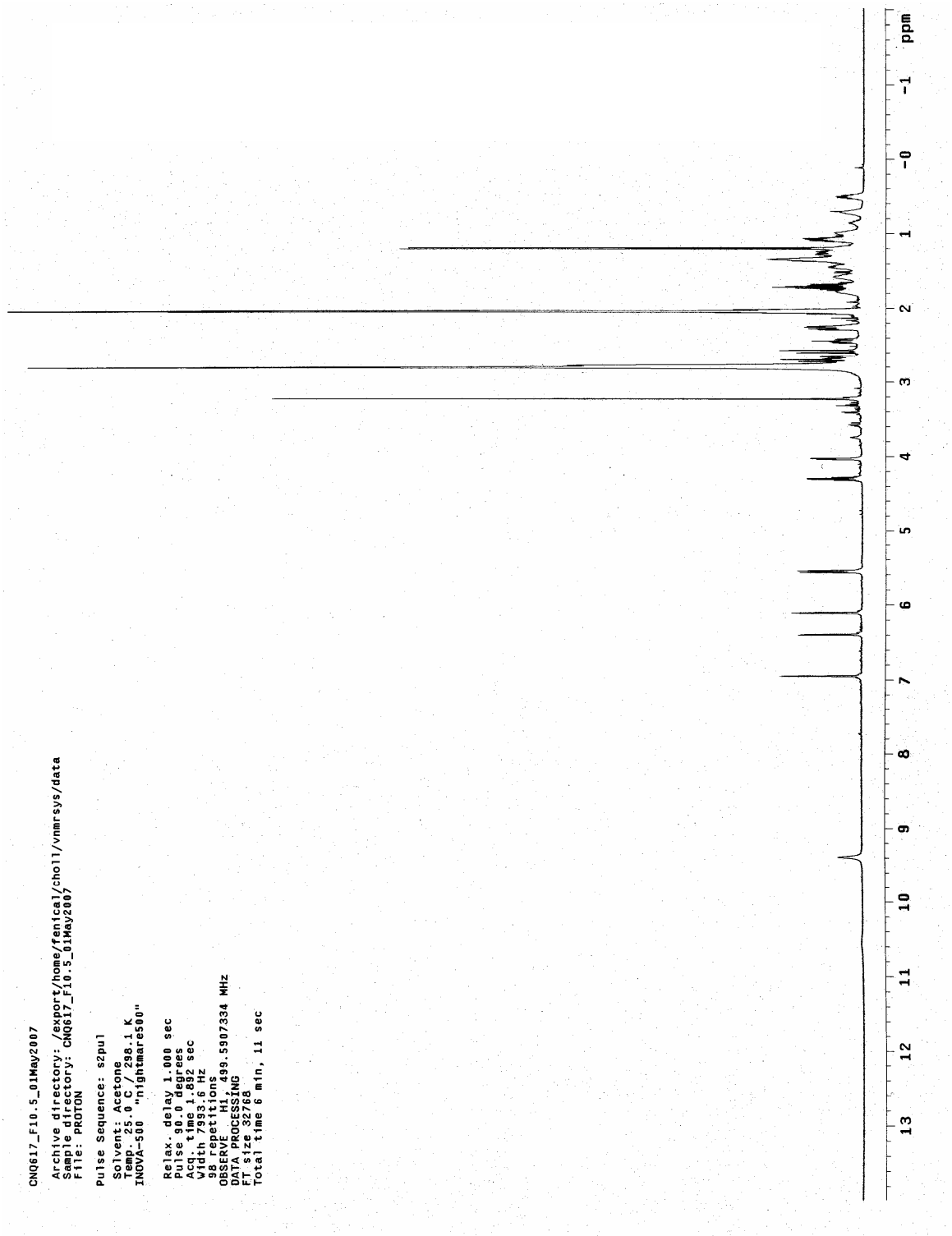

Figure III.5.6. ^{1}H NMR spectrum of marineosin B (**2**) (500 MHz, acetone-d_6)

Table III.5.2. ^{1}H, ^{13}C, COSY, HMBC, and ROESY NMR spectroscopic data (acetone-d_6) for marineosin B (**2**)

#	δ_C		δ_H	*J* (Hz)	COSY	HMBC	ROESY
1	122.6	CH	6.95 dd	1.5, 2.5	2	C-2, C-3, C-4	2
2	109.7	CH	6.10 dd	2.5, 3.5	1, 3		1, 3
3	113.4	CH	6.39 dd	1.5, 3.5	2		2, 6
4	128.8	C					
5	162.8	C					
6 a	41.0	CH_2	2.27 dd	6.0, 16.5	7	C-5	3, 25
b			2.58 dd	2.5, 17.0	7	C-5, C-7, C-8	3, 25
7	82.5	CH	4.03 dd	2.0, 6.0	6	C-5, C-25	10-NH, 21
8	105.9	C					
9	49.5	CH	2.71 d	13.0	21	C-7, C-8, C-10, C-11, C-21	11, 23
10	129.8	C					
11	110.4	CH	5.55 t	3.0	12, 10-NH		9
12	106.3	CH	5.57 t	2.5	11, 14, 10-NH		14a
13	131.8	C					
14 a	28.8	CH_2	2.44 m		15		12
b			2.67 m		15		10-NH
15 a	26.6	CH_2	1.44 m		14, 16		
b			1.77 m		14, 16		
16	27.4	CH_2	1.34 m		15, 17	C-14, C-18	10-NH
17 a	25.8	CH_2	0.51 m		16, 18	C-15	
b			0.72 m		16, 18		
18 a	25.8	CH_2	1.07 m		17, 19		
b			1.58 m		17, 19		
19 a	25.0	CH_2	1.00 m		18, 20		
b			1.28 m		18, 20		
20 a	33.7	CH_2	1.09 m		19, 21	C-21, C-22	
b			1.36 m		19, 21		
21	31.4	CH	2.26 m		9, 20, 22		7, 10-NH
22	38.9	CH_2	1.72 m	6.0	21, 23	C-9, C-20, C-21, C-23, C-24	23
23	66.1	CH	4.30 m	6.5	22, 24	C-8, C-21	9, 22, 24
24	22.3	CH_3	1.20 d	6.5	23	C-22, C-23	23, 25
25	57.8	CH_3	3.23 s			C-7	6, 24
1-NH			10.57 br				
10-NH			9.39 brs		11, 12		7, 14b, 16, 21

The major portion of this compound was assembled by the interpretation of COSY, TOCSY and HMBC NMR data. Although the yield of **2** is very small and there were difficulties which arose due to insufficient ^{13}C NMR data, the comparison of all spectral data with compound **1** allowed the structure of **2** to be established. Several of the carbon chemical shifts were obtained by interpretation of HMBC and HSQC NMR data. The only missing chemical shift was the quaternary carbon, C-13, which also proved to be the smallest carbon peak in **1**.

The correlation patterns derived from interpretation of COSY and HMBC NMR spectroscopic data were found to be similar to **1**, and consequently, the same planar structure was also assigned to **2**. Despite the fact that marineosin B (**2**) possessed the same planar structure as **1**, differences in the proton and carbon chemical shifts suggested that this compound had stereochemical defferences. Ultimately, the relative stereochemistry of **2** was also established by interpretation of ROESY NMR spectroscopic data and by analysis of vicinal coupling constants (Figure III.5.7).

The stereochemistry of the cyclic ether ring was found to be virtually identical to **1**. The methine protons H-9 (δ 2.71) and H-21 (δ 2.26) were both placed in axial positions due to their large vicinal coupling constants (J = 13 Hz). Proton H-21 was placed on the same side of the molecule as NH-1 (δ 9.39) based on observed mutual ROESY correlations. A ROESY correlation between H-9 and H-23 suggested that this six-member cyclic ring may not possess a chair conformation. The ROESY correlations from NH-1 to H-14b (δ 2.67), H-12 to H-14a (δ 2.44), and from H-9 to H-11 confirmed that the pyrrole ring also possessed a 2,5-disubstitution pattern.

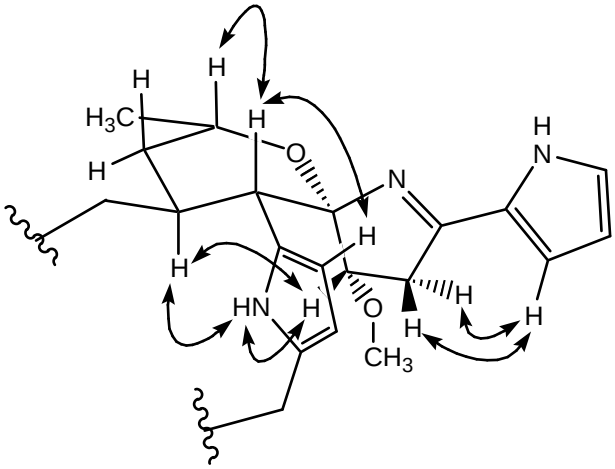

Figure III.5.7. Assigned relative configurations of **2** derived from selected ROESY NMR correlations.

The difference between marineosin A (**1**) and B (**2**) was concluded to result from the stereochemistry at the spiro carbon, C-8. ROESY correlations from **2** indicated that H-7 (δ 4.03) correlated to NH-1 and H-21, an observation which proved that these protons were aligned on the same side of the molecule. This assignment also explains why the chemical shifts of NH-1 and H-7 were shifted downfield in **2** since this part of the molecule became more structurally constrained than the same part of structure found in **1**.

Along with marineosins A (**1**) and B (**2**), an uncommon mixed biosynthetic terpenoid was also isolated from strain CNQ617. Marinoquinoline A (**3**) was obtained as a colorless oil which showed a LRMS $[M+Na]^+$ ion at *m*/*z* 550. The molecular formula of **3** was determined as $C_{35}H_{45}NO_3$ by high-resolution FABMS ($[M+H]^+$ *m*/*z* 528.3484). Initial analysis of **3** by ^1H and ^{13}C NMR methods, including interpretation

of HSQC spectroscopic data, revealed that marinoquinoline A (**3**) is consisted of a bicyclic heteroaromatic ring system with a linear chain of trisubstituted olefinic bonds. Evaluation of IR spectroscopic data showed a strong absorption band at 1562 cm^{-1}, which suggested the presence of an N-oxide functional group.[9]

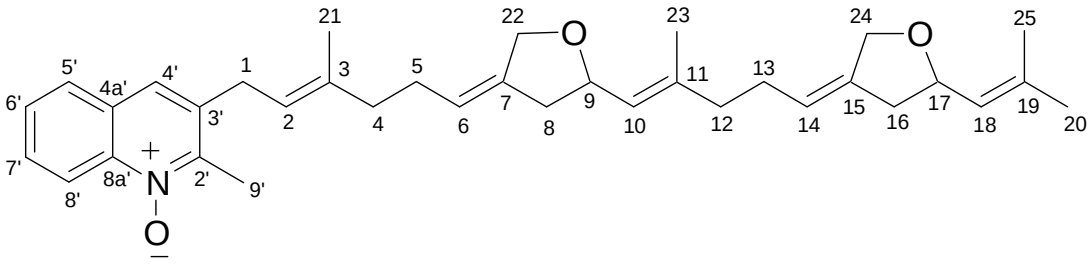

3

Figure III.5.8. The structure of marinoquinoline A (**3**)

The ^{1}H NMR spectrum of **3** (Figure III.5.9) measured in CD_3OD demonstrated five singlet methyl signals at δ 1.67 (3H, s), 1.69 (3H, s), 1.72 (3H, s), 1.79 (3H, s) and 2.73 (3H, s). Analysis of HSQC NMR data (Table III.5.3) illustrated that there were 10 olefinic and aromatic protons in this compound.

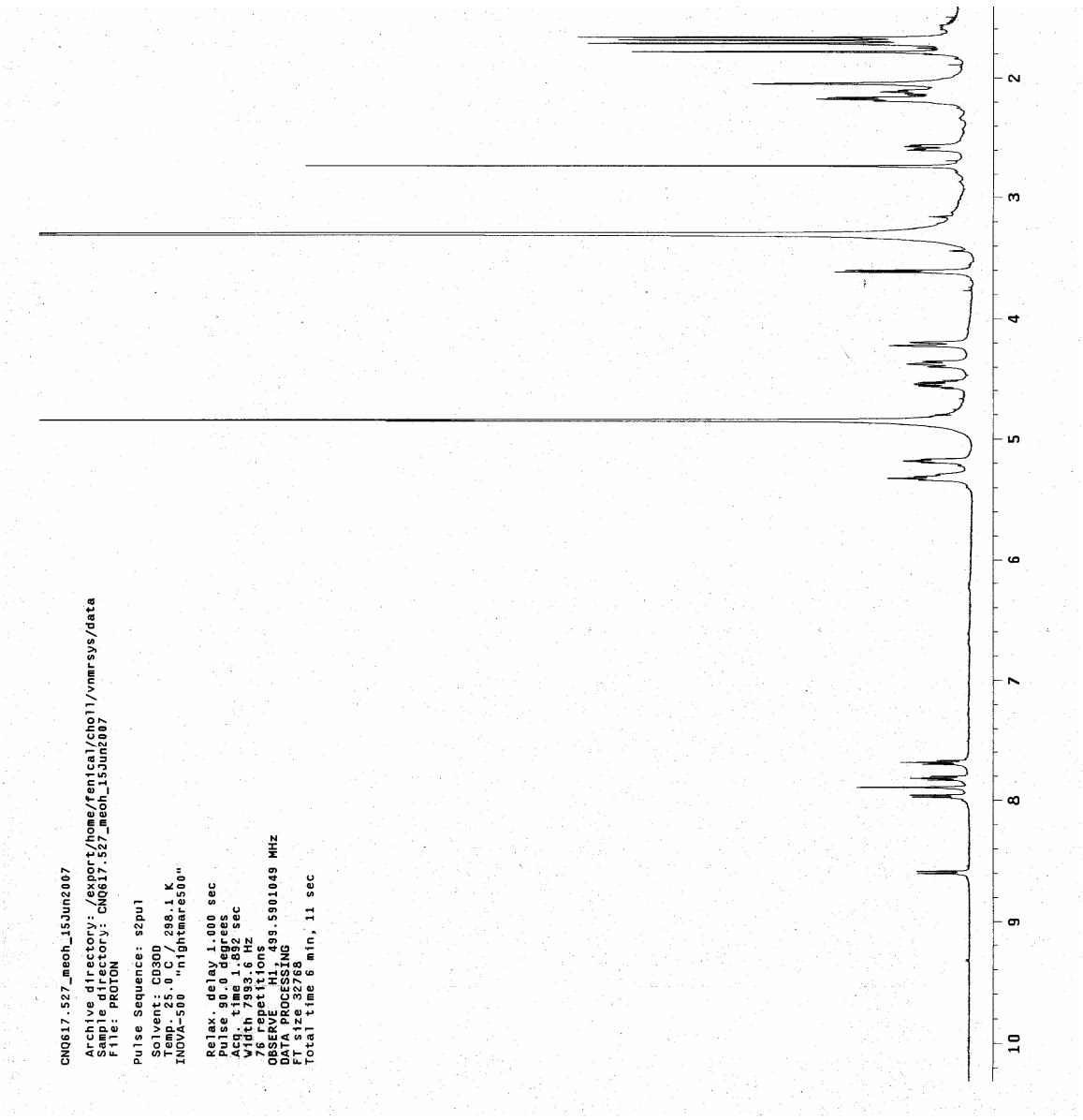

Figure III.5.9. ^{1}H NMR spectrum of marinoquinoline A (**3**) (500 MHz, CD_3OD)

Table III.5.3. ^{1}H, ^{13}C, COSY, HMBC, and NOESY NMR spectroscopic data (CD_3OD) for marinoquinoline A (**3**)

#	δ_C		δ_H	*J* (Hz)	COSY	HMBC	NOESY
1	33.1	CH_2	3.61 d	7.0	2	C-2, C-2′, C-3, C-3′, C-4′	9′, 21
2	122.1	CH	5.33 t	7.0	1, 21	C-1, C-4, C-21	4
3	139.4	C					
4	40.2	CH_2	2.18 m			C-5	2
5	28.7	CH_2	2.12 m	7.0	6	C-6, C-7	22a, 22b
6	121.0	CH	5.32 m		5, 22		8a, 8b
7	140.2	C					
8 a	40.3	CH_2	2.18 m		9	C-7	6
b			2.58 dd	5.5, 15.0	9	C-7, C-22	6, 9
9	77.5	CH	4.55 m		8, 10	C-22	8b, 23
10	126.3	CH	5.18 m		9	C-8, C-23	12
11	140.7	C					
12	40.0	CH_2	2.06 m			C-10, C-11, C-13, C-23	10
13	28.6	CH_2	2.05 m		14	C-14, C-15	24a, 24b
14	120.8	CH	5.29 m		13, 24		16a, 16b
15	140.2	C					
16 a	40.3	CH_2	2.18 m		17	C-15	14
b			2.58 dd	5.5, 15.0	17	C-15, C-24	17
17	77.4	CH	4.55 m		16, 18		16b, 25
18	125.9	CH	5.18 m		17, 20, 25	C-16, C-20, C-25	20
19	138.0	C					
20	25.9	CH_3	1.72 s		18	C-18, C-19, C-25	18
21	16.4	CH_3	1.79 s		2	C-2, C-3, C-4	1
22 a	69.0	CH_2	4.21 d	13.0	6	C-6, C-7	5
b			4.38 t	12.0	6	C-6, C-7, C-9	5
23	16.7	CH_3	1.67 s			C-10, C-11, C-12	9
24 a	69.0	CH_2	4.21 d	13.0	14	C-14, C-15	13
b			4.38 t	12.0	14	C-14, C-15, C-17	13
25	18.3	CH_3	1.69 s		18	C-18, C-19, C-20	17
1′							
2′	149.6	C					
3′	136.4	C					
4′	129.2	CH	7.89 s		1	C-1, C-2′, C-5′, C-8a′	5′
4a′	129.8	C					
5′	129.3	CH	7.97 d	8.0	6′	C-4′, C-7′, C-8a′	4′, 6′
6′	129.5	CH	7.69 t	7.5	5′, 7′	C-4a′, C-8	5′, 7′
7′	131.7	CH	7.82 t	8.0	6′, 8′	C-5′, C-8a′	6′, 8′
8′	119.7	CH	8.60 d	9.0	7′	C-6′	7′
8a′	140.5	C					
9′	15.0	CH_3	2.73 s			C-2′, C-3′	1

The heteroaromatic ring in **3** was assembled by the interpretation of COSY and HMBC spectral data (Figure III.5.10). COSY correlations of four methine signals from H-5′ to H-8′ (δ 7.97, 7.69, 7.82, and 8.60) established four consecutive aromatic protons. HMBC correlations from H-5′ to C-8a′, H-6′ to C-4a′, and from H-7′ to C-8a′ confirmed the presence of the benzene component of the quinoline system (C-4a′ to C-8a′). The downfield chemical shift of C-8a′ (δ 140.5) suggested that it was connected to the aromatic N-oxide. The remaining aromatic proton, observed as a singlet at δ 7.89, showed HMBC correlations to C-2′, C-5′ and C-8a′, thus suggesting the presence of the adjacent six-membered quinoline ring with the N-oxide nitrogen positioned between C-8a′ and C-2′ (δ 149.6) on the basis of their low field resonances. The aromatic methyl group, H_3-9′ (δ 2.73), was positioned at C-2′ on the basis of HMBC correlations from H-9′ to C-2′ and C-3′. Based upon the above analysis, this bicyclic heteroaromatic component of **3** was confirmed to be a disubstituted quinoline N-oxide.

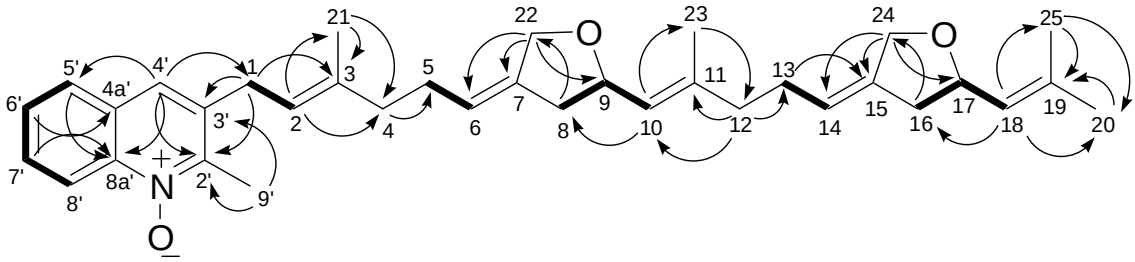

Figure III.5.10. Selected COSY (bold lines) and HMBC (arrows) NMR correlations observed for **3**.

The remainder of the molecule appeared to be a linear sesterterpenoid chain that was attached to the quinoline ring at the quaternary carbon C-3′ (δ 136.4). This was confirmed by the observation of a definitive HMBC correlation from C-1 to C-3′. Overall ^{1}H NMR spectroscopic analysis illustrated that the side chain contained repeating units of a similar oxygenated functional group, along with five double bonds in the side chain. Analysis by COSY and HMBC spectroscopic data allowed the side chain to be established as a regular sesterterpenoid, although there were difficulties in this interpretation due to several overlapping proton signals. Interpretation of COSY correlations allowed several fragments of the side chain to be established; these included correlations between H-1 and H-2, H-5 and H-6, H-13 and H-14, yielding the connectivity of C-8/C-9/C-10 and C-16/C-17/C-18.

The full sesterterpenoid side chain was assembled with high confidence based upon interpretation of HMBC data. The remaining four methyl singlet signals showed correlations (H-21 to C-2, C-3 and C-4, H-23 to C-10, C-11 and C-12, and from H-20/H-25 to C-18 and C-19) that allowed a major portion of the side chain to be established. Two tetrahydrofuran ether rings were easily assigned from the HMBC correlations from H-22 to C-9 and C-7, H-8 to C-22, H-24 to C-15 and C-17, and from H-16 to C-24. Oxygenation at C-22 (δ 69.0) and C-24 (δ 69.0) in these two ether rings was deduced from the ^{13}C NMR chemical shifts, which were considerably shifted downfield.

The geometries of the olefinic bonds in marinoquinoline A (**3)** were determined by interpretation of NOESY NMR spectroscopic data. The geometry of the double bond between C-2 and C-3 was established as *trans* (*E*) based upon a NOESY correlation of H-2 (δ 5.33) to H-4 (δ 2.18), and no correlation between H-2 and the methyl protons H_3-21. Using similar observations, notably an NOESY correlation between H-10 (δ 5.18) and H-12 (δ 2.06), a *trans* (*E*) configuration was also observed for the double bond between C-10 and C-11. A NOESY correlation observed between H-18 (δ 5.18) and H-20 (δ 1.72) also established the spatial relationship of the C-19 methyl groups. The geometry of the exocyclic double bonds attached to tetrahydrofuran ether rings were assigned *Z* configurations on the basis of observed NOESY correlations between H-6 and H-8 as well as between H-14 and H-16.

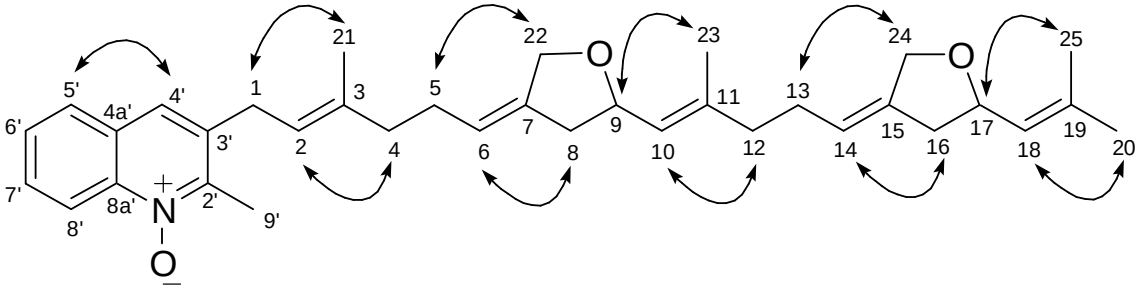

Figure III.5.11. Geometries of the olefinic bonds in **3** based on selected NOESY NMR correlations**.**

Neither the relative nor absolute configurations at C-9 and C-17 could be defined by any data obtained for marinoquinoline (**3**). Making this assignment will require alternative approaches perhaps capitalizing on the CD spectral features of this metabolite.

Biological Activity

The marine actinomycete strain CNQ617 (MAR3) was initially chosen for chemical investigation as the promising antifungal project. However, it was later discovered that this bacterial strain possesses very potent HCT-116 colon carcinoma cytotoxicity, while its antifungal activity was rather weak (MIC > 100 μg/mL) and not worth pursuing. Hence, bioassay-guided fractionation of the crude extract led to the isolation of marineosin A (**1**), which is the most cytotoxic metabolite from this bacterial strain.

Table III.5.4. Cytotoxic and antifungal activities of **1**-**3**

compound	HCT-116 inhibition IC_{50} (μg/mL)	*C. albicans* (WT) MIC (μg/mL)	*C. albicans* (AmBR) MIC (μg/mL)
1	0.2	NSA	NSA
2	19	NSA	NSA
3	NSA	NSA	NSA

Marineosins A (**1**) and B (**2**) were tested for their cytotoxic activities against the HCT-116 human colon tumor cell line and for inhibition against wild-type and amphotericin B-resistant strains of *C. albicans*. The results are demonstrated in Table III.5.4. Despite their structural similarities, **1** and **2** show rather different cytotoxic

activities, while both did not exhibit any antifungal activity. Marineosin A (**1**) was more active in the cytotoxic assay with a highly potent IC_{50} value of 0.2 μg/mL. On the other hand, marineosin B exhibited very weak cytotoxicity with IC_{50} = 19 μg/mL. The difference in stereochemistry at the spiro centers in marineosin A and B appear to significantly affect their bioactivities.

Marinoquinoline A (**3**), which is another new metabolite derived from CNQ617, was also tested in both antifungal and HCT-116 assay, but no biological activity was observed in any assay.

Experimental Section

General Experimental Procedures. Optical rotations were measured using a Rudolph Autopol III polarimeter. UV spectra were obtained using Varian Cary 50 Bio UV-Visible spectrophotometer. Infrared spectra were recorded on a Perkin-Elmer 1600 spectrophotometer. ^{1}H, ^{13}C, COSY, HMBC, HSQC, NOESY, ROESY, TOCSY, and HSQC-TOCSY NMR spectra were recorded on a Varian INOVA 500 MHz spectrometer. High-resolution mass spectrometer measurements were obtained on ThermoFinnigan MAT900XL instrument at University of California, San Diego, CA. All solvents were distilled prior to being used.

Collection and Phylogenetic Analysis of strain CNQ617. The marine actinomycete strain CNQ617 was isolated from a marine sediment sample collected off shore of La Jolla, CA by Alejandra Davo Prieto. The strain was designated as

MAR3 clade based on 16S rDNA analysis. The phylogenetic analysis revealed that this strain showed 98% similarity to *Streptomyces cacaoi*.

Fermentation and Extraction. Strain CNQ617 was cultured at 27°C with shaking at 250 rpm in fifteen 2.8-L Fernbach flasks each containing 1 L of the medium A1BFe-C [10 g starch, 4 g yeast extract, 2 g peptone, 5 mL $Fe_2(SO_4)_3 \cdot 4H_2O$ (8 g/L in DI water), 5 mL KBr (20 g/L in DI water), 1 L seawater]. After 5 days, the organic constituents from a 15 L culture were extracted by a solid-phase extraction method using Amberlite XAD-7 resin. The crude extract was prepared by washing the resin with acetone and concentrating by rotary evaporation.

Isolation and Purification. The crude acetone extract from a 15 L culture of strain CNQ617 was dried *in vacuo* to obtain a sticky dark brown substance (1.8 g), which was partitioned by HP20SS column chromatography (acetone/water) to yield eight fractions (20%, 40%, 50%, 60%, 70%, 80%, 90%, and 100% acetone mixtures). All eight fractions were concentrated to dryness and evaluated in the HCT-116 colon carcinoma cytotoxicity assay. The fraction that eluted with 90% acetone-water (173 mg) was found to possess very potent cytotoxic activity ($IC_{50} \leq 0.8$ μg/mL), and then fractionated by flash C18 column chromatography eluting with 30%, 50%, 75%, 80% and 100% MeOH-water mixtures. The 75% MeOH/water fraction from the flash C18 column was subjected to further purification by isocratic HPLC (Dynamax C_{18} semi-preparative, 3 mL/min; 77% MeOH/H_2O over 70 min) to yield marineosins A (**1**, 4.7 mg) and B (**2**, 1.7 mg). The 80% MeOH/water fraction was also further purified by

isocratic HPLC (Dynamax C_{18} semi-preparative, 3 mL/min; 80% MeOH/H_2O over 60 min) to obtain marinoquinoline (**3**, 1.6 mg).

Marineosin A (**1**): colorless oil; $[\alpha]_D$ –101.7 (*c* 0.06, MeOH); UV (MeOH) λ_{max} (log ε) 285 nm (4.06), 227 nm (3.88); IR ν_{max} (KBr) 2925, 2856, 1610, 1508, 1435, 1261, 763 cm^{-1}; NMR data, see Table III.5.1 ; ESIMS $[M+H]^+$ *m*/*z* 410; HREIMS $[M]^+$ *m*/*z* 409.2726 (calcd for $C_{25}H_{35}N_3O_2$, 409.2729)

Marineosin B (**2**): colorless oil; $[\alpha]_D$ +143.5 (*c* 0.09, MeOH); UV (MeOH) λ_{max} (log ε) 287 nm (3.24); IR ν_{max} (KBr) 2926, 2856, 1607, 1434, 1106, 743 cm^{-1}; NMR data, see Table III.5.2; ESIMS $[M+H]^+$ *m*/*z* 410; HRFABMS $[M+H]^+$ *m*/*z* 410.2804 (calcd for $C_{25}H_{36}N_3O_2$, 410.2807).

Marinoquinoline A (**3**): colorless oil; $[\alpha]_D$ +5.0 (*c* 0.08, MeOH); UV (MeOH) λ_{max} (log ε) 318 nm (2.89), 237 nm (3.72), 204 nm (3.80); IR ν_{max} (KBr) 3404, 2919, 2851, 1562, 1439, 1379, 1047 cm^{-1}; NMR data, see Table III.5.3; ESIMS $[M+Na]^+$ *m*/*z* 550; HRFABMS $[M+H]^+$ *m*/*z* 528.3484 (calcd for $C_{35}H_{46}NO_3$, 528.3478).

References

(1) Jensen, P. R.; Fenical, W. *Annu. Rev. Microbiol.* **1994**, *48*, 559-584.

(2) Goodfellow. M; Haynes, J. A. Actinomycetes in marine sediments. In *Biological, Biochemical and Biomedical Aspects of Actinomycetes*, edited by Ortiz-Ortiz; L. Bojalil; Yakoleff, V. London: Academic Press, **1984**, pp. 453-472.

(3) (a) Mincer, T. J.; Jensen, P. R.; Kauffman, C. A.; Fenical, W. *Appl. Environ. Microbiol*. **2002**, *68*, 5005-5011. (b) Jensen, P. R.; Gontang, E.; Mafnas, C.; Mincer, T. J.; Fenical, W. *Environ. Microbiol*. **2005**, *7*, 1039-1048. (c) Maldonado, L. A.; Fenical, W.; Jensen, P. R.; Kauffman, C. A.; Mincer, T. J.; Ward, A. C.; Bull, A. T.; Goodfellow, M. *Int. J. Syst. Evol. Microbiol*. **2005**, *55*, 1759-1766.

(4) Jensen, P. R.; Fenical, W. *Nat. Chem. Biol*. **2006**, *2*, 666-673.

(5) Shen, X.; Perry, T. L.; Dunbar, C. D.; Kelly-Borges, M.; Hamann, M. T. *J. Nat. Prod.* **1998**, *61*, 1302-1303.

(6) Hayakawa, Y.; Kawakami, K.; Seto, H.; Furihata, K. *Tetrahedron Lett.* **1992**, *33*, 2701-2704.

(7) (a) Carte, B.; Faulkner, D. J. *J. Org. Chem*. **1983**, *48*, 2314-2318. (b) Paul, V. J.; Lindquist, N.; Fenical, W. *Mar. Ecol. Prog. Ser*. **1990**, *59*, 109-118. (c) Lindquist, N.; Fenical, W. *Experientia*. **1991**, *47*, 504-506.

(8) (a) Wasserman, H. H.; McKeon, J. E.; Smith, L.; Forgione, P. *J. Am. Chem. Soc.* **1960**, *82*, 506. (b) Gerber, N. N. *Tetrahedron Lett.* **1970**, *11*, 809-812. (c) Gerber, N. N. *J. Heterocycl. Chem*. **1973**, *10*, 925-929.

(9) Pretsch, E.; Simon, W.; Seibl, J.; Clerc, T. *Tables of Spectral Data for Structure Determination of Organic Compounds*; Springer-Verlag: Berlin, 1989; p I205.

Acknowledgements

The text of III.4, in part, is the manuscript to be submitted to an academic journal as it appears in Boonlarppradab, C.; Kauffman, C. A.; Jensen, P. R.; Fenical, W. Marineosins A and B, A new class of macrocyclic pyrroles from the marine actinomycete “MAR3” clade. The dissertation author was the primary author and directed and supervised the research, which forms the basis for this chapter.